Manipulation of Macrophage Phagocytosis - Development of an Endogenous Delivery System

by

Johan Georg Visser

Dissertation presented in fulfilment of the requirements

for the degree of

Doctor of Philosophy in the Faculty of Science at Stellenbosch University

Study Leader: Prof. Carine Smith

Co-Study Leader: Dr. Anton Du Preez van Staden

March 2020

Declaration

By submitting this dissertation electronically, I declare that the entirety of the work contained therein is my own, original work, that I am the sole author thereof (save to the extent explicitly otherwise stated), that reproduction and publication thereof by Stellenbosch University will not infringe any third party rights and that I have not previously in its entirety or in part submitted it for obtaining any qualification.

This dissertation includes 1 original paper published in a peer-reviewed journal and 1 unpublished publication. The development and writing of the papers (published and unpublished) were the principal responsibility of myself and, for each of the cases where this is not the case, a declaration is included in the dissertation indicating the nature and extent of the contributions of co-authors.

Abstract

The need to administer more potent antimicrobial drugs is supported by the ever-increasing incidence of multidrug resistance. Given the (necessary) higher toxicity of these drugs, administration into host circulation comes at a high risk to the patient. Drug delivery systems that are capable of more localized drug deposition, could limit host exposure. Here we propose the use of an autologous delivery system to shuttle drugs through circulation to protect the host from premature drug exposure. Our approach encompassed a multidisciplinary method to include physiology and microbiology. From the physiology side, macrophages exhibit great capacity to transverse endothelial barriers during the inflammatory process. From the microbiology side, micro-organisms have evolved to evade the immune system by harboring within these macrophages to later induce their own expulsion for dissemination. The work presented here describes how we have utilized the pore forming and actin polymerising ability of the *Listeria monocytogenes* effectors, listeriolysin-O and actin assembly-inducing protein, to produce a novel drug delivery system: the synthetic microbe. Firstly, we synthesised these effectors by using a GFP-linked heterologous expression and purification system, with which we were able to produce effectors at a greater yield than previously reported. In vitro experiments further confirmed appropriate activity of synthesised proteins and finally, coating of these effector proteins onto polystyrene beads induced their expulsion from carrier macrophages. Furthermore, drug cargo expulsion did not result in lysis of the carrier cells, suggesting that macrophages could contribute to resolution of damage at target areas once cargo is released. In our opinion, this multidisciplinary approach may hold the solution to effective, controlled drug delivery.

Uittreksel

Die noodsaaklikheid om kragtiger antimikrobiese middels toe te dien, word beklemtoon deur die toenemende voorkoms van veelvuldige middel weerstandigheid. Gegewe die (noodsaaklike) hoër toksisiteit van hierdie medisyne, hou die sistemiese toediening daarvan 'n groot risiko vir die pasiënt in. Medisyne-afleweringstelsels wat meer gelokaliseer kan word, kan blootstelling van die gasheer beperk. Hier word voorgestel dat 'n outoloë afleweringstelsel gebruik word om dwelms deur die sirkulasie te vervoer, wat die gasheer teen voortydige blootstelling aan medisyne beskerm. Ons het 'n multidissiplinêre benadering ingespan wat beide fisiologie en mikrobiologie insluit. Van die fisiologiese kant af besit makrofage die vermoë om dwarsbrekings deur die endoteel te maak gedurende die inflammatoriese proses. Van die mikrobiologiese kant af het mikroörganismes ontwikkel om die immuunstelsel te ontduik deur binne hierdie makrofage weg te kruip en later hul eie uitsetting vir verspreiding te bewerkstellig. Die werk wat hier aangebied word, beskryf hoe ons die porievorming en aktienpolimerisasie-vermoë van die *Listeria monocytogenes*-effektore listeriolysien-O en aktien-samestellende induserende proteïen gebruik het om 'n nuwe medisyne-afleweringstelsel te vervaardig: die sintetiese mikroörganisme. Eerstens het ons hierdie effektore gesintetiseer deur gebruik te maak van 'n GFP-gekoppelde heteroloë uitdrukking- en suiweringstelsel, waarmee ons effektore met 'n groter opbrengs kon produseer as wat voorheen gerapporteer is. *In vitro*-resultate het die toepaslike aktiwiteit van gesintetiseerde proteïene verder bevestig. Laastens het die bedekking van hierdie effektorproteïene op polistireenkrale hul uitsetting uit draer-makrofage veroorsaak. Verder het die uitsetting van geneesmiddelvragte nie gelei tot lise van die draerselle nie, wat daarop dui dat makrofage kan bydra tot die genesing van skade in die teikengebiede nadat die vrag vrygestel is. Na ons mening kan hierdie multidissiplinêre benadering die oplossing vir effektiewe, beheerde medisyne-aflewering inhou.

Research Outputs

1. Conference contributions:

➢ International poster presentation

- **Visser JG**, Smith C. A macrophage shuttle for transendothelial stem cell delivery. EMBO Conference on Hijacking host signalling and epigenetic mimicry during infections, Paris, France, June 2017

2. Published manuscript:

- **Visser JG**, Van Staden ADP, Smith C. Harnessing Macrophages for Controlled-Release Drug Delivery: Lessons from Microbes. Frontiers in Pharmacology. 2019. Doi: 10.3389/fphar.2019.00022

Acknowledgements

I would like to thank the following for their contribution to the success of this project:

- Our God Jesus Christ for perpetual guidance and everlasting support
- My parents and family for making my dreams a reality
- Prof. Carine Smith for teaching me everything I know – I could not have asked for a better supervisor
- Dr. Du Preez van Staden for being an exceptional mentor and helping with all the molecular work done here
- Beate Jordaan for always listening and helping more than she realised
- National Research Foundation (NRF) of South Africa for financial support
- Mrs Lize Engelbrecht and Dr. Dalene de Swart for all things technical
- Stellenbosch University Central Analytical Facility (CAF), Fluorescence Microscopy unit, for technical assistance
- Tygerberg Central Analytical Facility (CAF), Flow Cytometry and Microscopy unit, for technical assistance
- All my friends for all the support I sometimes, unwillingly, received

Table of Contents

List of Figures

List of Tables

List of Abbreviations

aBCV	Autophagic BCV
ActA	Actin Assembly-Inducing Protein
ActABeads	ActA coated polystyrene beads
ActA-GST	ActA linked to GST
ADV	Acoustic Droplet Vaporization
ANOVA	Analysis of Variants
ARP	Actin Related Proteins
Atg	Autophagy-Related
BCV	*Brucella*-Containing Vacuole
CCL2	Chemokine (C-C motif) ligand 2
CFU	Colony-forming unit
Cn	*Cryptococcus neoformans*
COPII	Coat Protein Complex II
DAMP	Damage-Associated Molecular Pattern
Dot/Icm	Defective in Organelle Trafficking/Intracellular Multiplication
DTT	dithiothreitol
eBCV	Endosomal BCV
EDF	Extended Depth of Field
EEA1	Endosomal Early Antigen 1
ER	Endoplasmic Reticulum
ERK5	Extracellular Receptor Kinase 5
ESX-1	ESAT-6 secretion system
F-actin	Filamentous actin
FYCO1	FYVE and Coiled-coil Domain Containing Protein 1
FYVE	Fab 1, YOTB, Vac 1 and EEA1
G-	Gram-negative
G+	Gram-positive
gDNA	Genomic DNA
GAP	GTPase-Activating Protein
GEF	Guanine Nucleotide-Exchange Factor
GFP	Green Fluorescent Protein
GFP-ActA-GST	ActA linked to GFP and GST
GFP-LLO	GFP linked to LLO
GST	glutathione S-transferase
GTPase	Guanosine Triphosphate Phosphatase
HEPES	4-(2-hydroxyethyl)-1-piperazineethanesulfonic acid
HIFD	High Intensity Focused Ultrasound
His tag	polyhistidine-tag
HOPS	Homotypic Fusion and Protein Sorting
hVPS34	Human Vacuolar Protein Sorting 34
HREC	Subcommittee C Human Research Ethics Committee
HUVEC	Human Umbilical Vein Endothelial Cell
IgG	Immunoglobulin G
IFN-γ	Interferon gamma
IL-10	Interleukin 10
IL-1β	Interleukin 1 beta
IMAC	Immobilized Metal Affinity Chromatography
IPTG	thio-B-D-galactopyranoside
LAM	Lipoarabinomannan
LAMP	Lysosome-Associated Membrane Proteins
LB	Luria Bertani
LBPA	Lysobisphosphatidic Acid

LC3	Microtubule-Associated Protein 1A/1B-Light Chain 3
LCV	*Legionella*-Containing Vacuole
LepA	Legionella Effector Protein A
LepB	Legionella Effector Protein B
LLO	Listeriolysin-O
LLOActABeads	LLO and ActA coated polystyrene beads
M1	Classically Activated M1 Phenotype Macrophage
M2	Alternatively Activated M2 Phenotype Macrophage
MAP	Mitogen-Activated Protein Kinase
MCP-1	Macrophage Chemoattractant Protein 1
MES	2-(N-morpholino)ethanesulfonic acid
MIF	Macrophage Migration Inhibitory Factor
MPR	Mannose-6-Phosphate Receptor
Mtb	*Mycobacterium tuberculosis*
MTOC	Microtubule Organizing Centre
MyD88	Myeloid Differentiation Primary Response 88
NADPH	Nicotinamide Adenine Dinucleotide Phosphate
NK cell	Natural Killer Cell
N-WASP	Neuronal Wiskott-Aldrich Syndrome Protein
OD	optical density
ORP1L	Oxysterol-Binding Protein Related-Protein 1
PAMP	Pathogen-Associated Molecular Pattern
PBS	Phosphate Buffered Saline
PBS125	PBS containing 125 mM imidazole
PBS20	PBS containing 20 mM imidazole
PDIM	Phthiocerol Dimycocerosates
pDNA	Plasmid DNA
PI	Phosphatidylinositol
PI(3,5)P2	Phosphatidylinositol 3,5-Bisphosphate
PI3k	Phosphoinositide 3-kinase
PI3P	Phosphatidylinositol 3-Phosphate
PIKfyve	FYVE Finger-Containing Phosphoinositide Kinase
PKG	Protein kinase G
PNIPAAm	Poly-(NIPA-co-AAm)
PNP	Polymeric Nanoparticles
PRR	Pattern Recognition Receptor
PS	Phosphatidylserine
PtpA	Mycobacterium Tuberculosis Protein Tyrosine Phosphatase
T3SS	Type III Secretion System
T4BSS	Type 4B Secretory System
T4SS	Type IV Secretion System
T7SS	Type VII Secretion System
TACO	Tryptophan-Aspartate Containing Coat
TAM	Tissue Associated Macrophage
TB	Terrific Broth
TIM-4	T cell Immunoglobulin and Mucin-Domain Containing Protein 4
TNF-α	Tumour Necrosis Factor alpha
TLR	Toll-like Receptor
rBCV	Replication-Permissive BCV
RIG-like	Retinoic Acid-Inducible Gene-I-like
RILP	Rab7-Interacting-Lysosomal-Protein
RNS	Reactive Nitrogen Species
ROS	Reactive Oxygen Species
SapM	Secreted Acid Phosphatase
SB	Start Buffer

SB20	SB containing 20 mM imidazole
SB30	SB containing 30 mM imidazole
SCV	*Salmonella* Containing Vacuole
SDS-PAGE	sodium dodecyl sulphate–polyacrylamide gel electrophoresis
SEM	Standard Error of the Mean
SIF	*Salmonella* Induced Filaments
SKIP	SifA-and-Kinesin-Interacting-Protein
SLAP	Spacious *Listeria*-Containing Phagosome
SNARE	Soluble N-ethylmaleimide-Sensitive Factor-Attachment Proteins
SNX	Sorting Nexins
SPI	*Salmonella* Pathogenicity Island
VAMP	Vesicle Associated Membrane Protein
V-ATPase	Vacuolar-type H^+-ATPase
VPS33B	Vacuolar Protein Sorting-Associated Protein 33B

Units of Measure

%	percentage
˚C	degrees Celsius
µg/cm^2	microgram per square centimetre
µg/ml	microgram per millilitre
µl	microliter
µm	micrometre
µM	micromolar
g	gravitational acceleration
g/mol	gram per mole
h	hour
kDa	kilodalton
M	molar
Mb	megabase
mg	milligram
mg/ml	milligram per millilitre
min	minutes
ml	millilitre
mm	millimetre
mM	millimolar
mW	milliwatt
ng/ml	nanogram per millilitre
nm	nanometre
nM	nanomolar
kDa	kilo Dalton
RPM	revolutions per minute
U/µg	unit per microgram

Chapter 1: Introduction

Due to the time and cost involved in the research and development of novel pharmaceuticals, the approval of new antibiotics by regulatory bodies cannot keep up with the increasing multidrug resistance of many microbial pathogens. Furthermore, the increasing need for higher toxicity pharmaceuticals to eliminate these resistant bacteria or malignancies is associated with a plethora of undesired effects in the already compromised patient (Yasinzai et al., 2013; Hughes et al., 2015). Optimal delivery mechanisms are essential to ensure the effective delivery and release of these pharmaceuticals (cargo) and to limit side-effects. Apart from obvious problems such as toxicity, other problems are also encountered with systemic drug administration, which may affect drug efficacy. For example, drugs may bind to serum proteins, which may either inactivate the drug or prevent it from reaching its intended target areas (Ahsan et al., 2002; Khan et al., 2002). Also, in chronic diseases such as cancer, the high potency drugs required for treatment often have severe side-effects resulting in other chronic diseases, e.g. the chemotherapeutic drug doxorubicin, which is linked to cardiotoxicity and eventual chronic heart failure (Schlame et al., 2000; Shi et al., 2011; Sishi et al., 2013 a; b). Nanoscience has been incorporated in attempts to decrease occurrence of side-effects, but this has introduced new problems, for example in terms of pharmacodynamics. For example, doxorubicin has been packaged into liposome nanoparticles (Simpkins et al., 2013), however, these nanoparticles exhibited low tissue infiltration and the nanoparticle size generally limits delivery of larger drugs or proteins (Hoshyar et al., 2016). In addition, antimicrobial drugs have been reported to exert a plethora of neuropsychiatric effects (Zareifopoulos et al., 2017), such as anxiety, psychosis, mood disturbances, behavioural changes and seizures (Warstler et al., 2016).

The use of biopharmaceuticals is becoming more prevalent due to their high specificity and potency. However, due to their structural complexity, these molecules are often relatively unstable, and their size complicates the process of traversing biological barriers such as mucosal membranes (Youshia et al., 2016). These issues regarding drug delivery have invoked research and development initiatives into several drug delivery systems, including the use of polymer based micro- and nano- particles, which generally utilise encapsulation techniques for packaging drugs for delivery (Ahsan et

al., 2002). The limitations and advantages of different drug delivery systems have been comprehensively reviewed (Mitragotri et al., 2014; Patra et al., 2018). Although advancements have been made over the past few years, it is important to consider that these drug delivery systems are markedly diverse with each comprising of its own benefits and limitations. I present a short summary of the literature on some drug delivery systems to illustrate their diversity, benefits and limitations in **table 1.1**. Here I will only mention a few of these which are most pertinent to my thesis topic. For example, one benefit (and reason for use) of microparticles include the ability to delay drug release (Cohen et al., 1991). However, microparticles run the risk of increasing the inner pH as it degrades *in vivo*, that could lead to degradation of protein or peptide based drugs (Ding et al., 2006). Nanoparticles on the other hand can be used as vaccine adjuvants (Zhao et al., 2014), however, vascular epithelial elicits low permeability for nanoparticles, lowering bioavailability in deep tissue. It has been suggested that this issue could likely be addressed by optimising the geometry of nanoparticles (Banerjee et al., 2016), but this remains to be substantiated.

The quest for techniques to achieve successful focal *in vivo* delivery of pharmaceuticals or cargo – these may range from high-toxicity drugs to stem cells – thus remain an important niche within cell biology research and is of great clinical importance for future therapeutic interventions. Although a multitude of potential delivery systems have already been put forward, no broadly applicable delivery mechanism has been elucidated. It is clear that this problem can only be solved by taking an “out-the-box”, multidisciplinary approach. To this end, we believe that manipulation of an endogenous cellular “delivery system” would significantly address the above-mentioned limitations, limit the need for invasive surgery and allow delivery to normally inaccessible areas within bone or the central nervous system. Recently, we proposed packaging of cargo inside endogenous, living cells, for both protection and delivery to specific *in vivo* sites (Visser et al., 2019). More importantly – and the main topic for this project – we propose the development of a method for the release of cargo from these cells in a manner that is non-lytic to the host cell itself, so that drug delivery itself would not add to the magnitude of inflammation at the site of delivery.

Briefly, in my opinion, the monocyte/macrophage leukocyte subpopulation is the appropriate candidate for use as a delivery shuttle. (For a brief introduction of basic macrophage biology, please refer to **Appendix 1**.) Most pertinent to the current thesis

topic, these robust cells elicit an unrivalled capacity for migration from the circulation into and through various tissue compartments, during normal functioning, to exert their roles in the inflammatory process (Arnold et al., 2007 a; Abbas et al., 2014). We have recently successfully manipulated macrophages to ingest different cargo – ranging from polystyrene particles to live muscle stem cells – without the cargo being digested, by experimentally inducing transient phagosome maturation arrest (Visser et al., 2018). This approach immediately solves the problem of maintaining cargo intact for delivery, through shielding it from the *in vivo* environment until release. Furthermore, we have shown sustained phagocytic and transendothelial migration capacity of these manipulated, loaded, macrophages using *in vitro* models (Visser et al., 2018).

Although these results are very positive and novel, and optimisation for *in vivo* conditions is ongoing, the next major obstacle is related to actual delivery of the drug at required sites. Importantly, the method of delivery should not exacerbate inflammation or other degradative processes, as this would compromise recovery rate and recovery quality. As mentioned, here we propose using an unconventional, multidisciplinary approach to achieve delivery of intact cargo from an endogenous live cell without damage to the host cell. This would involve “hijacking” the mechanisms used by microbes to induce their non-lytic release from cells during infection and *in vivo* dissemination. This would produce a “synthetic microbe” which effectively encapsulates the cargo inside a macrophage phagosome, to facilitate its controlled, acute burst release.

In terms of dissertation layout, I provide an overview of the relevant literature in **Chapter 2**. This review has been published in Frontiers in Pharmacology in 2019 (Visser et al., 2019). This review is followed by a formulation of my hypothesis and specific aims, with methods employed presented in **Chapter 3**. I present the most significant results in **Chapter 4**, before interpreting data and contextualising findings in terms of relevant literature in **Chapter 5**. Finally, I present final conclusions and suggestions for further investigations in **Chapter 6**.

Delivery system	Method of administration	Pros	Cons	Pharmacodynamics	Pharmacokinetics
Microspheres: Poly(lactic-co-glycolic acid) (PLGA) polymers *1	Subcutaneous injection	Hydrophobic Mechanically strong Administer larger drugs	Protein aggregation. Degradation of protein cargo (Polymer degradation could raise pH). Needles clog due to size. Costly.	Low toxicity, degrading into biocompatible products	Sustained drug release
Nanoparticles: Liposomes *2	Subcutaneous injection	Cell-based delivery of tethered T cells Vaccine adjuvant Enhanced permeation-retention effect (tumour)	Additional research required for protein delivery Poor tissue penetration	Poor endothelial penetration and tissue diffusion Poor deep tumour penetration	Rapid clearance by RES and resident macrophages Endocytosed by host-cells reducing bioavailability
Depot injections *3	Subcutaneous injection or Surgical implant	Administer small or large drugs Easier to manufacture	Larger gauge needles Incisions made in skin Burst release	Non-immunogenic Drug diffusion largely site specific	Sustained drug release
Modified proteins and peptides: Pegylation *4	Subcutaneous injection	Sustained drug exposure	Sustained, but no control over drug exposure Fusion with native host protein	Increased size affects receptor binding via steric hindrance	Reduced renal clearance by increasing size above ~60 kDa Immunogenicity
Pulmonary delivery *5	Inhalation	Ease of administration (self-administration)	Limited delivery efficiency Sustained delivery problematic	Aggregation of drug particles	Macrophage drug clearance
Transdermal delivery *6	Skin patch	Painless	Limited to low kDa hydrophobic drugs Low bioavailability	Diffusion into dermis	Low bioavailability
Oral delivery *7	Capsule form	Ease of administration (self-administration) Easily manufactured	Poor absorption into systemic circulation Insufficient bioavailability	GIT irritation	Degradation in the GIT Limited intestinal epithelium permeation

Table 1.1: Examples of drug delivery systems: Reticuloendothelial System (RES), Gastrointestinal Tract (GIT). **1**: (Langer et al., 1976; Cohen et al., 1991; Kim et al., 1999; Ding et al., 2006) **2**: (Sugahara et al., 2010; Nance et al., 2012; Bertrand et al., 2014; Zhao et al., 2014; Hoshyar et al., 2016) **3**: (Ghalanbor et al., 2010) **4**: (Pasut et al., 2012) **5**: (Edwards, 1997) **6**: (Abla et al., 2005; Chen et al., 2006; Alkilani et al., 2015) **7**: (Morishita et al., 2006).

Chapter 2: Literature Review

This literature review has been published in its current form: Visser JG, Van Staden ADP, Smith C. (2019). Harnessing Macrophages for Controlled-Release Drug Delivery: Lessons from Microbes. *Frontiers in Pharmacology* 10:22, 1-18. doi: 10.3389/fphar.2019.00022. Impact factor 3.845

2.1. Introduction

In recent years, drug delivery has become a well-documented research niche across various disciplines in science. Approaches of drug delivery into pathogenically damaged areas or poorly vascularised cancer tissues has been largely focused on treatments incorporating nanoparticles (Zhao et al., 2011; Dreaden et al., 2012; Feng et al., 2014; Huang et al., 2015; Lv et al., 2016; Tanei et al., 2016). These nanoparticles generally serve to shield harsh/labile drugs from the host and subsequently activate or release it after reaching target tissues. With the potential exception of nanoparticle uptake into target cells via complementary receptor ligands, this approach is however still more comparable to drug saturation than with specialised drug delivery *per se*.

In this review we propose an alternative to the strategies/approaches used until now: a novel macrophage-mediated drug delivery method that more accurately fits the term “drug delivery”, via incorporation of both nanomedicine and cellular manipulation. Macrophages are highly mobile cells. By loading host macrophages with appropriate cargo (e.g. chemotherapeutic agents such as doxorubicin or high-potency antimicrobials), one can thus theoretically use the inherent homing capabilities of these immune cells to reach target damaged, infected or malignant tissue, in order to treat the affected cellular areas only. Such an approach would reduce the total concentration of drug required (when compared to systemic administration) and significantly reduce or even eradicate the risk of drug-associated adverse effects. Achieving this goal would indeed require substantial research into phagocytosis, macrophage chemotaxis, pathogenic immune evasion and controlled release of therapeutics. Here, we propose such a system where cargo is introduced into the macrophage, maintained within “inactivated” phagosomes and released in a controlled manner at the appropriate time and *in vivo* location.

The system as proposed in its entirety here, is novel. However, some aspects of this system have been investigated individually before (discussed in detail later) and testifies to the feasibility of the approach we suggest. In order to fully understand cellular role players, a multidisciplinary approach is clearly required. We propose that the literature on host-microbe interactions may provide the insight required. While research have described the ability of microbes to evade the immune system by hiding (and proliferating) inside immune cells before orchestrating their own expulsion or transfer directly into new host cells, the mechanisms by which they achieve this have received very little attention by non-microbiologists. In our opinion, harnessing these microbial strategies could prove useful in the drug delivery niche. Thus, if a paradigm shift can be made to embrace the fact that host-affecting microbial mechanisms may potentially have therapeutic application, we believe that biologists could learn valuable lessons from microbes, to the benefit of technological advancement in medicine.

The aim of this paper is therefore to present a summary of pertinent literature on microbial mechanisms known to modulate the course of endocytic processes and to evaluate their feasibility in the context of therapeutic drug delivery. A specific novel focus will be on potential mechanisms through which to achieve controlled expulsion. We believe that this paper elucidates an exciting new avenue for research in the context of drug delivery.

In order to facilitate clarity of our argument, we first provide a brief overview of the most pertinent literature describing the mechanisms that would come into play in a complete cell-based delivery system. Considering the complexity of these processes, one can appreciate the enormity of the task to elucidate which perturbations in this process may be used for application to our proposed drug delivery system. Thus, we will describe the different phases – namely cargo loading, maintenance of cargo integrity, *in vivo* motility of the carrier cell toward delivery sites and cargo expulsion – individually below, before discussing in more detail, the lessons to be learnt from microbes.

2.2. Components of a Cell-Based Delivery System

2.2.1. Cargo Loading into Macrophages

Circulating monocytes form part of the innate immune system and are largely responsible for the initial recognition of foreign material or microbes (Abbas et al., 2014). Recognition and internalisation, for the purpose of neutralisation, are generally very effective. This is evidenced by the absence of adaptive B and T cell responses in almost 95% of Animalia (Mills et al., 2015). However, many microbes have been able to survive within macrophages by manipulating phagocytic processes (discussed later). A summary of the most relevant normal human phagocytic processes is presented visually in **Figure 2.1**.

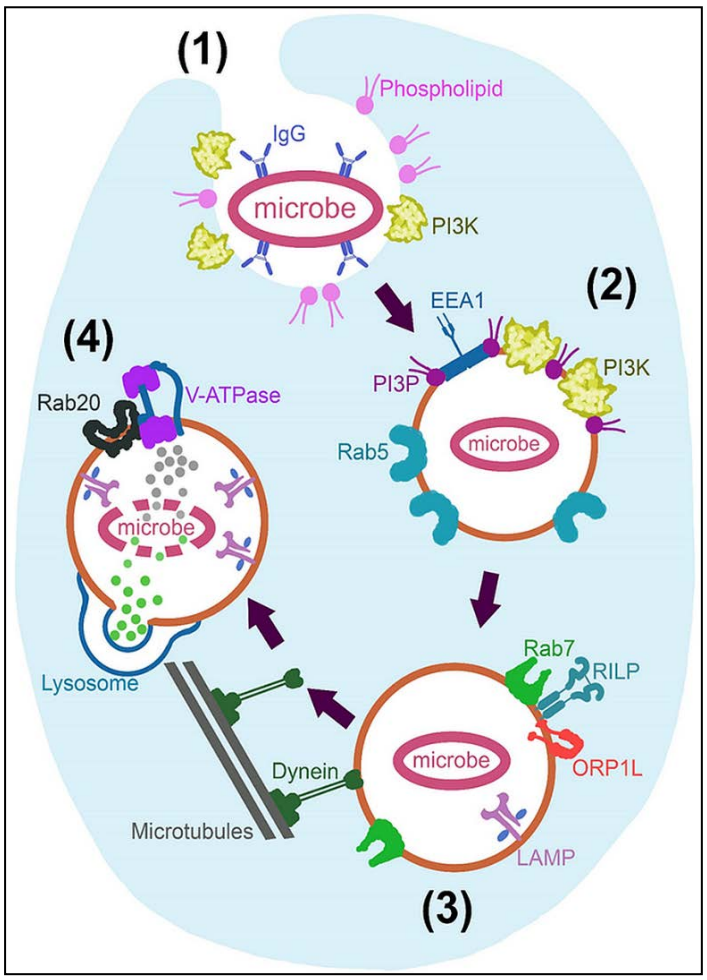

Figure 2.1: Fundamental mechanisms of phagosome maturation. Initiated through (1) Recognition and engulfment of opsonised microbe and expression of phospholipids and phosphoinositide 3-kinase (PI3k), at the extending pseudopodia. (2) Nascent phagosome is formed after actin polymerisation facilitates pseudopod closure behind the microbe. This phagosome is characterized by Rab5, phosphatidylinositol 3-phosphate (PI3P) and endosomal early antigen 1 (EEA1) expression. (3) The late phagosome is characterized by Rab7 recruitment; resulting in Rab5 inactivation and PI3P degradation as well as recruitment of lysosome-associated membrane proteins (LAMP) while achieving dynein linkage and centripetal movement for later lysosomal fusion. Rab7 achieves these processes via Rab7-interacting-lysosomal-protein (RILP) and oxysterol-binding protein related-protein 1 (ORP1L). Lysosome fusion initiates the last stage in maturation; (4) Phagolysosome biogenesis, where LAMP expression is increased, and lysosomal content is dumped into the phagosome. Rab20 also allows an acidic environment through the action of vacuolar-type HC-ATPase (V-ATPase).

The most important aspect of our topic is that of immune recognition and intake into the macrophage. It is commonly known that pattern recognition receptors (PRRs) on phagocytes recognise several different molecular patterns – such as damage-associated molecular patterns (DAMPs) or pathogen-associated molecular patterns

(PAMPs) – on the target for potential phagocytosis (Abbas et al., 2014). Toll-like receptors (TLRs) present on phagocytes also indirectly regulate phagocytosis through Myeloid differentiation primary response 88 (Myd88) signalling and activation of the p38 residue (Shi et al., 2016). Several other minor role players in pathogen recognition, such as receptors for lectin, mannose, complement and Retinoic acid-inducible gene-I-like (RIG-like) receptors, has been identified, but the immunoglobulin G (IgG) receptors are most directly associated with phagocytosis of material. In fact, antibody-opsonised material binds and activates IgG receptors to induce engulfment independently of co-stimulation by T cells or NK (natural killer) cells (Liu et al., 2013), making this mechanism an obvious choice for ex vivo cargo loading into macrophages. Engulfment is reliant on phosphoinositide 3-kinase (PI3k) recruitment and its production of various phosphatidylinositides that, together with actin polymerisation, result in pseudopod formation around the material and subsequent internalisation.

Once material has been engulfed, it is enveloped inside a double-membraned (nascent) phagosome, which is innocuous and undergoes various maturation phases, that culminates in fusion with lysosomes, which enables it to acidify and break down its contents. Characterisation of this maturation process is well-established (Patki et al., 1998; Fratti et al., 2001; Vieira et al., 2002; Kinchen et al., 2008; Fairn et al., 2012) and are not discussed in detail here, as we do not envisage a requirement for huge manipulation of this phase. Indeed, previous research by our group and others have demonstrated that macrophages readily take in a variety of purpose-designed materials and particles of varying sizes via endocytic pathways (Zhao et al., 2011; Dreaden et al., 2012; Feng et al., 2014; Oh et al., 2014; Huang et al., 2015; Miller et al., 2015; Tanei et al., 2016; Fan et al., 2018; Visser et al., 2018).

2.2.2. Cargo Maintenance

Of more direct relevance, lysosomal fusion marks the start of the last stage in maturation, that of phagolysosome biogenesis (Seto et al., 2011), which is an obvious threat to cargo maintenance. Normally, this lysosome fusion is mediated by endoplasmic reticulum (ER) soluble N-ethylmaleimide-sensitive factor-attachment proteins (SNARE) such as syntaxin 7, syntaxin 8 and vesicle associated membrane protein (VAMP) -7 and -8 (Becken et al., 2010). Lysosome-associated membrane protein (LAMP) concentration is increased after fusion (Jahraus et al., 1994) and

cathepsin D proteases are recruited from the Golgi via Rab-22b, -32, -34, -38 and -43 (Ng et al., 2007). The vacuolar-type H+-ATPase (V-ATPase) is also incorporated via Rab20 co-localisation at this time (Curtis et al., 2005). In this way, fusion ultimately effectuate an acidic environment within the macrophage phagosome, as well as supplying it with proteases, reactive oxygen species (ROS) and reactive nitrogen species (RNS) to facilitate decomposition of phagosomal content.

To date, the majority of literature employing macrophages as delivery shuttles, have used either nanoparticle-encapsulated drugs travelling inside the cell, or drugs "backpacked" on the outside of the cell. The most popular protocol used are to load cargo into macrophages to create a "Trojan horse". However, this approach has some limitations: firstly, there is a significant risk of drug-associated cytotoxicity, secondly, drugs are released at a relatively slow rate and thirdly, they are vulnerable to lysosomal degradation inside the macrophage (Yousefpour et al., 2014). In an attempt to address these limitations, transport of drugs on the outer surface of macrophages were attempted. However, prevention of internalisation of the backpacked cargo into carrier macrophages was a major obstacle (Watson et al., 2010; Doshi et al., 2011).

In our opinion, perhaps the most feasible option to ensure integrity of cargo that are either labile or highly toxic – so that premature delivery should not be risked – would be their maintenance intracellularly by modification of normal phagocyte function. It is here where we could substantially learn from microbial strategies (refer to **Section 2.4**). Indeed, we have previously demonstrated maintenance of cargo inside primary human M1 macrophages chemically treated to transiently inhibit phagosomal cargo destruction (Visser et al., 2018). Briefly, protein-coated polystyrene beads, used as simulative cargo, were maintained intact (i.e. with no digestion of the protein coating) inside macrophages after in vitro treatment with a phagosome maturation inhibiting cocktail, consisting of Wortmannin, Concanamycin A and Chloroquine. This inhibition cocktail was only administered in vitro, and treated cells were washed prior to use, thus lowering risk to patient in the context of in vivo application. Furthermore, this intervention did not affect chemotactic or migratory capacity – macrophages were able to transverse an in vitro Human Umbilical Vein Endothelial Cell (HUVEC) membrane while carrying the bead cargo.

Another modern technique relevant here, is the use of nano- or microparticle encapsulation of drugs prior to loading into carrier cells (Dou et al., 2006; Zhao et al., 2011; Blaudszun et al., 2014; Feng et al., 2014; Klyachko et al., 2014; Pang et al., 2016; Tanei et al., 2016; Gnanadhas et al., 2017; Evans et al., 2018; Fan et al., 2018). In addition to host protection, polymeric particles may also be used for maintenance of drug integrity itself. Emerging evidence indeed indicates a role for polymeric particles as protective modality for both host and drug cargo. Cargo can be rendered innocuous via, for example, poly-(NIPA-co-AAm) (PNIPAAm) micelle or microbubble encapsulation. PNIPAAm micelles are reported to degrade in response to an increase in temperature above the lower critical solution temperature (Feng et al., 2014), enabling control over bio-activation of encapsulated drugs. As an example, these micelles could be incorporated during treatment of peripheral diseases, such as melanoma or myopathy, where an external stimulus can be administered to increase the local temperature and release drug cargo from PNIPAAm micelles. Incorporation of microbubbles together with nanoparticles has also shown some promise during in vivo delivery of resveratrol for treatment of cancer (Lv et al., 2016). In this study, resveratrol was loaded into acetylated β-cyclodextrin nanoparticles (PNP), which were then loaded into microbubbles. The outer microbubble coating served to protect the pH sensitive PNP while in circulation, whereas PNP in turn released resveratrol upon exposure to the low pH tumour niche. These studies indicate that polymeric particles may be powerful tools to incorporate into delivery systems to address current limitations.

2.2.3. *In Vivo* Macrophage Migration for Cargo Delivery

Literature focusing on macrophage (or other phagocyte) migration are normally aimed at the prevention of this migration, e.g. in the context of cancer metastasis or inflammation. Despite the different focus to ours, these studies have elucidated the process of migration in detail.

For example, in the context of muscle inflammation, M1 macrophages have been illustrated to be the most motile, pro-inflammatory phenotype, while M2 macrophages are less likely to infiltrate tissues and associated with a relatively anti-inflammatory outcome (Arnold et al., 2007 a; Smith et al., 2008; Kruger et al., 2014). Our previous work on M1 macrophages (Visser et al., 2018) confirms the choice of this phenotype

as superior for drug delivery. However, it should be noted that macrophage phenotype has a large degree of plasticity, which will have to be taken into account when designing drug delivery protocols for application in particular disease states. To this end, a recent review (Ruytinx et al., 2018) comprehensively provide information on macrophage polarisation in the context of inflammatory diseases such as neurological disease, cancer, metabolic and cardiovascular disorders.

Similarly, in terms of chemotactic signals for macrophage migration, chemotaxins generally expressed on tissue cells in many different disease conditions have been identified. Most notably, inflammation – which would be present in any disease state with a requirement for drug delivery – is known to result in increased levels of the chemokines macrophage migration inhibitory factor (MIF) and/or macrophage chemoattractant protein 1 (MCP-1 or CCL2), which are strong signals for macrophage recruitment into the tissue (Lee et al., 2010; Baeck et al., 2012). Additionally, oxidative stress – which is a known complication of both chronic disease and infection (Nimse et al., 2015; Petersen et al., 2016) – have been shown to initiate macrophage migration in vivo (Wang et al., 2016). In terms of systemic migration towards chemotactic signals originating from hypoxic tissue, such as in cancer, evidence also exist to confirm the inherent capacity of macrophages to migrate toward tumours (Owen et al., 2004; Batrakova et al., 2011). Although finer detail on the regulation of macrophage migration has been reported, such as its dependence of on integrin β1 expression and recycling (Gnanadhas et al., 2017) and numerous proteases (Van Goethem et al., 2010), these details are likely of academic value only, at least for the context under discussion. In our opinion, these factors are unlikely to be a limiting factor, since integrin β1 is expressed by almost all cell types and some degree of redundancy is in place. For example, in contrast to the fairly uniform amoeboid movement of neutrophils, macrophages were reported to exhibit multiple different migration mechanisms that are more mesenchymal in nature (Van Goethem et al., 2010; Barros-Becker et al., 2017), which could confer greater resilience to macrophages in terms of mobility under adverse conditions. Interestingly, the latter study also demonstrated a greater degree of directionality of macrophages vs. neutrophils in a zebrafish tail transection model of leukocyte migration. Another ability of macrophages pertinent to the current topic, is their ability to maintain their mobility after ingestion of cargo, even when the cargo is much larger than anticipated to be required for the purpose of drug

delivery (Chang et al., 2013; Evans et al., 2018; Visser et al., 2018). These reports again confirm that this phase of the system is unlikely to require major intervention, as it seems to already have been fine-tuned by evolution.

The only potential limitation we foresee is interference with chemotactic signal originating from the intended site for drug delivery, by e.g. an acute, severe infection/damage in another organ, which may have chemotactic priority above that of the signal originating from the intended delivery site. However, the practise of isolating patients for a period prior to a medical procedure is not uncommon and could avoid this complication. Furthermore, pathogen-associated infection has been shown to take priority above other, relatively less life-threatening, situations, which would in fact favour directional macrophage migration, rather than limit it.

2.2.4. Cargo Expulsion

The final step to complete such a delivery system, would be a mechanism by which the cargo can be released or expelled at the appropriate time and location in vivo. Normally, following phagolysosomal destruction of ingested material, digested material is either recycled by the phagocytic cell or expelled into the extracellular matrix. Recycling of re-usable “waste” such as amino acids, glucose and phosphates occur via diffusion through the phagolysosome membrane into the cytosol (Guyton et al., 2011). Of particular interest here, the insoluble components are expelled from the macrophage either via the ER-Golgi secretory pathway or utilised for antigen presentation through Ca^{2+}- and vesicle-associated membrane protein 7 (VAMP7)-dependant lysosome exocytosis (Samie et al., 2014). We believe that the manipulation of these expulsion mechanisms could facilitate controlled drug delivery.

In terms of published studies on drug delivery systems, most systems either rely on non-specific release of nanoparticles containing drugs (Miller et al., 2015), or employ release of drugs inside the carrier cell. For example, rupture of doxorubicin-containing microbubbles inside macrophages was achieved by high intensity focussed ultrasound techniques (Fan et al., 2018). However, this strategy for drug release resulted in significant carrier cell death. We believe this is an undesirable mechanism, as this would likely contribute to inflammation and thus delayed recovery. Therefore, to date, a controlled cell-based drug release system does not seem to exist.

In the next section, we evaluate microbially employed strategies, in terms of their feasibility for adaptation into therapeutic contexts. We will focus on the two phases of this system which seems to be most commonly and effectively manipulated by microbes, namely immune evasion by intracellular survival and programmed expulsion from host cells.

2.3. What Can We Learn from Microbes?

Pathogenic phagosome maturation arrest or modulation thereof, and subsequent escape from the host cell are hallmarks of bacterial host immune evasion and dissemination. Well characterized mechanisms include interfering with PI3k and PI3P biogenesis (*M tuberculosis* & *Candida glabrata*) (Vergne et al., 2003; Rai et al., 2015), establishing microbe-containing vacuoles (*Legionella pneumophila* & *Brucella*) (Celli, 2015; Bärlocher et al., 2017), blocking of fission and fusion with lysosomes and endosomes (*Mycobacterium tuberculosis* & *Legionella*) (Vergne et al., 2003, 2005; Bärlocher et al., 2017), raising pH levels via induction of phagosomal acid leakage (*Cryptococcus neoformans*) (Tucker et al., 2002), lysis of the phagosomal membrane (*Listeria monocytogenes*) (Alberti-Segui et al., 2007), hijacking of the endocytic recycling pathway (*Legionella pneumophila*) (Xu et al., 2013) and even active macrophage killing (filamentous *Candida albicans*) (Gaur et al., 2013). Manipulation of the endocytic pathways by microbes is achieved via highly diverse and complex mechanisms. Intracellular microbes secrete hundreds of proteins, known as effectors, capable of modulating these pathways (Santos et al., 2015; Schroeder, 2018). These effectors have diverse functions and microbes employ multiple layers of redundancy to ensure their survival (Ghosh et al., 2017; Schroeder, 2018). The abundance and variety of these effectors provide an ideal bioprospecting opportunity to identify effectors that can be utilized to modulate the endocytic pathways as needed. Keeping in mind that not all microorganisms have effectors capable of manipulating the endocytic pathway for both maintenance and expulsion. Identified effectors can then be further investigated to optimise the cocktail of effectors (possibly from different organisms) best suited for application in a macrophage-based delivery system.

Organism	Disease State	Type of endocytic modulation	Outcome of endocytic modulation	Egress and Dissemination
Brucella (G-) **1*	Brucellosis / Malta Fever	Modulation of phagosome maturation	VirB (T4SS) dependent modulation of phagosome, Suppression of macrophage polarization	Cell necrosis / apoptosis (VirB and bacterial dissociation dependent) followed by extracellular dissemination
Legionella pneumophila (G-) **2*	Legionnaires disease	Prevention of phagosome maturation	Dot/Icm (T4BSS) dependent prevention of phagosome maturation	Pyroptosis, Apoptosis, Cell lysis
Listeria monocytogenes (G+) **3*	Listeriosis	Prevention of phagosome maturation, phagosome rupture	Listeriolysin-O dependent lysis of phagosome or induction of autophagy for replication	Cell-to-cell spread (ActA/LLO-dependent)
Chlamydia (G-) **4*	Genital / respiratory infections	Subversion of endocytic pathway via inclusion formation	Inc/CT229 dependent inclusion development	Cell lysis, Inclusion extrusion
Mycobacterium tuberculosis (acid fast) **5*	Tuberculosis	Prevention of phagosome maturation, phagosome rupture	LAM/SapM dependent interference of PI3k and PI3P biogenesis. Inhibition of H+ V-ATPase assembly. ESX-1/EsxA and PDIM dependent phagosome rupture	Cell necrosis / apoptosis
Salmonella enterica (G-) **6*	Salmonellosis	Modulation of phagosome maturation	Modulation of phagosome maturation via T3SS effector (SifA, SopB) dependent development of SCV	Pyroptosis
Cryptococcus neoformans (Yeast) **7*	cryptococcal meningoencephalitis	Unknown effectors. Possible pH dependent phagosome damage. Capsular protection.	Unknown effectors. Possible pH modulation through phagosome damage.	Non-lytic expulsion, cell lysis, cell-to-cell spread

Table 2.1: Examples of intracellular microbes and main outcomes of endocytic pathway modulation. Gram negative (G-), Gram positive (G+). ***1** (Pizarro-Cerdá et al., 1998; Hong et al., 2000; Comerci et al., 2001; Boschiroli et al., 2002; Celli et al., 2003; Arellano-Reynoso et al., 2005; Celli, 2006; Pei et al., 2006, 2008; Starr et al., 2008; Chen et al., 2009, 2011; Starr et al., 2012; von Bargen et al., 2012; Smith et al., 2016). ***2** (Kirby et al., 1998; Roy et al., 1998; Gao et al., 1999; Alli et al., 2000; Gerhardt et al., 2000; Bachman et al., 2001; Tilney et al., 2001; Molmeret, 2002; Chen et al., 2004; Molmeret et al., 2004; Chen et al., 2007; Xu et al., 2013; Schroeder, 2018). ***3** (Smith et al., 1995; Skoble et al., 2000; Veiga et al., 2005; Henry et al., 2006; Shaughnessy et al., 2006; Alberti-Segui et al., 2007; Birmingham et al., 2008; Czuczman et al., 2014; Mitchell et al., 2015). ***4** (Perfettini et al., 2003; Rzomp et al., 2003; Scidmore et al., 2003; Hybiske et al., 2007; Betts-Hampikian et al., 2010; Capmany et al., 2010; Chin et al., 2012; Volceanov et al., 2014). ***5** (Sturgill-Koszycki et al., 1994; Ferrari et al., 1999; Renshaw et al., 2002; Walburger et al., 2004; Vergne et al., 2005; de Jonge et al., 2007; Seto et al., 2010; Wong et al., 2011; Simeone et al., 2015; Zhang et al., 2016; Augenstreich et al., 2017; Queval et al., 2017; Quigley et al., 2017). ***6** (Hersh et al., 1999; Steele-Mortimer et al., 1999; Jesenberger et al., 2000; Sano et al., 2007; Bujny et al., 2008; Mallo et al., 2008; Bakowski et al., 2010; Braun et al., 2010; McGourty et al., 2012; Chakraborty et al., 2015; D'Costa et al., 2015; LaRock et al., 2015; Li et al., 2016; Knuff et al., 2017). ***7** (Wozniak et al., 2008; Johnston et al., 2010; Nicola et al., 2011; Qin et al., 2011; Nicola et al., 2012; Chen et al., 2015; Davis et al., 2015; Smith et al., 2015; Bojarczuk et al., 2016; Gilbert et al., 2017).

Examples of intracellular microbes and their mechanisms for modulation of the endocytic pathway are summarised in **table 2.1**. In order to provide more detail on the variety and complexity of methods used, modulatory mechanisms of different microbes in the context of both phagosome maturation and expulsion are presented in the next sections.

2.3.1. Intracellular Survival Mechanisms

Due to the high incidence of tuberculosis in especially developing countries, much research has been focused on the causative agents of this illness. As a result, relatively detailed knowledge is available on the route of immune evasion by this pathogen in particular, as well as on how bacterially secreted effectors and cell wall components modulate phagosome maturation. The primary route of *Mycobacterium tuberculosis* (Mtb) into the body is through inhalation, where it reaches the lungs' alveolar space and is preferentially taken up by alveolar macrophages. Mtb survive intracellularly by working against PI3ks to prevent EEA1 docking. This is achieved in two ways: 1) Mtb secretes a PI 3'-phosphatase (SapM) that dephosphorylates PI3P and 2) a component in the microbial cell wall, lipoarabinomannan (LAM), interferes with recruitment/activation of the human PI3k (hVPS34) (Vergne et al., 2005). *Mycobacterium*-containing phagosomes also retain the tryptophan-aspartate containing coat (TACO) protein (normally expressed on the cytosolic leaflet of the plasma membrane and involved in intracellular membrane trafficking, cytokinesis and cytoskeletal remodelling) (Ferrari et al., 1999). TACO retention causes prolonged Rab5 expression - although some maturation effectors can still bind the phagosome, this effectuates a relative absence of PI3P, so that the FYVE domain-mediated binding of EEA1 is greatly perturbed (Simonsen et al., 1998) and lysosome fusion inhibited (Ferrari et al., 1999). Additionally, secretion of the soluble serine/threonine kinase Protein kinase G (PKG) by Mtb into the host cytosol is essential for prevention of phagosome-lysosome fusion (Walburger et al., 2004). Furthermore, a more alkaline and hydrolase deficient phagosome is also brought about in two ways. Firstly, hydrolysis is weakened by limited expression of Rab7. This GTPase has been shown to only transiently localise to mycobacterial phagosomes, preventing sufficient Rab7-interacting lysosomal protein (RILP) recruitment, but also limiting cathepsin D protease delivery (Seto et al., 2010, 2011). Secondly, acidification is regulated by Mtb by interfering with V-ATPase complex assembly and retention, thereby maintaining a

stable, slightly alkaline pH (6.2-6.5) (Sturgill-Koszycki et al., 1994; Seto et al., 2011; Queval et al., 2017). The Mtb phosphatase, PtpA, is involved in inhibition of complex assembly by binding to the subunit H of the V-ATPase where it then dephosphorylates and inactivates hVPS33B, effectively inhibiting the membrane fusion machinery (Wong et al., 2011).

In contrast to Mtb, the survival mechanisms of C. glabrata is largely dependent on active PI3ks. *C. glabrata* encodes the enzyme PI3k and produces fungal PI3P (Strahl et al., 2007; Rai et al., 2015). In this manner, the PI3P content of phagosomes increase prematurely during the early stages of maturation, where PI3P has not yet come into play. This could lead to a PI3P rich phagosome being identified as already partly matured, thus halting further maturation. Additionally, increased PI3P content could overburden PI3P degradation capacity of the phagosomal lumen. Deletion of the functional subunits of fungal PI3k led to ameliorated phagosome maturation and significantly reduced fungal survival and virulence (Rai et al., 2015). The differences between the strategy of *C. glabrata* vs. Mtb illustrates how the same cellular role players may be modulated in different ways for different outcomes, depending on the intended requirement of the modulating microbe, and in our opinion also demonstrates the susceptibility of this system to exogenous modulation or control.

Reminiscent of Mtb, *Leishmania* (the causative agent of Leishmaniasis) promastigotes are also harboured in phagosomes that retain TACO on their membranes, blocking lysosome fusion and ensuring a neutral pH in which this parasite can differentiate into the amastigote stage (Ferrari et al., 1999; Gogulamudi et al., 2015). However, after differentiation, the parasite allows phagosome fusion with lysosomes to achieve an acidic environment in which the amastigotes thrive. Interestingly, these phagosomes still exhibit low expression of late phagosomal markers (LAMP, V-ATPase and Rab7), after lysosome fusion (Vinet et al., 2009). In addition, Leishmania protects itself by inhibiting recruitment of NADPH oxidase to the phagosome, perturbing ROS production (Moradin et al., 2012). Similarly, *M. tuberculosis* was reported to stimulate release of TNF-α and IL-10 from infected macrophages (Sendide et al., 2005), resulting in a deactivation of ROS and RNS release (Redpath et al., 2001). IL-10 specifically down-regulates secretion of pro-inflammatory cytokines (Redpath et al., 2001) like INF-γ and TNF-α and results in a shift toward a Th2-type cell expansion in the alveoli (de Almeida et al., 2012), bringing about a shift towards an alternatively

activated, anti-inflammatory, M2 macrophage phenotype (Smith et al., 2008), which itself produces more IL-10, sustaining this phenotype and a relatively more anti-inflammatory environment. This implies that these microbes not only alter the response of the host cell to the ingested microbe itself, but that it may also affect systemic signalling by the host cell, which may affect the rate at which these bacteria are able to spread.

Brucella and *Legionella* are examples of intracellular pathogens that manipulate the endocytic pathway to create a niche in which they can replicate and thrive. They accomplish this by hijacking host proteins and membrane organelles to establish a bacterium-containing vacuole with morphological features reminiscent to that of host membrane compartments (Xu et al., 2013; Celli, 2015). Effectors secreted by *Brucella* within the *Brucella*-containing vacuole (BCV) manipulates maturation by altering interactions with late endosomes and lysosomes (Celli, 2015). During initial phagocytosis a large portion of *Brucella* cells are rapidly degraded (~90%), however surviving cells are capable of prolonged intracellular proliferation (von Bargen et al., 2012). Previously it was thought that *Brucella* evade fusion of BCVs with lysosomes by secretion of effectors via a functional VirB type IV secretion system (T4SS) and cyclic β-1-2-glucan (Pizarro-Cerdá et al., 1998; Celli et al., 2003; Arellano-Reynoso et al., 2005). Cyclic β-1-2-glucan was thought to prevent fusion of the BCV with lysosomes by modulating lipid raft organization on phagosome membranes but is not a requirement for subsequent BCV maturation (Arellano-Reynoso et al., 2005). Rather, live cell imaging has shown that the BCV interacts with lysosomes, thus fusion is not completely prevented (Starr et al., 2008). Early stages of BCV maturation involve the recruitment of late endosome markers, LAMP-1 and Rab7 to the BCV membrane, with acidification of the BCV being crucial for VirB expression (Boschiroli et al., 2002; Starr et al., 2008). This early BCV is also known as the endosomal BCV (eBCV) due to its interaction with the endocytic pathway. These findings highlight the importance of the initial interactions with the endocytic pathway in determining outcome. Unlike *Brucella*, *Legionella* diverts from the canonical endocytic pathway soon after being phagocytosed (Tilney et al., 2001). Departure from the canonical endocytic pathway starts minutes after being phagocytosed – the *Legionella*-containing vacuole (LCV) is covered with smooth vesicles, ER in origin, and mitochondria is recruited to the LCV (Tilney et al., 2001). The LCV is also devoid of early endosome markers such as Rab5

and LAMP-1, with the exception of Rab7 (Roy et al., 1998). *L. pneumophila* utilizes early mild caspase-3 activation to prevent lysosome fusion by cleavage of rabaptin5 (effector of Rab5) (Gao et al., 1999; Molmeret et al., 2004). The eBCV and LCV both eventually interact with components of the ER. In the case of the eBCV, LAMP-1 is progressively lost as the eBCV interacts with the ER and maturation proceeds to the formation of a replication-permissive BCV (rBCV) (Celli et al., 2003; Celli, 2006; Starr et al., 2008), with the rBCV subsequently converted from an intermediate vacuole into an ER-derived organelle which is ideal for bacterial proliferation (Celli et al., 2003). The smooth vesicles recruited to the LCV early on, eventually come to resemble rough ER and become studded with ribosomes (Gerhardt et al., 2000; Tilney et al., 2001). The specific recruitment of GTPases usually required for fusion of ER-derived vesicles with the Golgi apparatus aids in this process. Similar to *Brucella*, the hijacking of the host's secretory trafficking pathway results in a replication-permissive LCV. The rapid formation of an ER-like LCV and subversion of the endocytic pathway is dependent on the Dot/Icm T4BSS (Defective in Organelle Trafficking/Intra-Cellular Multiplication Type 4B Secretory System) of *Legionella* (Roy et al., 1998). Indeed, mutants deficient in the T4BSS ultimately fuse with the lysosome, indicating that effectors secreted by the T4BSS directly influence the endocytic pathway (Roy et al., 1998; Molmeret et al., 2004; Schroeder, 2018). The Dot/Icm T4BSS secretes hundreds of potential virulence effector molecules that aid in the formation of the LCV. However, no one effector has been shown to be crucial, again indicative of multiple layers of redundancy (Schroeder, 2018). Similarly, the VirB T4SS is essential for *Brucella* survival, as illustrated in virB– mutants (Hong et al., 2000; Comerci et al., 2001; Celli et al., 2003; Pei et al., 2008). Several other pathogens utilize T4SS and other secretion systems to release effector molecules that are capable of manipulating host function. The VirB and Dot/Icm systems are certainly also capable of releasing effector molecules that, in the case of *Brucella* and *Legionella*, are used to manipulate ER membrane dynamics and fusion.

Similar to some vacuole-inhabiting bacteria, *Chlamydia* also subverts the endocytic pathway to create a replicative niche. *Chlamydia* is also a very proficient modulator of the host cytoskeleton through complex interactions of its secreted effectors with the host cell. This manipulation is even more interesting when considering that *Chlamydia* has a relatively small genome for bacteria (1.04 Mb and 1.23 Mb for *C. trachomatis* and *C. pneumoniae* respectively) and relies on the host for their metabolic

requirements (Stephens et al., 1999). Furthermore, ~10% of its genome encodes for virulence effectors (Betts-Hampikian et al., 2010) which, as for some other intracellular pathogens, are delivered through specialized secretion systems. Similar to *Legionella*, the *Chlamydia*-containing inclusion (the term used for the replicative vacuole) is diverted from the endocytic pathway early on and is rather trafficked to the microtubule organizing centre (MTOC) via dynein-mediated movement. From here, they are in an ideal position to intercept lipids and nutrient-rich exocytic vesicles. Markers for early endocytic- and late endocytic-compartments are absent from the inclusion (such as Rab5, Rab7 and LAMP-1) (Rzomp et al., 2003; Scidmore et al., 2003). However, several other Rab GTPases are recruited to the inclusion, such as Rab1, -4, -6 (*C. trachomatis* only), -10 (*C. pneumoniae* only), -11 and -14 (Rzomp et al., 2003; Capmany et al., 2010). The recruitment of the different Rab GTPases is important for the modulation of fusion events, for example the prevention of lysosomal fusion and promoting of fusion with lipids and nutrient-rich exocytic vesicles. *Chlamydia* further modulate vesicle fusion via interaction with SNARE proteins.

Subversion of the canonical phagocytic pathway by *Salmonella* uses similar mechanisms to that of, both, the vacuole-residing bacteria and those opting for a cytosolic lifestyle. After internalization, *Salmonella* remains in a modified phagosome – the *Salmonella* containing vacuole (SCV). Similar to the microbes already mentioned, *Salmonella* utilize secretory systems to deliver their effectors to the host and have two T3SS encoded on different pathogenicity islands (SPI-1 and SPI-2) (LaRock et al., 2015). The early effectors secreted by *Salmonella* (via T3SS-SPI1) are important for the establishment of this early SCV. Shortly after being phagocytosed SCV associates with early endosome markers EEA-1 and Rab5 and via its effector SopB (a phosphatase), delays lysosome fusion by indirectly preventing Rab GTPases from binding to the phagosomal membrane (Steele-Mortimer et al., 1999; Mallo et al., 2008; Bakowski et al., 2010). Recruitment of sorting nexins (SNX) help in the progression of SCV maturation, SNX1 specifically induces tubulation and is involved in the removal of the cation-dependent mannose-6-phosphate receptor (MPR) that may be important for the lack of lysosomal enzymes in the late SCV (Bujny et al., 2008). Additionally, SNX3 transiently interacts with the early SCV and is required for tubule formation and recruitment of late endosomal markers Rab7 and LAMP-1 (Braun et al., 2010). The replacement of early markers at this stage is accompanied by a

decrease in both bacterial cytoplasmic and SCV pH (Chakraborty et al., 2015). This drop in pH is crucial for induction of SPI-2 genes required for subsequent effector secretion. The effectors secreted by T3SS-SPI-2 change the early SCV into a late SCV that is uniquely suited for bacterial replication. Examples of SPI-2 effectors involved in SCV maturation include SifA and SopD2. SifA complexes with SifA-and-Kinesin-Interacting-Protein (SKIP). The SifA-SKIP complex sequesters and binds Rab9, thereby inhibiting Rab9-dependent recruitment of MPR (McGourty et al., 2012). SopD2 impairs the Rab7-dependent recruitment of RILP and FYCO1 (FYVE and Coiled-coil domain Containing protein 1). RILP and FYCO1 are involved in vesicular trafficking along microtubules and indirect inhibition of their recruitment by SopD2 delays delivery of the SCV to lysosomes (D'Costa et al., 2015). At this stage, the SCV is similar to a late endosome (with markers LAMP-1, Rab7 and V-ATPase), but not enriched with lysosomal enzymes, possibly due to the lack of MPR and incomplete lysosome fusion (McGourty et al., 2012). Similar to *Chlamydia*, *Salmonella* exploit dynein-mediated transport (via its effectors) to arrive at a juxtanuclear position near the microtubule organizing centre (MTOC). At this location, *Salmonella* distinguishes itself from other intracellular pathogens with the formation of a dynamic tubular network composed of *Salmonella* induced filaments (SIFs) (Knuff et al., 2017). SIFs are required for SCV integrity, enabling continuous fusion of host vesicles to SCV and are associated with late endosomal markers such as LAMPs, Rab7, V-ATPase, cholesterol and lysobisphosphatidic acid (LBPA), as well as low levels of MPR and cathepsin D. Furthermore, another similarity with other vacuole-living bacteria, is the communication between the SCV and the ER, illustrating the extensive interactions of SIFs/SCV with the host cell (Santos et al., 2015). However, unlike the other vacuolar bacteria's interaction with ER-derived components, the *Salmonella* SCV interaction with the ER-derived coat protein complex II (COPII) can result in SCV rupture and *Salmonella* hyper-replication in the cytosol (Santos et al., 2015).

In comparison to the more meticulous modulations mentioned, *L. monocytogenes* takes a relatively more radical (and perhaps destructive) approach to ensure intracellular survival. Manipulation of the clathrin-mediated endocytic pathway facilitates entry into non-phagocytic cells (Veiga et al., 2005), whereas entry into macrophages is achieved via phagocytosis and initial engulfment of bacteria to form phagosomes. However, with the help of the cholesterol-dependent pore forming toxin

listeriolysin-O (LLO), phagosome-lysosome fusion is disrupted via dysregulation of pH and calcium gradients across the phagosome membrane (Henry et al., 2006; Shaughnessy et al., 2006). Additionally, with the help of two phospholipases (PlcA and PlcB), LLO promotes escape of the bacteria from phagosomes into the cytosol (Smith et al., 1995; Mitchell et al., 2015). Once in the cytosol, bacteria undergo rapid growth and subsequently hijack the host's actin polymerisation machinery to move within the cytosol and ultimately spread in a cell-to-cell manner (Skoble et al., 2000; Mitchell et al., 2015). Although not as intricate as *Brucella* and *Legionella*, *Listeria* is also capable of slow replication in macrophage vacuoles (instead of rapid cytosol replication) via the formation of spacious *Listeria*-containing phagosomes (SLAPs) (Birmingham et al., 2008). SLAP formation is dependent on LLO, but unlike phagosome rupture observed with cytosolic life, intermediate LLO expression is required for interference with phagosomal pH, without phagosomal rupture. Bacteria containing SLAPs are LAMP-1+, which indicates that these are endocytic compartments. However, no drop in pH is observed, due to LLO-mediated uncoupling of pH gradients across the membrane and prevention of lysosome fusion. Furthermore, SLAP formation is dependent on autophagy and is hypothesized to be triggered by the damage caused to phagosomes by LLO.

The opportunistic pathogen *Cryptococcus neoformans* (Cn) is also capable of infecting and replicating at high numbers in macrophages and may possibly utilize these phagocytes as shuttle for their dissemination across the blood brain barrier. An important virulence factor of Cn is its capsule, which ensures survival by protecting against phagocytic uptake and oxidative stress, once infiltrated into the host circulation (Zaragoza et al., 2008; Bojarczuk et al., 2016). However, phagocytosis can be triggered by direct recognition of Cn capsule components or indirectly via complement (Johnston et al., 2013). After Cn internalisation by macrophages, it resides in phagosomes which mature into a phagolysosome, as usual. Interestingly, this microbe does not seem to radically modulate the phagosomal maturation process, but rather seems able to thrive at the lower pH of the maturing phagosome. Some early- and late-endosomal markers are present on these phagosomes, including EEA-1, Rab5, Rab11, MPR, LAMP-1 and cathepsins, with live Cn inducing premature removal of Rab5 and Rab11 from the Cn phagosome, which may influence phagosome acidification (Tucker et al., 2002; Davis et al., 2015; Smith et al., 2015). The

phagolysosomes still acidify, but final pH is maintained slightly higher, at around 5.3 (vs. normal phagolysosome pH of ~4.5), which is the optimal pH for Cn growth. Additionally, damage to the phagolysosome membrane favours Cn survival and possibly contributes to the slight increase in pH observed with live Cn (Davis et al., 2015). Recently urease activity was found to influence phagosomal pH, which through production of urease-derived ammonia can increases pH (Lerm et al., 2017; Fu et al., 2018). Furthermore, membrane damage to the phagolysosome results in permeabilization of the membrane and subsequent leakage of lysosomal enzymes (e.g. cathepsins), the loss of which may also increase survival of Cn within the phagolysosome (Wozniak et al., 2008). Furthermore, the release of these enzymes, can result in activation of inflammasomes and subsequent cell death (Chen et al., 2015). It is clear that Cn is capable of modulating phagosome maturation to some extent, but the search for responsible effectors is still ongoing.

These studies illustrate how some pathogens manipulate the phagocytic process in seemingly divergent ways to reach an identical end goal of intracellular survival. In doing so they ensure their own propagation and dissemination to elicit disease. Importantly, in our opinion, this demonstrated susceptibility to manipulation of the phagocytic process supports the feasibility of drug delivery systems that harness one or more of the microbial strategies presented here. Although there is still much research to be done on the exact microbial effectors involved in manipulation of the endocytic pathway, the available literature can already be used to make informed decisions as to which effectors can be used in the development of autologous drug delivery systems.

In the context of a complete macrophage-based drug delivery system, the manipulation of the endocytic pathway for retention and protection of cargo is only the first step. The next step to consider in the development of an effective delivery system, is the expulsion of drug cargo from macrophage vehicles. To this end, the mechanisms used by microbes can again be mined and possibly exploited to achieve cargo expulsion.

2.3.2. Expulsion from Host Cell

Turning attention now to the expulsion phase, which is a vital requirement for pathogenic dissemination of microorganisms, and which can be induced by either the

infected host cell, or by the pathogen itself. Some microorganisms utilise host cell machinery to facilitate their escape, while others induce either accidental or intended host cell death, resulting in their release from the cell as a "side-effect". Many microorganisms have been identified to have the ability to egress via one or more methods and some effectors in this process have been identified. However, in terms of manipulation of egress through upregulation or elimination of these effectors, very little data is available and substantial experimental work is still required in this niche. This can be attributed, at least in part, to a large degree of redundancy. This degree of redundancy is also seen in the bacterial mechanisms employed to modulate phagosome maturation, which adds complexity to the process of identifying a controllable pathway. Below, we provide a summary of the current knowledge regarding microbial egress, with an integrated discussion of its potential for therapeutic application.

Probably the most obvious technique used, given the ability of many microbes to manipulate phagosomal pH for intracellular survival, is the manipulation of pH to induce host cell death. This technique has been described in some detail for Mtb, which stabilises phagosomal pH at ~6.2-6.5 by interfering with the V-ATPase complex (Sturgill-Koszycki et al., 1994; Seto et al., 2011; Queval et al., 2017). This raised pH level is a pre-requisite for the ESX-1 dependent rupture of the phagosome (Simeone et al., 2015). The ESX-1 (T7SS) secretory system secretes two effector proteins, namely EsxA and EsxB, which form a heterodimer and are secreted by Mtb in a co-dependent manner (Renshaw et al., 2002). EsxA has membrane permeabilizing properties and EsxB is thought to act as a chaperone to prevent degradation and/or premature lytic activity (de Jonge et al., 2007; Zhang et al., 2016). EsxA effects phagosome rupture and escape to the cytosol, while being aided by the cell wall lipid phthiocerol dimycocerosates (PDIM) (Augenstreich et al., 2017; Quigley et al., 2017). This lipid has been proposed to primarily aid in phagosomal rupture, resulting in increased numbers of cytosolic bacteria – which in turn induces host cell necrosis and ultimately Mtb dissemination (Augenstreich et al., 2017; Quigley et al., 2017).

Other bacteria have also been described to escape through host cell membrane rupture resulting in cell death, albeit achieved by slightly different techniques. *Brucella* for example replicates within host cells, dissociating into two phenotypes, namely a smooth and a rough type. The rough phenotype has cytotoxic activity which breaks

down the cellular membrane and is essential for bacterial dissemination (Pei et al., 2006, 2014). In this way, *Brucella* egress and dissemination are achieved through caspase-2 mediated cell death (Chen et al., 2009, 2011). Furthermore, this mode of cell death results in a pro-inflammatory response and recruitment of additional macrophages - that can be infected - in further aid of *Brucella* dissemination (Pei et al., 2014). It has however been proposed that *Brucella* can disseminate via cell-to-cell spread using an autophagy related mechanism (Starr et al., 2012; Smith et al., 2016). The final phase of *Brucellas'* intracellular life cycle is the formation of an aBCV which results from the engulfment of rBCVs into autophagosome-like structures via an autophagic process (Starr et al., 2008, 2012). This transformation to an aBCV is an essential prerequisite for bacterial egress via cell-to-cell spread (Starr et al., 2012; Smith et al., 2016). Interestingly, the VirB T4SS has been implicated in *Brucella* release via cell death and cell-to-cell spread, although the bacterial effectors have not been identified (Pei et al., 2008; Smith et al., 2016). The different modes of dissemination are possibly due to differences in experimental conditions, such as bacterial strains and cell lines used. Different bacterial strains may have different effectors or altered expression profiles that may result in different post-replicative outcomes (i.e. cell death or cell-to-cell spread) and different cell lines will also react differently to secreted effectors.

Legionella can also be placed in the category of intracellular pathogens that escape through macrophage cell death. Once a replicative LCV is established inside the macrophage, the bacteria converts to a replicative form and multiplies within the enclosed LCV. At high multiplicities of infection and subsequent termination of replication *Legionella* exhibit contact-dependent cytotoxicity, resulting in formation of pores in the host cell membranes (Kirby et al., 1998; Bachman et al., 2001). Initially pores are formed within the phagosomal membrane (of the LCV), resulting in release of bacteria into the cytosol. The cytosolic bacteria are then able to form pores within the plasma membrane, resulting in osmotic lysis and release of bacteria (i.e. necrosis) (Kirby et al., 1998; Alli et al., 2000). The importance of the Dot/Icm secretory system of *Legionella* for pore-formation mediated lysis, and specifically that of the small inner membrane protein, IcmT, has been illustrated (Molmeret, 2002). Interestingly, in primary protozoan host cells, *Legionella* is capable of non-lytic release. The bacterial effectors LepA and LepB have been shown to play a role in manipulating the amoeba

hosts exocytic pathway for dissemination (Chen et al., 2004, 2007). These effectors may also play a role in *Legionella* release from human cells or phagosome maturation and can potentially form part of an artificial microbe drug delivery system.

Literature indicates that *Salmonella* exits cells via several mechanisms, including programmed cell death and flagella-facilitated escape. For example, the SPI-1 effector SipB can act by inducing caspase-1-dependent pyroptosis in macrophages (Hersh et al., 1999; Li et al., 2016). Briefly, SipB binds to and activates caspase 1, resulting in the cleavage of pro-IL1β and its secretion (Hersh et al., 1999; Li et al., 2016). While this inflammatory response should result in elimination of *Salmonella*, the over-activation during infection results in release of large amounts of bacteria capable of infecting naïve recruited cells. SipB is also able to induce apoptosis in a caspase-1 independent manner involving activation of caspase-2, -3, -6, and -8 (Jesenberger et al., 2000). In addition to apoptosis and pyroptosis, *Salmonella* is also able to induce oncosis in macrophages (Sano et al., 2007). Oncosis is associated with macrophage swelling resulting in cell death, with *Salmonella*-induced oncosis characterized by F-actin dissociation. Subsequently the flagellated *Salmonella* escapes from oncotic macrophages via flagellar movement (Sano et al., 2007).

Although the methods presented here will effectively release intracellular cargo, the associated host cell death may significantly contribute to tissue damage and secondary inflammatory damage, which may further delay recovery of patients. While certainly an option to consider for further development, specifically where cell death and increased inflammation would not be as detrimental (e.g. cancerous tissue), a more optimal solution in scenarios where minimisation of inflammation – as well as the availability of functional macrophages - might be more critical, would be achieving release of drugs without the sacrifice of host cells.

Manipulation of the host cell's expulsion mechanics without killing the host has indeed been described for a few microbes, although much less information is available in this context. From the literature, it seems that only two egress methods have been described: direct spread into neighbouring cells and expulsion into the extracellular environment. As briefly eluded to earlier, *L. monocytogenes* escapes from the host phagosome into the cytosol through activity of pore forming LLO (Alberti-Segui et al., 2007). However, complete escape from the host macrophage is aided by the effector

responsible for modulation of the host actin polymerisation machinery. Surface anchored actin assembly-inducing protein (ActA) interacts with the ARP2/3 complex to mediate actin polymerisation on the bacterial surface, which in turn creates sufficient force to induce membrane protrusion and cell-to-cell spread (Skoble et al., 2000). The actin-propelled bacteria creating these membrane protrusions induce uptake into neighbouring cells via a process called efferocytosis (Czuczman et al., 2014). Here, LLO damages the plasma membrane of protrusions, resulting in surface presentation of the inner membrane leaflet lipid, phosphatidylserine (PS) (Czuczman et al., 2014). The PS+ protrusions are recognised by the T cell immunoglobulin and mucin-domain containing protein 4 (TIM-4) on macrophages, which subsequently mediates the uptake of PS+ protrusions (Czuczman et al., 2014). The bacteria may also be present in PS+ vesicles, formed as a result of Ca2+ dependent membrane repair and scission of the initial PS+ protrusion (Czuczman et al., 2014). Both PS+ vesicles and protrusions are similarly taken up by neighbouring cells via TIM-4. *Listeria* are one of the few phagocytically internalised microorganisms that allow host cell survival after escape. Thus, the processes regarding expulsion of *Listeria* is of great interest as target for manipulation or adoption in therapeutic drug delivery systems.

Chlamydia is also known to exit the host cell by extrusion, although it can also induce cell lysis (Hybiske et al., 2007). These methods exhibit almost identical prevalence but are markedly distinct and independent. The exact bacterial trigger facilitating either one or the other outcome has yet to be fully elucidated. Cell lysis is known to be protease and calcium dependant and entails perforation of the inclusion body (*Chlamydia*-containing vacuole) and plasma membrane (Hybiske et al., 2007). *Chlamydia*-infected host cell lysis has been suggested to be linked to microbe-associated apoptotic cell death, although minimal direct evidence exists in support of this notion (Perfettini et al., 2003). Regardless, the extrusion capability of *Chlamydia* from host cells without cell lysis is of greater interest here. With this technique, inclusion body extrusion requires actin polymerisation, myosin II, RhoA and Neuronal Wiskott-Aldrich Syndrome Protein (N-WASP) (Hybiske et al., 2007). The formation of an actin coat around the inclusion is correlated to extrusion out of the host cell. Host- and bacterium-derived factors play a role in the formation of the actin coat. For example, in humans, host-derived septins (GTP-binding proteins) form structures around the inclusion and co-localize with F-actin, resulting in the formation of F-actin

fibres around the inclusion (Chin et al., 2012; Volceanov et al., 2014). This process facilitates normal extrusion of *Chlamydia* inclusions from host cells (Volceanov et al., 2014). Actin stabilisation by jasplakinolide (actin polymerisation agent) alone was reported to induce extrusion, which substantiates the role of septins in extrusion (Hybiske et al., 2007). In terms of therapeutic application, this may suggest that the intervention achieved by *Chlamydia* on the host cell mechanics may be less detrimental to the host cell compared to other microbial exit strategies. In a therapeutic context, this may result in faster normalisation of function in the host cell, which is much desired, as these host cells may then be able to participate in the normal inflammatory process that would be required for clean up after the drug has fulfilled its function.

Non-lytic release into the extracellular space has also been observed for *Cryptococcus neoformans*, albeit at low frequencies of 5-15% in vivo (Bojarczuk et al., 2016). Autophagy has been implicated in Cn intracellular lifestyle with components such as Atg-2a, -5, -9a, -12 and LC3 observed in close proximity to the Cn containing phagosome (Qin et al., 2011; Nicola et al., 2012). The effect of autophagy is dependent on opsonin, macrophage type and activation state (Nicola et al., 2012). Autophagy does seem to play a role in host defence against Cn, with disruptions in autophagy affecting host fungistatic activity and fungal growth (Qin et al., 2011; Nicola et al., 2012). However, this is a double-edged sword with autophagy also seemingly playing a role in Cn release. This is evident by the observation of Atg-5-knockout clones of J774.16 and RAW264.7 cells having reduced incidence of non-lytic exocytosis events (Qin et al., 2011; Nicola et al., 2012). This, along with the observation of LC3 surrounded cells outside macrophages, suggests a possible role of autophagy in non-lytic release of Cn (Nicola et al., 2012). Therefore, while autophagy aids in the host defence against Cn, it also participates in the dissemination of Cn through non-lytic release. This eludes to a balance that must be maintained by the host regarding autophagy, with either decreased fungistatic activity combined with decreased non-lytic release, or vice versa. In addition to the potential role of autophagy in the non-lytic release of Cn, other factors can also play a role in this route of Cn dissemination. The increase in pH of the Cn-containing phagosome results in increased occurrence of non-lytic release. Artificially increasing phagosomal pH results in increased expulsion of Cn and when compared to the in vivo situation, the damage caused by

Cn to the phagosome could result in a similar pH increase (Nicola et al., 2011). Unfortunately, the Cn effectors responsible for non-lytic release have not yet been elucidated. However, in addition to the potential role of autophagy, the MAP extracellular receptor kinase 5 (ERK5) of host cells is implicated in the regulation of non-lytic release, with its inhibition resulting in increased release rates (Gilbert et al., 2017). Furthermore, actin polymerisation also plays a role in release of Cn from the host (Johnston et al., 2010). In contrast to other pathogens such as *Listeria* and *Chlamydia*, actin polymerisation inhibits Cn release through actin flashes on the Cn containing phagosome (Johnston et al., 2010). Although some information regarding the non-lytic release of Cn is available, it remains poorly understood and the exact mechanism for this escape method is still elusive.

The body of research investigating intracellular pathogens and their host-interacting mechanisms is significant. However, specific information on the microbial effectors is still largely lacking, probably owing to the fact that the main focus of research was the prevention of these microbial actions, rather than full elucidation thereof for implementation. In addition, effectors secreted by invading microbial forces exhibit a large degree of built in redundancy, so that it is not surprising that the task of identifying specific roles for specific effectors has remained largely unaccomplished. Specifically, in terms of microbial expulsion, information is largely lacking, with only a handful of known microbial effectors. Considering this, clearly a new approach is required. The recent advancements in gene editing, heterologous expression, live cell imaging and -omics technologies may provide a more powerful platform from which to investigate the complex host-pathogen interaction and the effectors involved, especially in the context of expulsion from immune cell hosts.

2.4. The Impossible Made Possible?

From our review of the literature, we propose that most of the limitations of current drug delivery systems can be overcome by harnessing microbial strategies. We hypothesize that the synthetic microbe drug delivery system we describe here would a) address poor drug-delivery to target tissue – especially at sites with low blood supply – b) increase treatment efficacy with lower treatment doses and thereby c) reduce adverse host reactions. A visual representation of the proposed system is provided in **Figure 2.2**.

In terms of the system we propose, we foresee two novel preparatory steps to be done in parallel. Firstly, monocytes should be isolated from peripheral blood collected from individuals with a requirement for drug delivery, to enable autologous re-infusion. These macrophages can then be propagated in culture, differentiating and polarizing them into M1 phenotype macrophages, as previously described (Mia et al., 2014), to achieve the phenotype known to be most capable of translocating out of circulation and into tissue (Arnold et al., 2007 a; Africa et al., 2015 a; b). In order to prevent intracellular degradation, polarized macrophages can be treated to achieve transient phagosome maturation arrest, by in vitro exposure to arresting agents such as Wortmannin, Concanamycin A and Chloroquine, which we have previously successfully illustrated (Visser et al., 2018). The fact that phagosome maturation arrest is achieved by in vitro intervention is a strength of this model, as this eliminates patient exposure to these potentially harsh chemicals and their related adverse effects. Secondly, the drug should be packaged in multiple layers of nanoparticle coatings (**Figure 2.2A**). These layers will serve to protect the drug from degradation, and can be peeled away in sequential, controlled steps to achieve controlled expulsion and release of the drug after delivery at its required site. With advancements in polymer sciences, smart polymers can be designed that have effectors conjugated to the polymers and can also be developed for directed multiphasic release of effectors at certain checkpoints. (The nature of the different layers will be clarified in the discussion of the expulsion phase and illustrated in **Figure 2.2**).

To construct the synthetic microbe drug delivery system, phagosome maturation arrested macrophages will engulf opsonized nanoparticle-enclosed drugs (the synthetic microbe) and form a phagosome containing this cargo (**Figure 2.2**). The number of synthetic microbes taken up per macrophage may be optimized by adjusting macrophage-microbe exposure time. Uptake is largely dependent on particle proximity to the macrophage as well as size and shape of particles (Beningo et al., 2002; Champion et al., 2006; Underhill et al., 2012). Determining the exact onset of engulfment, following introduction of particles into cell media, is complex and may need optimization on a case-specific basis. Unpublished data from our group suggests initiation of engulfment to occur within 5 min, with particles included at a 1:4 ratio with cells. From the literature, the last stage of phagosome maturation (phagolysosome biogenesis) occurs around 1h after engulfment (Jahraus et al., 1998). Our

implementation of an arbitrary exposure time of one hour resulted in significant 4.5µm particle engulfment (>1 particle per cell, in ~70% of cells) by both arrested and untreated macrophages. Since macrophages are capable of repeated engulfment cycles (irrespective of arrest), carrier cells should be removed from drug-containing media and washed after the appropriate engulfment period, to prevent overloading of macrophages and potentially compromising their ability to traverse endothelial barriers, as well as eventual cell death (if particle load exceeds cytosol volume or steric hindrance causes membrane rupture during transmigration) (Champion et al., 2006; Visser et al., 2018). At this point, the drug-loaded macrophages are ready for autologous re-administration into the patient via infusion into the peripheral circulation (**Figure 2.2B**).

As stated earlier, macrophage migration to sites for delivery will rely on the inherent macrophage capacity for chemotactic mobility. However, in vivo testing of the system will elucidate whether further optimization is required. Upon arrival at the site for delivery, controlled expulsion of the cargo and subsequent release of the drug will be achieved through multiple consequential steps. Specifically, the phagosome lysing and membrane escaping agents (i.e. microbial effectors) would be released upon arrival at target location. This can only be achieved after transient phagosome maturation has expired and phagolysosomal degradation agents activate this layer. This biphasic layer would, in turn, allow escape of cargo into the cytosol, as well as expulsion thereof into the extracellular environment through microbial effectors. The substantial amount of genome data currently available should enable relatively comprehensive genomic data mining for novel and existing microbial effectors. The use of genome mining in this context will only be useful if information (e.g. homology regions, structural information) about effectors are available. The use of techniques such as proteomics along with bioinformatic mining/analysis has been suggested as more useful tools in combination to identify effectors (Na et al., 2015; Cheng et al., 2017). For example, in recent studies, proteomics has been used to identify novel effectors in *Salmonella*. Although proteomics can be a useful tool in identification of effectors it is only the first step. Next would be to heterologously express the identified effectors. Several bacterial effectors have been expressed in heterologous systems with success (Skoble et al., 2000; Churchill et al., 2005; Weigele et al., 2017). Most notably, the *Listeria* effectors LLO and ActA have been recombinantly expressed, with

recombinant LLO also being used for the effective delivery of several compounds to the cytosol of cells (Lee et al., 1996; Skoble et al., 2000; Mandal et al., 2002; Provoda et al., 2003; Stier et al., 2005). The ability to identify and express possible effectors creates the opportunity to manipulate the host endocytic pathway. However, these effectors need to be protected from degradation and secreted in a sequential manner to effectively modulate host processes.

In order to prevent asynchrony of final drug release and arrival of synthetic microbe at the target site (i.e. release of drug at inappropriate sites), an innocuous, bio-compatible layer, such as PNIPAAm (mentioned above), could be incorporated. This layer would be the inner most layer and protect the drug until controlled drug dissemination at the required site is achieved via external stimulus (e.g. temperature or ultrasound). In the case of a PNIPAAm layer, final drug dissemination can be achieved by temperature increase (Feng et al., 2014). In addition, microbubbles could also be incorporated as protective drug micelle, instead of PNIPAAm. These microbubbles would then be degraded by external ultrasound stimulation (Huang et al., 2015; Lv et al., 2016; Fan et al., 2018). This layer should ideally consist of non-biodegradable but bio-compatible constituents, to prevent drug release into circulation and exposure to off-target tissue. Furthermore, augmented host protection can be achieved by allowing the safe extrusion of intact drug-micelles through the urinary tract.

The redundancy employed in the aforementioned approach is another characteristic we could adopt from the plethora of redundancy employed by microbes during immune evasion, in order to maximize control over drug delivery and minimize risk of undesired effects.

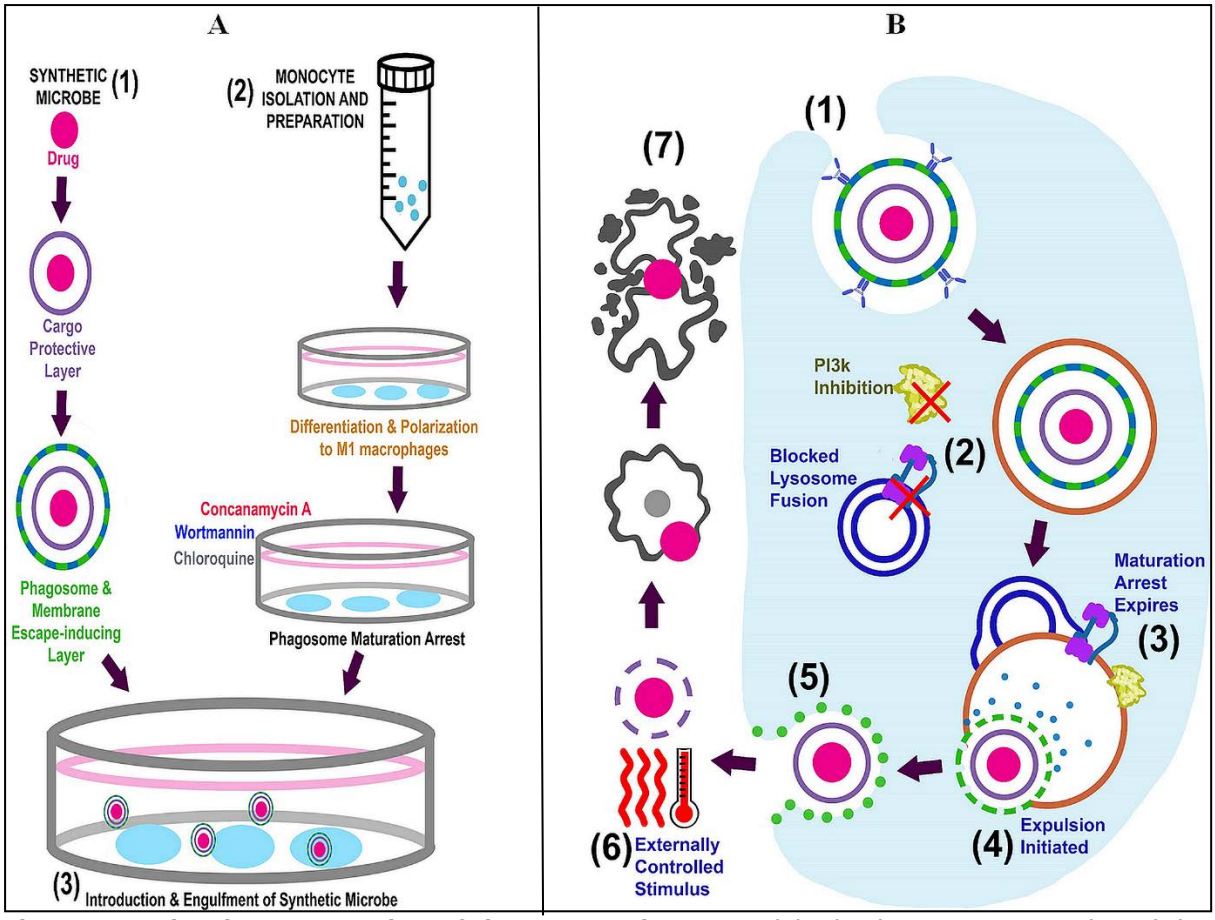

Figure 2.2: Visual representation of the proposed system. (A) Simultaneous preparation of the synthetic microbes (1) and autologous macrophages (2) are followed by introduction of the synthetic microbe into phagosome maturation arrested macrophages (3). The complete system can now be administered into circulation for in vivo delivery. (B) Intracellular events for in vitro engulfment of synthetic microbe (3), in vivo maintenance/expulsion (4–7) and final delivery of drug at target site (8–9).

2.5. Post-Delivery Clearance of the System

Given the potential complication of polymer accumulation in vivo, or premature drug release, it is perhaps relevant to briefly discuss safety aspects of this system. The utilization of M1 macrophages would be advantageous as they would remain at target locations post-delivery and could potentially contribute to faster resolution of either primary inflammation (present due to the disease state) or secondary inflammation (required to clear bacterial debris after effective treatment). In support of this theory, the M1/M2 phenotype presents with some plasticity as tissue resident macrophages have been shown to change phenotype following appropriate effector exposure or systemic infection and activation by pathogens (Arnold et al., 2007 a; Mills, 2012). This low risk feature is the result of the non-lytic mechanisms employed to achieve expulsion, which is novel.

In terms of clearance of the components of the nanoparticle layers themselves, polymeric nanoparticles have demonstrated clearance rates of hours to several days (Alexis et al., 2008; Feng et al., 2014). Macrophages failing to reach their intended target sites may still release the encapsulated drug, but final dissemination of drugs at unintended sites is unlikely, due to the requirement for external stimulus. Thus, encapsulated drugs, polymeric debris and loaded macrophages should be efficiently cleared from the system, so that no long-term implications due to residual drugs or synthetic microbe components are expected.

Clearly, a model proposing quite significant paradigm shifts, such as the one we described here, requires substantial in vitro and in vivo testing and optimization by multiple laboratories. Given the requirement for in vivo tracking of cells, a zebrafish model may be the ideal choice for pilot studies, as the basic anatomy of the fish facilitates leukocyte migration tracking (Langenau et al., 2004) and this model has been employed in the context of macrophage migration (Wang et al., 2016; Barros-Becker et al., 2017). Additionally, in vivo tracking can also be achieved by permanent intracellular cell labeling and/or lasing techniques (Schubert et al., 2015) that would elucidate the exact location of carrier macrophages as well as their cargo over an extended period.

2.6. Conclusion

Intracellular pathogens have developed a unique arsenal of tools to evade the immune system and thrive within host cells. The modulation of host processes, specifically modulation of the endocytic pathway, not only make these pathogens difficult to treat and dangerous, but also provides the opportunity to utilize and modify their methods for human gain. If the right combination of these effectors are repurposed, they can be used to develop a macrophage-based delivery system for the transport and controlled delivery of therapeutic agents packaged into a “synthetic microbe” as described here, to significant benefit of patients currently struggling with diseases at non-accessible sites or those caused by multi-drug resistant pathogens.

The success of a host-derived or biological delivery system is dependent on a key understanding of how microbial effectors work and what combination would result in effective release without severe side-effects, keeping in mind that the effectors are

indeed potent virulence factors. Advancements in molecular biology, -omics, bioinformatics and live cell imaging have resulted in the identification of effectors and their roles in the host-microbe/pathogen interaction, using and building on this information, effectors can be chosen that would result in the desired outcome. Utilizing synthetic biology and heterologous expression, effectors can be produced and tailored for specific functions. Although some developmental steps for the proposed synthetic microbe drug delivery model remains to be addressed in more detail, we believe that rapid development in e.g. polymer design and the aforementioned advancements in techniques that are used to characterize and tailor effectors, can be used to overcome these limitations in the very near future.

2.7. Hypothesis

We hypothesize that it is possible to employ microbial effectors - *Listeria monocytogenes* effectors LLO and ActA - to induce cargo expulsion from human carrier cells (primary M1 polarised macrophages) in the absence of infection, in a manner that would not result in lysis of carrier cells. Secondly, we hypothesise that it is possible to synthesise LLO and ActA in significant amounts using an *E.coli* heterologous GFP-linked protein expression system.

2.8. Aims and Objectives

In order to test our hypothesis, we formulated the following aims and objectives:

Aims:

1. Developing an expression system to synthesise microbial effectors
2. Using these effectors to induce expulsion from carrier cells

Objectives:

1. Synthesis of sufficient amounts of the chosen microbial effectors LLO and ActA
2. Determining appropriate activity of synthesised effectors *in vitro*
3. Determining expulsion of effector coated beads from carrier macrophages

Chapter 3: Methods

3.1. Plasmid Design

The *Listeria monocytogenes* effectors LLO and ActA, were translationally fused to green fluorescent protein (GFP) and expressed in *Escherichia coli.* Generation of a backbone plasmid containing *mgfp5* (GFP gene) including an N-terminal 6x polyhistidine-tag (His tag) and C-terminal WELQut protease site was done according to previous reports (van Staden et al., 2019) (**Figure 3.1, 3.2**). Briefly, the *mgfp5* gene was amplified from the pTRKH3-ermGFP using the primers listed in **Table 3.1** and purified using the pJET PCR purification kit according to the manufacturer's instructions (Thermo Fisher Scientific). The PCR product and pRSFDuet-1 were digested with the restriction enzymes BamHI/PstI. The digestion products were electrophoretically separated on an agarose gel and bands corresponding to the corrected sizes were excised and purified from the gel pieces using the ZymoClean gel DNA recovery kit according the manufacturer's instructions (Zymo Research). The purified digestion products were ligated using T4 ligase according to the manufacturer's instructions (New England Biolabs). The resulting pRSFGFP was used to transform chemically competent *E. coli* BL21 (DE3) cells. For transformation, the ligated plasmid DNA (pDNA) was added to competent cells (thawed on ice) and incubated, on ice, for 5 minutes. Cells were subsequently heat shocked at 37°C for 10 min, after which warm (37˚C) Luria Bertani (LB) broth was added to a total volume of 1 mL. Cells were recovered at 37°C for 1 hour and plated onto LB agar containing 50 µg/mL kanamycin. Plates were incubated at 37°C until visible colonies were observed. Colonies were selected and used to inoculate 5 mL of LB broth and incubated with agitation at 37°C for 18 hours. Plasmid DNA was isolated from these cells using the Pure Yield plasmid isolation kit according to the manufacturer's instructions (Promega). Listeriolysin-O was amplified from *L. monocytogenes* EDG-e genomic DNA (gDNA, isolated using the Zymogen fungal/bacterial gDNA Miniprep kit) using the primers listed in **Table 3.1**, with the forward primer designed to exclude the N-terminal signal peptide (**Figure 3.1**). Digested (PstI/NotI) and purified LLO was cloned into pRSF-GFP on a PstI/NotI fragment using T4 ligase, resulting in the translational fusion of LLO to His tagged GFP (**Table 3.1**) The resulting pRSFGFP-LLO construct was transformed into chemically competent *E. coli* BL21 cells as described elsewhere.

Plasmid DNA was isolated from positive transformants and used in sequencing reactions (CAF Stellenbosch). Correct transformants were used in subsequent expression experiments.

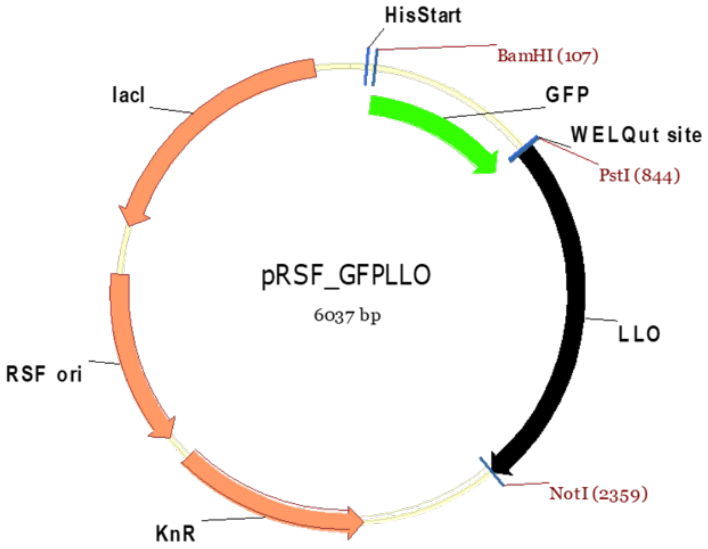


```
                                                                                                                                M  G  S  S  H  H  H  H  H  H
1       GGGGAATTGT GAGCGGATAA CAATTCCCCT GTAGAAATAA TTTTGTTTAA CTTTAATAAG GAGATATACC ATGGGCAGCA GCCATCACCA TCATCACCAC
        CCCCTTAACA CTCGCCTATT GTTAAGGGGA CATCTTTATT AAAACAAATT GAAATTATTC CTCTATATGG TACCCGTCGT CGGTAGTGGT AGTAGTGGTG
         S  Q  D  P  M  S  K  G  E  E  L  F  T  G  V  V  P  I  L  V  E  L  D  G  D  V  N  G  Y  K  X  X  X  X
101     AGCCAGGATC CGATGAGTAA AGGAGAAGAA CTTTTCACTG GAGTTGTCCC AATTCTTGTT GAATTAGATG GTGATGTTAA TGGGTACAAA
        TCGGTCCTAG GCTACTCATT TCCTCTTCTT GAAAAGTGAC CTCAACAGGG TTAAGAACAA CTTAATCTAC CACTACAATT ACCCATGTTT
                                      PstI
                                      ~~~~~~~
           H  G  M  D  E  L  Y  K  T  G  W  E  L  Q  A  S  A  F  N  K  E  N  S  I  S  S  M  A  P  P  A  S  P
801     CACATGGCAT GGATGAACTA TACAAAACCG GTTGGGAACT GCAGGCATCT GCATTCAATA AAGAAAATTC AATTTCATCC ATGGCACCAC CAGCATCTCC
        GTGTACCGTA CCTACTTGAT ATGTTTTGGC CAACCCTTGA CGTCCGTAGA CGTAAGTTAT TTCTTTTAAG TTAAAGTAGG TACCGTGGTG GTCGTAGAGG
         P  A  S  P  K  T  P  I  E  K  K  H  A  D  E  I  D  K  Y  I  Q  G  L  D  Y  N  K  N  N  V  X  X  X  X
901     GCCTGCAAGT CCTAAGACGC CAATCGAAAA GAAACACGCG GATGAAATCG ATAAGTATAT ACAAGGATTG GATTACAATA AAAACAATGTA
        CGGACGTTCA GGATTCTGCG GTTAGCTTTT CTTTGTGCGC CTACTTTAGC TATTCATATA TGTTCCTAAC CTAATGTTAT TTTTGTTACAT

         V  Y  A  K  E  C  T  G  L  A  W  E  W  W  R  T  V  I  D  D  R  N  L  P  L  V  K  N  R  N  I  S  I  W
2201    GTTTACGCTA AAGAATGCAC TGGTTTAGCT TGGGAATGGT GGAGAACGGT AATTGATGAC CGGAACTTAC CACTTGTGAA AAATAGAAAT ATCTCCATCT
        CAAATGCGAT TTCTTACGTG ACCAAATCGA ACCCTTACCA CCTCTTGCCA TTAACTACTG GCCTTGAATG GTGAACACTT TTTATCTTTA TAGAGGTAGA
                                                                  NotI
                                                                  ~~~~~~~~~
           G  T  T  L  Y  P  K  Y  S  N  K  V  D  N  P  I  E  *  A  A
2301    GGGGCACCAC GCTTTATCCG AAATATAGTA ATAAAGTAGA TAATCCAATC GAATAAGCGG CCGCATAATG CTTAAGTCGA ACAGAAAGTA ATCGTATTGT
        CCCCGTGGTG CGAAATAGGC TTTATATCAT TATTTCATCT ATTAGGTTAG CTTATTCGCC GGCGTATTAC GAATTCAGCT TGTCTTTCAT TAGCATAACA
```

Figure 3.1: GFP-LLO plasmid map and sequence. **Plasmid map**: pRSFDuet-1 with GFP fused to LLO. Relevant restriction sites and WELQut protease site are indicated. **Sequence**: GFP-LLO including relevant restriction sites and protease cleavage sites. GFP sequence is indicated in green and LLO sequence indicated in black.

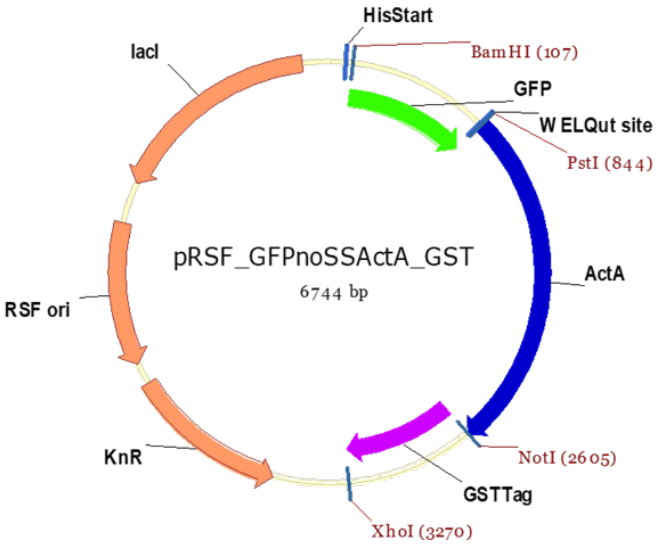


```
                                                                                                  M  G  S  S  H  H  H  H  H  H
1     GGGGAATTGT GAGCGGATAA CAATTCCCCT GTAGAAATAA TTTTGTTTAA CTTTAATAAG GAGATATACC ATGGGCAGCA GCCATCACCA TCATCACCAC
      CCCCTTAACA CTCGCCTATT GTTAAGGGGA CATCTTTATT AAAACAAATT GAAATTATTC CTCTATATGG TACCCGTCGT CGGTAGTGGT AGTAGTGGTG
       S  Q  D  P   M  S  K   G  E  E   L  F  T  G   V  V  P   I  L  V   E  L  D  G   D  V  N   G  Y  K   X  X  X  X·
101   AGCCAGGATC CGATGAGTAA AGGAGAAGAA CTTTTCACTG GAGTTGTCCC AATTCTTGTT GAATTAGATG GTGATGTTAA TGGGTACAAA
      TCGGTCCTAG GCTACTCATT TCCTCTTCTT GAAAAGTGAC CTCAACAGGG TTAAGAACAA CTTAATCTAC CACTACAATT ACCCATGTTT
                                                PstI
                                                ~~~~~~~
      · H  G  M   D  E  L   Y  K  T  G   W  E  L   Q  D  S   E  D  S  S   L  N  T   D  E  W   E  E  E  K   T  E  E ·
801   CACATGGCAT GGATGAACTA TACAAAACCG GTTGGGAACT GCAGGATAGC GAAGATTCTA GTCTAAACAC AGATGAATGG GAAGAAGAAA AAACAGAAGA
      GTGTACCGTA CCTACTTGAT ATGTTTTGGC CAACCCTTGA CGTCCTATCG CTTCTAAGAT CAGATTTGTG TCTACTTACC CTTCTTCTTT TTTGTCTTCT
      ·Q  P  S   E  V  N  T   G  P  R   Y  E  T   A  R  E  V   S  S  R   D  I  K   E  L  E  K   S  N  K  X  X  X  X
901   GCAACCAAGC GAGGTAAATA CGGGACCAAG ATACGAAACT GCACGTGAAG TAAGTTCACG TGATATTAAA GAACTAGAAA AATCGAATAA
      CGTTGGTTCG CTCCATTTAT GCCCTGGTTC TATGCTTTGA CGTGCACTTC ATTCAAGTGC ACTATAATTT CTTGATCTTT TTAGCTTATT

       N  R  S  A   G  I  E   E  G  K   L  I  A  K   S  A  E   D  E  K   A  K  E  E   P  G  N   H  T  T   A  V  P  R ·
2501  AATCGTTCTG CTGGCATTGA AGAAGGAAAA CTAATTGCTA AAAGTGCAGA AGACGAAAAA GCGAAGGAAG AACCAGGGAA CCATACGACG GCAGTACCAC
      TTAGCAAGAC GACCGTAACT TCTTCCTTTT GATTAACGAT TTTCACGTCT TCTGCTTTTT CGCTTCCTTC TTGGTCCCTT GGTATGCTGC CGTCATGGTG
          NotI
          ~~~~~~~~~
      · A  A  A   S  P  I   L  G  Y  W   K  I  K   G  L  V   Q  P  T  R   L  L  L   E  Y  L   E  E  K  Y  X  X  X  X
2601  GCGCGGCCGC GTCCCCTATA CTAGGTTATT GGAAAATTAA GGGCCTTGTG CAACCCACTC GACTTCTTTT GGAATATCTT GAAGAAAAAT
      CGCGCCGGCG CAGGGGATAT GATCCAATAA CCTTTTAATT CCCGGAACAC GTTGGGTGAG CTGAAGAAAA CCTTATAGAA CTTCTTTTTA

       M  D  P  M   C  L  D   A  F  P   K  L  V  C   F  K  K   R  I  E   A  I  P  Q   I  D  K   Y  L  K   S  S  K  Y ·
3101  ATGGACCCAA TGTGCCTGGA TGCGTTCCCA AAATTAGTTT GTTTTAAAAA ACGTATTGAA GCTATCCCAC AAATTGATAA GTACTTGAAA TCCAGCAAGT
      TACCTGGGTT ACACGGACCT ACGCAAGGGT TTTAATCAAA CAAAATTTTT TGCATAACTT CGATAGGGTG TTTAACTATT CATGAACTTT AGGTCGTTCA
                                                                                XhoI
                                                                                ~~~~~~~
      · I  A  W   P  L  Q   G  W  Q  A   T  F  G   G  G  D   H  P  P  K   S  *  L   E
3201  ATATAGCATG GCCTTTGCAG GGCTGGCAAG CCACGTTTGG TGGTGGCGAC CATCCTCCAA AATCGTAACT CGAGTCTGGT AAAGAAACCG CTGCTGCGAA
      TATATCGTAC CGGAAACGTC CCGACCGTTC GGTGCAAACC ACCACCGCTG GTAGGAGGTT TTAGCATTGA GCTCAGACCA TTTCTTTGGC GACGACGCTT
```

Figure 3.2: GFP-ActA-GST plasmid map and sequence. **Plasmid map**: pRSFDuet-1 with N-terminal GFP fusion to ActA and C-terminal fusion to GST. Relevant restriction sites and WELQut is indicated. **Sequence**: GFP-ActA-GST including relevant restriction sites and protease cleavage sites WELQut and AVPR for thrombin). GFP sequence is indicated in green, ActA sequence indicated in blue and GST sequence indicated in purple.

Table 3.1: Primers used in this study

ID	Primer Name	Primer Sequence	Description	Ref
1	GFP_BamHI_F	GGATCCGATGAGTAAAGGAGAAGAACTTTTCACTGGAGTTGTCCCAATTC	PCR of GFP from pTRKH3-ermGFP including sequence for C-terminal WELQut site	$
2	GFPWELQ_PstI_R	CTGCAGTTCCCAACCGGTTTTGTATAGTTCATCCATGCCATGTGTAATCC		
3	GST_NotI_F	GCGCGGCCGCGTCCCCTATACTAGGTTATTGGAAA	PCR of GST tag from pET41a (+)	*
4	GST_XhoI_R	CAGACTCGAGTTACGATTTTGGAGGATGGTCGCCA		
5	WLLO_PstI_F	GGGAACTGCAGGCATCTGCATTCAATAAAG	PCR of truncated LLO from *L. monocytogenes* EDGe gDNA	*
6	LLO_NotI_R	ATTATGCGGCCGCTTATTCGATTGGATTAT		
7	WActA_PstI_F	GGGAACTGCAGGATAGCGAAGATTCTAGTCTAAACAC	PCR of truncated ActA from *L. monocytogenes* EDGe gDNA	*
8	ActA_NotI_R	ATGCGGCCGCTTACGTCGTATGGTTCCCTG		
9	mCherry_NotI_F	CACGCGCGGCCGCGATGGCAATCATCAA	PCR of mCherry for fusion to C-terminal of GFP-ActA	*
10	mCherry_XhoI_R	ACCAGACTCGAGTTTATATAATTCATCCATA		
11	pRSFMCS1_F	GGATCTCGACGCTCTCCCT	Sequencing primer for inserts in MCS1 of pRSF-Duet 1	#
12	pRSFMCS1_R	GATTATGCGGCCGTGTACAA		

$ (van Staden et al., 2019). * This study. # Sequences obtained from Novagen

Several plasmid constructs were generated for the expression of ActA (refer to **Appendix 2**), due to degradation products observed during the expression and purification of ActA. The final construct resulted in the translational fusion of ActA to His tagged GFP on its N-terminal and a glutathione S-transferase (GST) tag on the C-terminal (**Figure 3.2**). Actin Assembly-Inducing Protein was amplified from *L. monocytogenes* EDG-e gDNA with the primers designed to exclude the N-terminal and C-terminal signal peptide and transmembrane domain, respectively (**Figure 3.2, Table 3.1**). The GST tag was amplified from pET41a(+) using primers listed in **Table 3.1**. Purified ActA PCR product was digested with PstI/NotI and ligated into pRSFGFP

previously digested with PstI/NotI. The ligation product was transformed and purified as described elsewhere. The resulting pRSFGFP-ActA construct was subsequently digested with NotI/XhoI and used in a ligation reaction with the GST tag (digested with NotI/XhoI). The product from the ligation reaction was used to transform chemically competent *E. coli* BL21 (DE3) cells and pDNA isolated as described elsewhere. To further increase the stability of ActA during expression an *E. coli* BL21 (DE3) strain, ArcticExpress, harbouring the cold-adapted chaperonins Cpn10 and Cpn60 was employed. Transformation and culturing of ArcticExpress *E. coli* BL21 (DE3) is essentially performed as described for *E. coli* BL21 (DE3) with one exception. During culturing, gentamicin (20 µg/mL) is included in order to maintain the plasmid harbouring *cpn10* and *cpn60* (pACYC-based plasmid).

3.2. Protein Synthesis and Purification

The GFP-linked heterologous expression method used for purification of LLO and ActA allowed real time validation of purification products through visible GFP fluorescence in samples and SDS PAGE gels (**Figure 3.3**) (van Staden et al., 2019).

3.2.1. Listeriolysin-O (LLO)

Escherichia coli BL21 (DE3) cells expressing GFP-LLO were inoculated in 10 mL LB broth containing 50 µg/mL kanamycin and incubated overnight at 37°C under agitation. For thio-B-D-galactopyranoside (IPTG) optimization, the overnight culture was used to inoculate 200 mL Terrific Broth (TB; 1% v/v) containing 50 µg/mL kanamycin. Flasks were incubated at 30°C on a shaker until an optical density (OD_{600nm}) of 0.6 was reached. Cells were induced with 0.25, 0.5 and 1.0 mM IPTG and expressed for 24 hours at 26°C with agitation. Cells were collected via centrifugation at 7500 rpm for 15 min at 10°C and wet weight recorded. The pellets were frozen before cells were lysed with lysis buffer (5 mL/g cell wet weight) for 30 min on ice. Lysis buffer was made up in Start Buffer (SB) containing 30 mM imidazole (SB30), 1 mg/mL lysozyme, 1 U/mL RNAse (NEB) and 6 U/mL DNAse (NEB) and SigmaFast (EDTA free) protease inhibitors (Sigma-Aldrich; added according to manufacturer's instructions). Cells were sonicated on ice three times at 70% power output, 90% pulses for 3 min and centrifuged at 13000 rpm for 45 min at 10°C to separate cell debris from GFP-LLO containing lysate. Prior to isolating protein via immobilized metal

affinity chromatography (IMAC), His Trap HP Ni-NTA His tag columns (1 mL, GE Healthcare) were equilibrated with 5 column volumes of SB30, followed by application of cell-free supernatant. Columns were washed with SB30 for 10 column volumes and GFP-LLO eluted using SB containing 500 mM imidazole over 5 column volumes. The eluted samples were desalted against PBS (pH 7.4) using 10 kDa spin columns (Thermo Fisher). Protein concentration for yield determination of desalted proteins were determined using the BCA protein assay according to the manufacturer's instructions (Thermo Fisher).

Desalted GFP-LLO concentration was adjusted to 1 mg/mL for determination of optimal cleavage conditions. Listeriolysin-O was liberated from its GFP fusion partner by cleavage with 0.5 U, 1.0 U, 5.0 U and 10 U WELQut protease for 16 hours at 26°C in a total reaction volume of 25 µL. Optimal WELQut concentration was evaluated by SDS-PAGE analysis. Using optimal cleavage conditions, LLO was further purified to remove the GFP fusion partner and WELQut protease (also His tagged). Imidazole was added to the cleavage reaction to a final concertation of 10 mM and applied to a His Trap HP Ni-NTA column previously equilibrated with 10 mM imidazole. The LLO containing flow through was collected, with His tagged-GFP and -WELQut protease remaining on the column. The purified LLO was desalted with PBS (pH 7.4) using 10 kDa protein concentrators and used in subsequent experiments.

3.2.2. Actin Assembly-Inducing Protein (ActA)

Purification of GFP-ActA-GST was done in a similar manner to that of GFP-LLO with the exception of additional GST tag purification (**Figures 3.3**). *Escherichia coli* BL21 (DE3) ArcticExpress cells expressing GFP-ActA-GST were inoculated in 10mL LB broth containing 50 µg/mL kanamycin and 20 µg/mL gentamycin and incubated overnight at 30°C under agitation. The overnight culture was used to inoculate 500mL TB (2 % v/v) containing 50 µg/mL kanamycin and 20 µg/mL gentamycin. Flasks were incubated at 30°C on a shaker until an OD_{600nm} of 0.5 was reached. Cells were subsequently induced with 0.5 mM IPTG and allowed to express at 26°C with agitation for 18 hours. After expression cells were collected via centrifugation at 7500 rpm for 15 min at 10°C and wet weight recorded. The pellets were frozen before cells were lysed with 5 mL/g wet weight lysis buffer for 30 min on ice. Lysis buffer was made up in SB containing 20 mM imidazole, 1 mg/mL lysozyme, 1 U/mL RNAse (NEB) and 6

U/mL DNAse (NEB) and protease inhibitors (Sigma-Aldrich). Cells were sonicated on ice three times at 70% power output, 90% pulses for 3 min, centrifuged at 13000 rpm for 45 min at 10°C. All subsequent purification steps were done on ice to reduce degradation of GFP-ActA-GST. Prior to isolating protein via IMAC, His Trap HP Ni-NTA His tag columns (1 mL, GE Healthcare) were equilibrated with 5 column volumes of SB containing 20 mM imidazole (SB20) supplemented with protease inhibitors (1x stock made up according to manufacturer's instructions), followed by application of cell-free supernatant. Columns were first washed with SB20 containing protease inhibitors for 10 column volumes. Columns were further washed with PBS containing 20mM imidazole (PBS20) for 10 column volumes before eluting GFP-ActA-GST with PBS containing 125 mM imidazole. The eluent was diluted 1:1 in PBS (pH 7.4) and dithiothreitol (DTT) was added to a final concentration of 5 mM. The diluted eluent was applied to a column packed with glutathione agarose (2 mL; Thermo Fisher) and allowed to bind with continuous circulation for 1 hour to allow adequate binding of GST-tagged protein. Columns were washed with 10 column volumes of PBS (pH 7.4) and bound GFP-ActA-GST eluted from the column with PBS containing 10 mM reduced glutathione (pH 8).

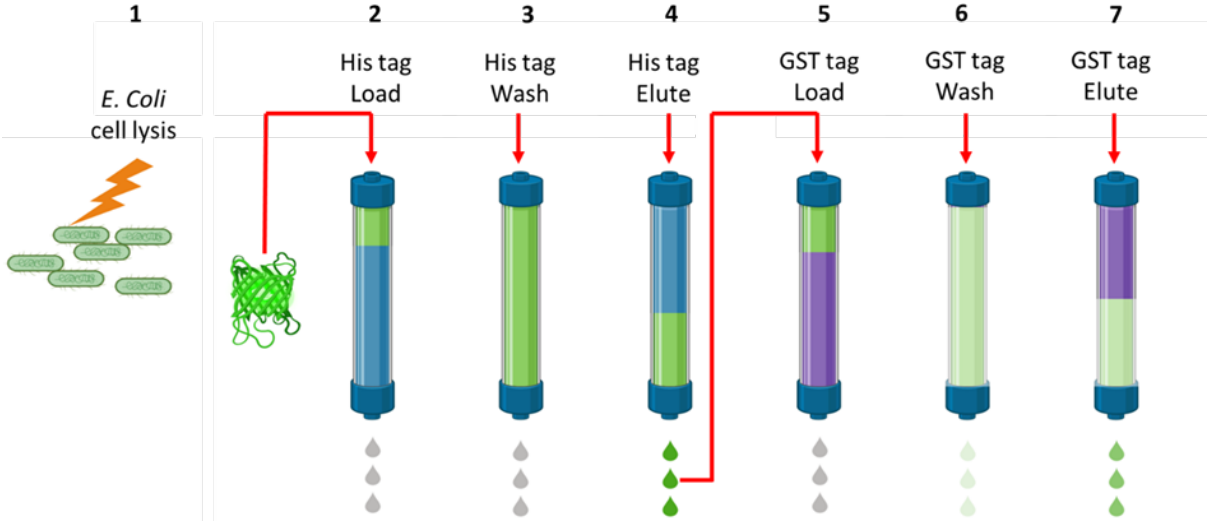

Figure 3.3: Schematic of Protein Purification: Immobilized metal affinity chromatography (IMAC; steps **1-4**) and glutathione S-transferase (GST; steps **1-7**) purification used in this study. Image created in BioRender.

Liberation of ActA-GST from the GFP fusion partner was achieved through cleavage with WELQut protease. The eluent from GST-tag purification was cleaved with 10 U

WELQut protease per millilitre of eluent and incubated for 16 hours at 8°C. After cleavage, imidazole was added to the reaction to a final concentration of 10 mM and applied to a His Trap HP Ni-NTA column pre-equilibrated with 10 mM imidazole. The flow through containing the liberated ActA-GST was collected and desalted in a 4-(2-hydroxyethyl)-1-piperazineethanesulfonic acid (HEPES) buffer (20 mM HEPES, 50 mM KCl; pH 7.5) using a 10 kDa protein concentrator. Desalted samples were used in subsequent experiments and for determination of protein yield (protein concentration determined using BCA protein assay). Samples were collected throughout purification and cleavage reactions for analysis by SDS-PAGE.

3.3. SDS-PAGE

Samples were electrophoretically separated using tricine SDS-PAGE (Schägger, 2006). Briefly, samples were added to tricine sample buffer (1:1) and incubated at 37°C for 30 min. Subsequently, 7 µL sample was loaded into the wells of a 10% tricine SDS-PAGE gel. After separation GFP fluorescence was visualized using either a MiniBIS Pro DNR Bio-imaging system (DNR Bio-imaging systems, Israel) or Dark Reader DR195M Transilluminator (Integrated Scientific Solutions) (van Staden et al., 2019). Gels were fixed with 25% Isopropanol and 10% acetic acid fixing buffer and stained using blue silver Coomassie stain until protein bands could be visualized (Candiano et al., 2004).

3.4. Processing Donor Peripheral Blood Samples

Ethical clearance exemption was obtained from Subcommittee C Human Research Ethics Committee (HREC) of Stellenbosch University (Reference # X15/05/013) for isolation of primary human monocytes and erythrocytes from donor blood. Monocyte isolation, differentiation and polarization into M1 macrophages was performed as previously described (Visser et al., 2018). Briefly, collected donor buffy coats from the Western Province Blood Transfusion Service was mixed at a 2:1 ratio with RPMI in order to facilitate layering onto a Histopaque gradient. This was centrifuged at 400 x g for 30 min after being washed in PBS containing 1 mM EDTA. The PBMC sample was then layered onto a 46% iso-osmotic Percoll solution containing PBS, RPMI and FBS before being centrifuged at 550 x g for 30 min. The monocyte layer was removed and plated onto 35 mm culture dishes and cultured for a total of 6 days in RPMI containing

10% Human Serum, 100 U/mL Penicillin-Streptomycin, 2 mM Glutamax and 50 ng/ml GM-CSF. To induce polarisation into M1 phenotype 50 ng/ml LPS and 20 ng/ml IFN-γ was added at 5 days into culture. Cells were harvested or imaged on day 6.

3.5. pH-Dependant Protein Activity

Haemolytic activity of LLO and GFP-LLO was determined at varying concentrations and pH, using human erythrocytes prepared from donated whole blood. The different pH levels were chosen to determine appropriate LLO activity, which is reported to occur from pH 6 and lower (Alberti-Segui et al., 2007). At physiologically relevant concentrations, LLO should have no haemolytic capacity at physiological pH of 7.4. Activity of LLO at lower pH levels is also in accordance with its pore forming activity within mature phagolysosomes (Friedrich et al., 2012). Furthermore, the concentration was chosen at 10x serial dilutions of the maximum protein yield obtained. This was conducted due to the lack of literature on the exact concentration of LLO haemolysis. Peripheral blood was centrifuged at 400 x g for 10 min and plasma removed. Erythrocytes were washed in PBS (pH 7.4) followed by centrifugation. Supernatant was removed and erythrocytes resuspended to original volume followed by dilution at 1:50 in PBS at pH 7.4, 6.0 or 5.5 before 190 µL of these dilutions were loaded into wells of a 96-well plate and mixed with 10 µL LLO or GFP-LLO at varying concentrations. A positive control of 0.1% Triton X100 was included to induce complete lysis of erythrocytes in a separate reaction. An untreated sample and blank were also included. Plates were incubated at 37°C for 1 hour after which absorbance readings were measured at 540 nm. Zero (blank) and 100% haemolysis was determined using PBS (pH 7.4, 6.0 and 5.5) and 0.1% Triton X100, respectively. All other groups were expressed as a percentage of the positive control, as previously described (van Staden et al., 2012).

3.6. Microbial Effector Coating onto Carboxylate Modified Beads

For *in vitro* testing with primary macrophages, the microbial effectors were coated onto 200 nm carboxylate modified crimson polystyrene beads (Thermo Fisher; F8806). Bead stock ($3.4x10^{12}$ beads/mL) was diluted into 100 µL 2-(N-morpholino)ethanesulfonic acid (MES) buffer (50mM, pH 5.2) to a final concentration of $3.4x10^{11}$ beads/mL and incubated for 1 hour at 23°C. Beads were collected by

centrifugation at 10 000 rpm for 10 min at 23°C. The supernatant was removed and 100 µL LLO (470 µg/mL) and 100 µL ActA (450 µg/mL) were added to the bead solution and incubated at 23°C for 4 hours. Beads were then washed three times with PBS before adding 100 µL O+ donor serum.

Effective bead coating was evaluated using SDS-PAGE, samples were collected of stock LLO, ActA and LLO/ActA mixture before coating as well as supernatant after coating. Gels were analysed using ImageJ software (1.52a) to determine intensities of bands. The LLO and ActA (intact) stock bands were used to determine purity of respective effectors added to beads. In order to estimate bead coating the intensities of bands corresponding to LLO or ActA (intact) originally added to beads was subtracted from that remaining in the supernatant after coating.

3.7. Confocal Microscopy for Actin Polymerisation Activity

Sodium citrate (3.2%) vacutainers were used to isolate donor peripheral blood. Blood was centrifuged at 1500 x g for 10 min at 4˚C, supernatant was removed and washed with PBS. After washing, $2.16x10^{10}$ cells were lysed in 2x lysis buffer (2 M Tris-HCl, pH 7.0, 1.2 M KCl, 2 mM DTT, 1 mM $MgCl_2$, 2 mg/mL Tween-20, 7.5% (w/v) Triton X100, and 0.2 mM protease inhibitors) for 30 min at 23˚C (modified from Schafer et al., 1998). Buffer was removed by centrifugation at 10 000 RPM for 10 min at 23˚C. Lysate was resuspended in ddH_2O and transferred to a protein concentrator tube. Lysate was centrifuged 3 times at 4000 x g for 30min to desalt the sample, after which it was resuspended in PBS and centrifuged again. This reduced the Tris-HCl concentration to 0.013M. Additional 0.2 mM protease inhibitors were added. Lysated RBCs were labelled with Oregon Green Phalloidin at 0.5 µL/mL (0.5x working concentration) and exposed to ActA coated beads (ActABeads) at $6.8x10^8$ beads/mL. In order to facilitate actin polymerisation, free ATP was added at 2 µL/mL of 10x assay buffer (500 mM Tris-HCl, 100 mM $MgCl_2$, 10 mM ATP, 100 mM DTT, pH 7.5). Lysates were loaded into an 8-chamber slide and imaged at 100x magnification using a Carl Zeiss LSM780 confocal microscope with ELYRA S.1 super resolution platform (Carl Zeiss, Germany) and analysed using the ZEN black edition imaging software.

3.8. Confocal Microscopy of Fixed Actin Polymerisation

Isolated human macrophages ($1x10^6$ cells/mL) were treated with $3.4x10^8$ beads coated with LLO and ActA (LLOActABeads) and incubated at 37˚C with 5% CO_2 under 80% humidity 1 hour and 2 hours, respectively, before being fixed with 4% paraformaldehyde for 10 min. Fixed cells were labelled with 1 µL/mL (1x) Oregon Green Phalloidin to determine actin polymerisation. Cells were imaged using a Carl Zeiss LSM780 confocal microscope (Carl Zeiss, Germany) and analysed with ZEN black edition imaging software. This pilot study was done to test ActA activity prior to higher throughput assessment using imaging flow cytometry.

3.9. Live Cell Imaging of *Listeria monocytogenes*

Listeria monocytogenes EDG-e was inoculated in 10 mL Brain heart infusion broth overnight. An aliquot of the overnight culture (1 mL) was centrifuged at 10 000 rpm and cells washed three times with PBS (pH 7.4). After wash steps cells were resuspended in 1 mL PBS (pH 7.4), resulting in a concentration of ~ 3.9×10^9 CFU/mL. *Listeria monocytogenes* EDG-e were added to macrophages at a concentration of 6.83×10^6 CFU/150µL culture media (multiplicity of infection > 22).

Time lapse videos of infected macrophages were taken on a Carl Zeiss LSM780 confocal microscope (Carl Zeiss, Germany) with ZEN black edition imaging software at 100x magnification.

3.10. Bead Expulsion Assay using Imaging Flow Cytometry

The AMNIS imaging flow cytometer has the unique ability of analysing samples at high throughput while simultaneously taking an image of every event, producing a highly reliable quantitative as well as qualitative results. Different methods of lifting macrophages from culture surfaces were tested to determine optimal conditions in terms of cell survival and immunocytochemistry fluorophore preservation prior to analysis via imaging flow cytometry (**Appendix 3**). The optimal detachment method of '23°C Accutase Fix' is described here. In order to assess time dependant expulsion of beads, macrophage populations were exposed to either $6.8x10^8$ LLOActABeads or serum coated beads (SerumBeads). These cells were then incubated at 37°C with 5% CO_2 under 80% humidity in separate 35 mm tissue culture dishes (Bio-Smart

Scientific; 20035) for each time point. Culture dishes were removed from incubation from the 15 min time point at 10 min intervals up to 75 min, media was aspirated and replaced with 1 mL 23°C Accutase. Dishes were then incubated at 23°C for 10 min before adding an additional 1 mL 23°C Accutase and incubating for another 10 min. Cells were carefully scraped using a cell scraper and transferred to 15 mL tubes for centrifugation at 400 x g for 10 min at 23°C in a swinging bucket centrifuge. Supernatant was discarded and pellet resuspended in 200 µL BD Fixation/Permeabilization solution (BD Biosciences; 554714) containing Hoechst (Sigma-Aldrich; 33342) and Oregon Green 488 Phalloidin at 5 µL/mL (0.5x) and 0.25 µL/mL (0.25x), respectively. Cells were then incubated at 4°C for 20 min to allow for fixing, permeabilization and staining before centrifugation at 400 x g for 10 min at 23°C. Supernatant was discarded and the stained cell pellet was resuspended in 50 µL BD Perm/Wash solution (BD Biosciences; 554714) before being analysed on the ImageStream Mark II AMNIS imaging flow cytometer (Millipore Sigma, United Kingdom) using IDEAS acquisition software (version 6.2). Appropriate gates were drawn on the Aspect Ratio vs. Area graph to exclude debris, and the autosampler was set to record and count 10 000 events in the cell gate per sample. Illumination settings were set at 40 mW for 405 nm laser (Hoechst: nuclei), 100 mW for 488 nm (Oregon green phalloidin: actin) and 75 mW for the 642 nm laser (Crimson red: beads). Magnification was set at 60x with EDF (Extended Depth of Field) selected and instrument set to highest sensitivity with lowest speed. A spot count analysis was set up to determine intracellular bead count. After applying the previously determined focussed cells and single cells, the truth populations were chosen. Cells were organised according to Intensity MC Channel11 (bead channel). Low truth populations were chosen by selecting cells containing 0-1 bead and high truth populations were chosen from cells containing the highest number of beads in this channel. A total of 50 cells were chosen for each truth population. To determine the average amount of beads/cell, the cumulative number of beads present in all bead-containing cells were averaged according to the number of cells in the sample for each time point. To determine the number of phagocytically active cells, the percentage cells of the total cell population containing 1 or more beads was recorded.

3.11. Statistical Analysis

All statistical analysis was done using Graph Pad Prism 5. All data are presented as means ± SEM. Linear regression and ANOVA with Bonferroni host-hoc tests were conducted where appropriate. A p-value of < 0.05 was considered statistically significant.

Chapter 4: Results

4.1. Heterologous Expression and Yield of LLO and ActA GFP Fusions

Recombinant GFP-LLO and GFP-ActA-GST were successfully expressed in *E. coli* and expression/purification were validated using SDS-PAGE analysis. SDS-PAGE analysis indicated fluorescent protein products corresponding to a size slightly lower than that of LLO fused to GFP (~85 kDa; **Figure 4.1**). This is due to the samples not being boiled, which is important to maintain GFP fluorescence, causing GFP-LLO to migrate faster through the gel (**Appendix 4**). Liberation of LLO from its GFP fusion partner was achieved using the WELQut protease with amino acid recognition sequence W-E-L-Q-↓-X. Cleavage with WELQut was performed at several concentrations and as expected, liberated LLO increased with protease concentration, with 0.4 U/µg resulting in the best cleavage (**Figure 4.2**). Both GFP and WELQut protease contain His-tag sequences, making it possible to remove them through IMAC. Using this method LLO was separated from its fusion partner and from the protease (**Figure 4.3**). Liberated LLO corresponded to the correct size of ~56 kDa when separated using SDS-PAGE (**Figure 4.4**). The purity of LLO after purification was satisfactory with a single band observed after separation with SDS-PAGE (**Figures 4.3, 4.4**).

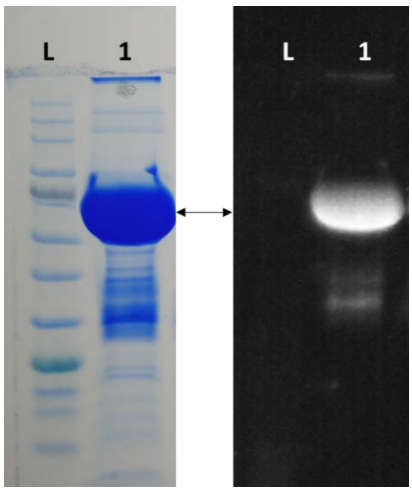

Figure 4.1: SDS-PAGE of heterologously expressed GFP-LLO. **Left**: Stained gel, **Right**: Fluorescent image of GFP-LLO. **L**: Ladder (NEB ladder #P7712), **1**: GFP-LLO eluted from IMAC column

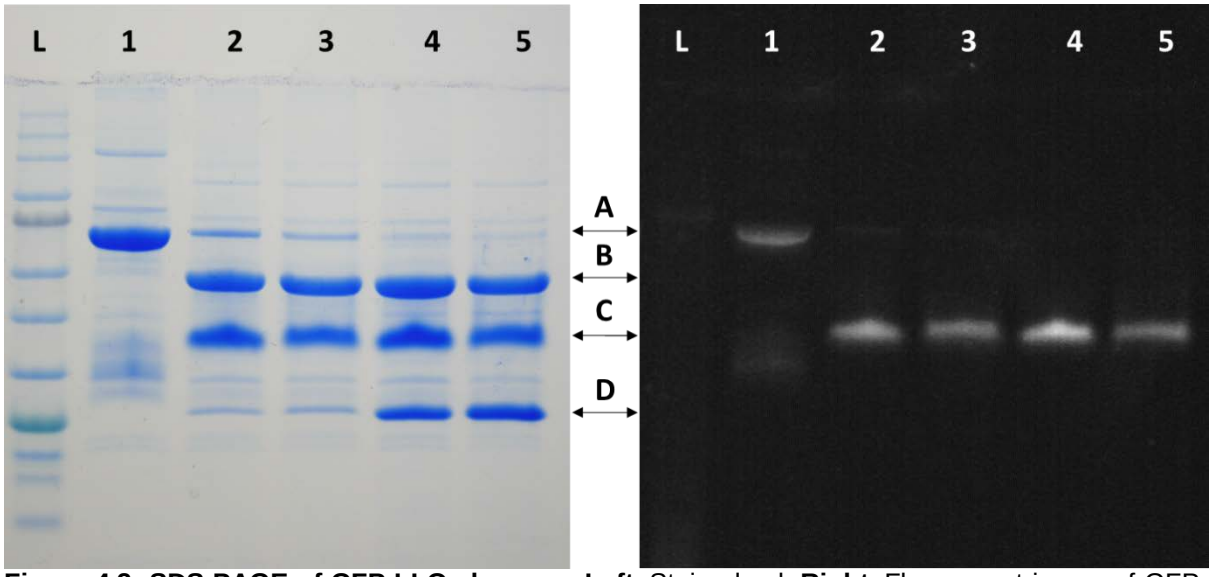

Figure 4.2: SDS-PAGE of GFP-LLO cleavage. **Left**: Stained gel, **Right**: Fluorescent image of GFP-LLO and GFP. **L**: Ladder (NEB ladder #P7712), **1**: GFP-LLO (1 mg/mL), **2-5**: GFP-LLO cleaved with WELQut protease at 0.02 U/µg, 0.04 U/µg, 0.2 U/µg 0.4 U/µg, respectively. **A**: GFP-LLO, **B**: LLO, **C**: GFP, **D**: WELQut protease.

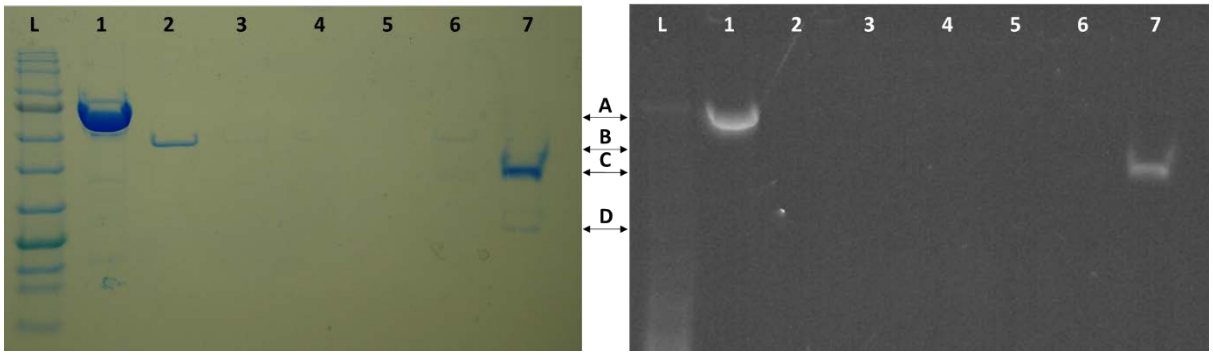

Figure 4.3: SDS-PAGE of GFP-LLO cleavage and IMAC purification. **Left**: Stained gel, **Right**: Fluorescent image of GFP-LLO and LLO. **L**: Ladder (NEB ladder #P7712), **1**: Uncut GFP-LLO, **2-7**: Flow through from IMAC purification using increasing concentrations of imidazole, 10 mM, 20 mM, 30 mM, 40 mM, 50 mM and 500 mM, respectively. **A**: GFP-LLO, **B**: LLO, **C**: GFP, **D**: WELQut protease. Cleavage reaction adjusted to final imidazole concentration of 10 mM before loading onto gel

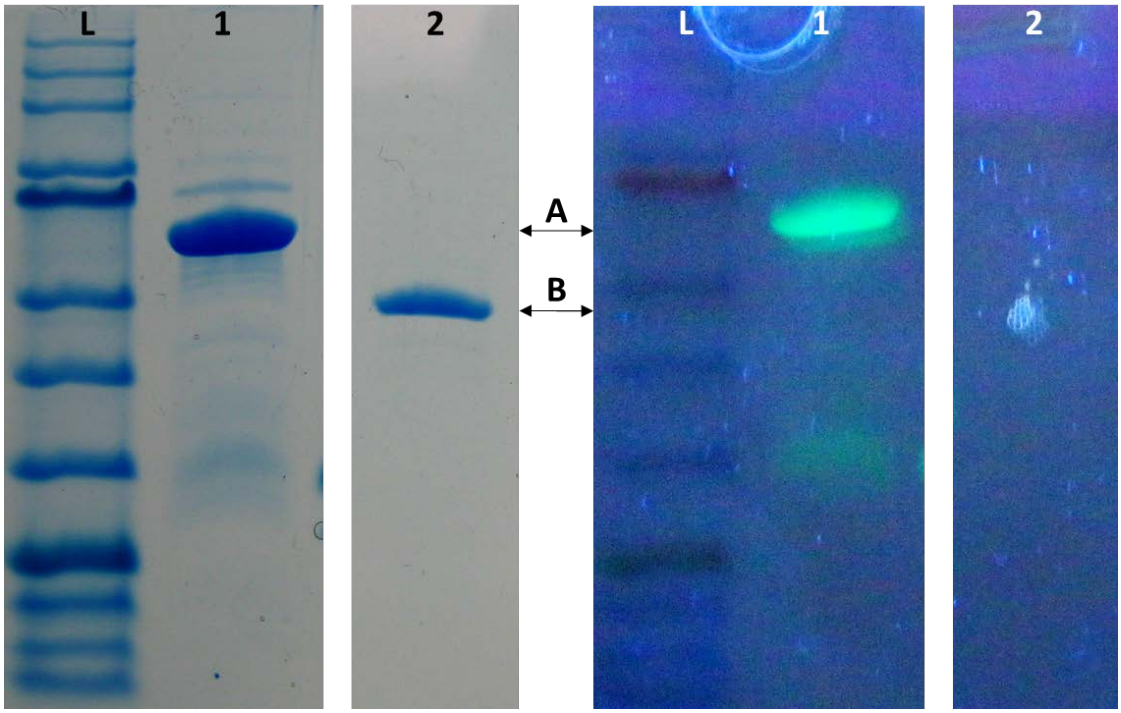

Figure 4.4: SDS-PAGE of purified GFP-LLO and LLO used in erythrocyte lysis assay. **Left**: Stained gel, **Right**: Fluorescent image of GFP-LLO and GFP. **L**: Ladder (NEB ladder #P7712), **1**: Uncut GFP-LLO, **2**: Cleaved, IMAC purified and desalted LLO. **A**: GFP-LLO, **B**: LLO.

Purification of ActA proved to be more challenging due to degradation during expression and purification and required some optimisation (**Appendix 2**). In order to increase yields of intact ActA a dual purification method was used. In order to use two affinity chromatography methods His tagged GFP and GST was fused to the N- and C-terminals of ActA, respectively. From SDS-PAGE analysis, clear degradation can be seen in samples collected from the first IMAC purification steps (in red frames **Figure 4.5**). The second purification step, utilizing the GST-tag (and glutathione agarose), yielded a pure product with little to no degradation (lane 5 of **Figure 4.5**). It should be noted that ActA has been shown to have aberrant migration when separating with SDS-PAGE, this is most likely due to its high proline content (Noireaux et al., 2000). To liberate ActA-GST from its fusion partner the same protease employed for GFP-LLO was used. After cleavage of GFP-ActA-GST a clear drop in the band (and fluorescence) corresponding to GFP could be observed along with the liberation of ActA-GST (lane 6 of **Figure 4.5**). Additional bands were observed after desalting and concentrating steps and possible degradation of the ActA product during the 16 hours cleavage step can be observed (**Figure 4.5**). The purity of ActA-GST after affinity chromatography and desalting/concentration was also satisfactory (lane 8 of **Figure 4.5**).

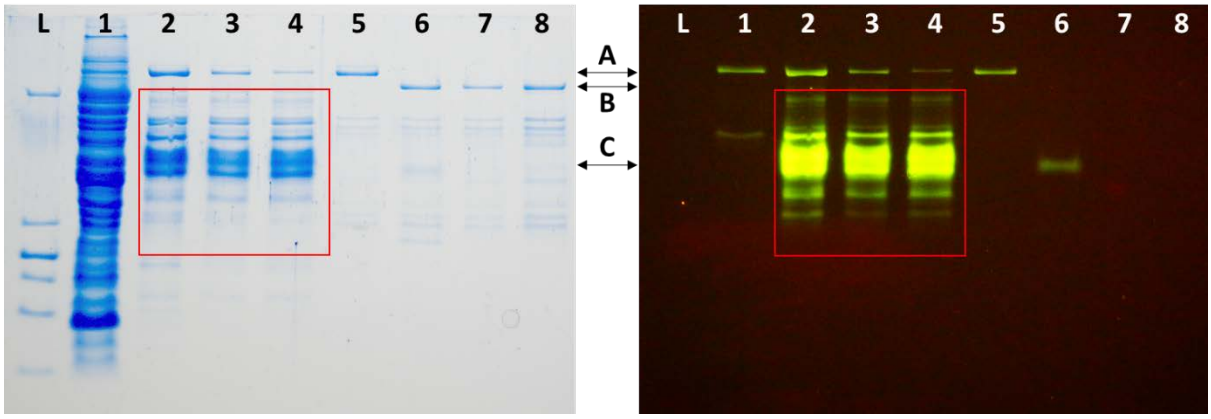

Figure 4.5: SDS-PAGE of GFP-ActA-GST purification. **Left**: Stained gel, **Right**: Fluorescent image of GFP-ActA-GST and GFP. **L**: Ladder (PageRuler #26632), **1**: IMAC flow through, **2**: IMAC elution containing GFP-ActA-GST, **3**: Dilution of IMAC elution before GST purification, **4**: Flow through from GST column, **5**: Elution from GST column containing GFP-ActA-GST, **6**: WELQut protease cleavage of GFP-ActA-GST eluted from GST column, **7**: Flow through from IMAC column containing ActA-GST after WELQut digestion, **8**: Desalted and concentrated ActA-GST obtained from IMAC flow through. **A**: GFP-ActA-GST, **B**: ActA-GST, **C**: GFP. Degradation products are outlined in **red**.

Optimal GFP-LLO yields where obtained when expression was induced with 0.5 mM IPTG resulting in a GFP-LLO concentration of 109.01 mg/L and LLO concentration (after cleavage and purification) of 51.48 mg/L. Degradation of GFP-ActA-GST during expression and purification (**Figure 4.5**) resulted in a lower yield compared to GFP-LLO with a final yield of ActA-GST of 890.35 µg/L.

4.2. Microbial Effector Activity

4.2.1. Haemolytic Activity of GFP-LLO and LLO

The activity of purified GFP-LLO and LLO was determined in terms of its capacity for haemolysis of human donor erythrocytes (**Figure 4.4** and **4.6**). Potent LLO haemolytic activity was observed at pH 6.0 and 5.5, with LLO concentrations as low as 0.043 ng/200µL (0.215ng/mL) resulting in haemolysis (13.03 % ± 0.4561), whereas significant reductions in haemolysis is observed at higher pH (pH 6.0: 4.026% ± 0.4478 and no relative haemolysis at pH 7.4; **Figure 4.6**). This trend is also seen at 0.43ng/200µL (2.15ng/mL) LLO where a pH of 7.4 (0.2110% ± 0.06090) resulted in significantly less haemolysis when compared to pH 6.0 and 5.5 (pH 6.0: 41.63% ± 0.8381 and pH 5.5: 63.01% ± 0.6482). Thus, purified LLO had potent activity by inducing haemolysis especially at pH levels below that of physiological pH 7.4. Higher concentrations seemed to have saturated the sample to overburden pH dependency, subsequently inducing complete haemolysis at all pH levels including pH 7.4 (**Figure**

4.6). Of note, an upward trend in haemolysis from pH 7.4 to 5.5 is still observed, indicating that pH levels still play some role at higher concentrations. A two-way ANOVA of the data presented in **Figures 4.6** and **4.7** was conducted to determine the effect of dose as well as pH.

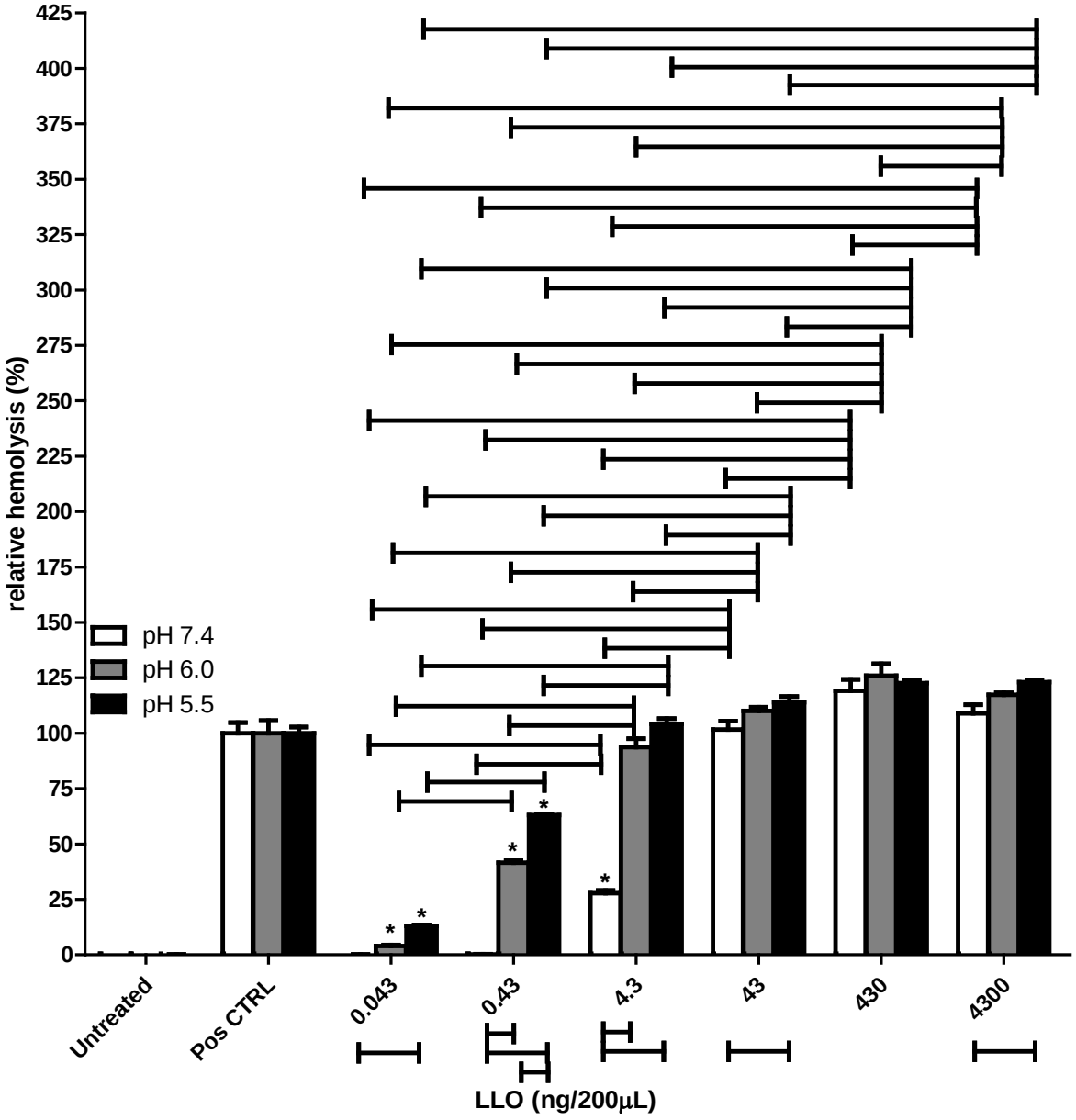

Figure 4.6: Erythrocyte haemolysis following LLO exposure at varying pH. Relative haemoglobin absorbance was collected at 540 nm, values expressed as percentage of positive control, mean ± SEM (n=3). Analysis via Two-way ANOVA. Brackets indicate $p < 0.05$. * = $p < 0.05$ vs Untreated.

The activity of GFP bound LLO was also determined (**Figure 4.7**). The GFP-LLO haemolytic activity was significantly active below physiological pH at concentrations of 0.0125ng/200µL (0.0625ng/mL) (pH 6.0: 4.890% ± 0.5885, pH 5.5: 14.17% ± 1.144;

Figure 4.7). Similar to LLO, haemolytic activity increased with increasing GFP-LLO concentration with haemolytic activity observed at pH 7.4 when GFP-LLO concentration is increased to and above 12.5ng/200µL (62.5ng/mL; 52.51% ± 1.206)

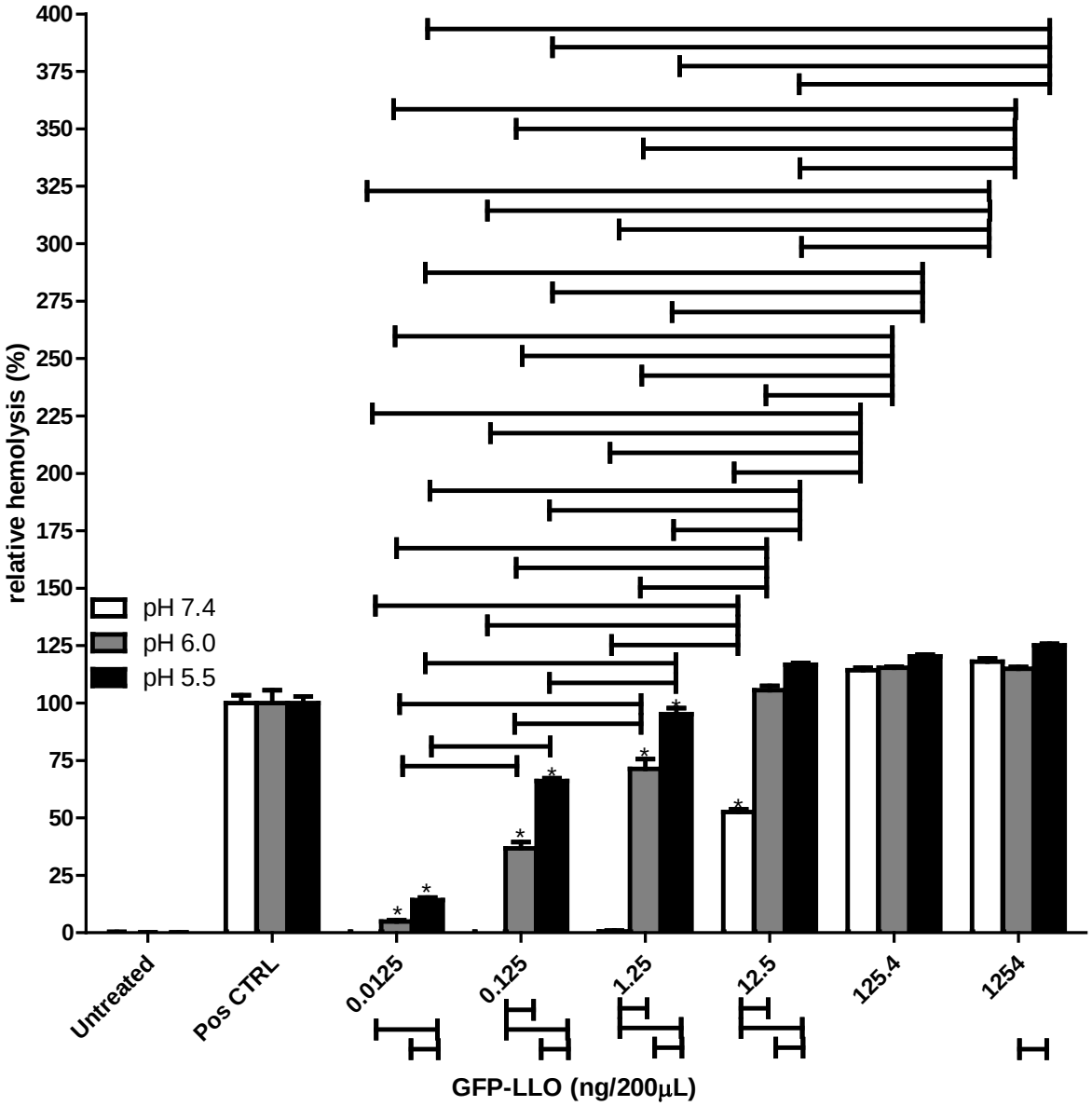

Figure 4.7: Erythrocyte haemolysis following GFP-LLO exposure at varying pH. Relative haemoglobin absorbance was collected at 540 nm, values expressed as percentage of positive control, mean ± SEM (n=3). Analysis via Two-way ANOVA. Brackets indicate $p < 0.05$. * = $p < 0.05$ vs Untreated.

4.2.2. Bead Coating

The approximate concentration of the LLO and ActA-GST (intact) coating was determined at ~21.02 µg and ~11.09 µg, respectively coated onto $3.4x10^{10}$ beads

(**Figure 4.8**). Indicating ~0.62 ng LLO with ~0.33 ng ActA coated onto each 0.2 µm bead.

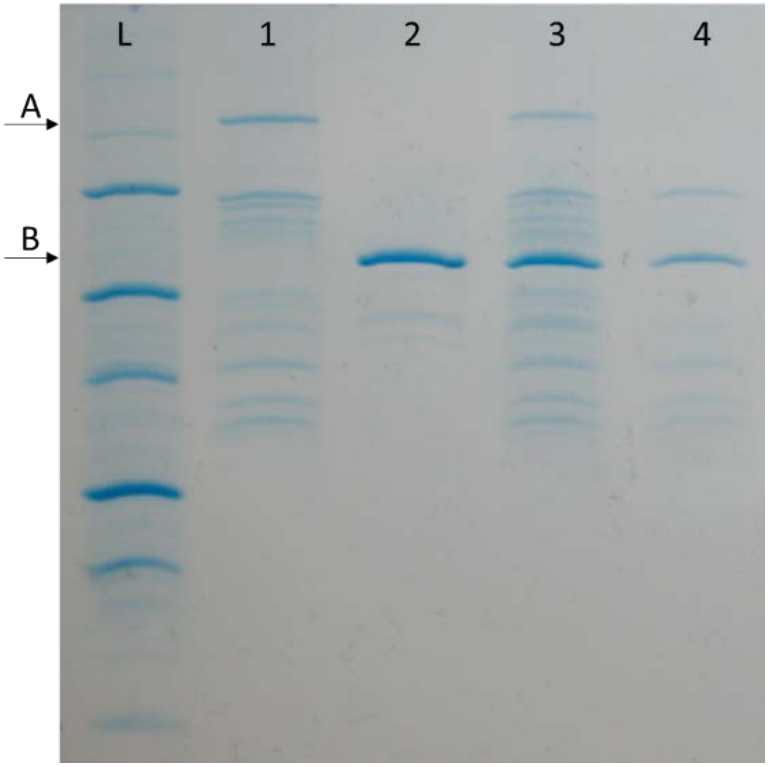

Figure 4.8: SDS-PAGE of LLO and ActA before and after coating onto beads. **L**: Ladder (Biorad #1610363), **1**: ActA stock, **2**: LLO stock, **3**: Mixed LLO and ActA stock, **4**: Supernatant of mixed LLO and ActA stock after coating (residual LLO and ActA left over after coating). **A**: ActA, **B**: LLO.

4.2.3. Actin Polymerisation Activity of ActA

The ability of ActA to polymerise actin was assessed by exposing erythrocyte lysates to polystyrene beads coated with ActA (ActABeads). **Figure 4.9** shows actin polymerisation 'clouds' (white arrows) occurring in response to ActA. These clouds seem to start forming at 60 min post introduction of beads and tether beads to one another. This is apparent when considering the absence of these 'clouds' during SerumBeads exposure at the same time point. Some background polymerisation is observed.

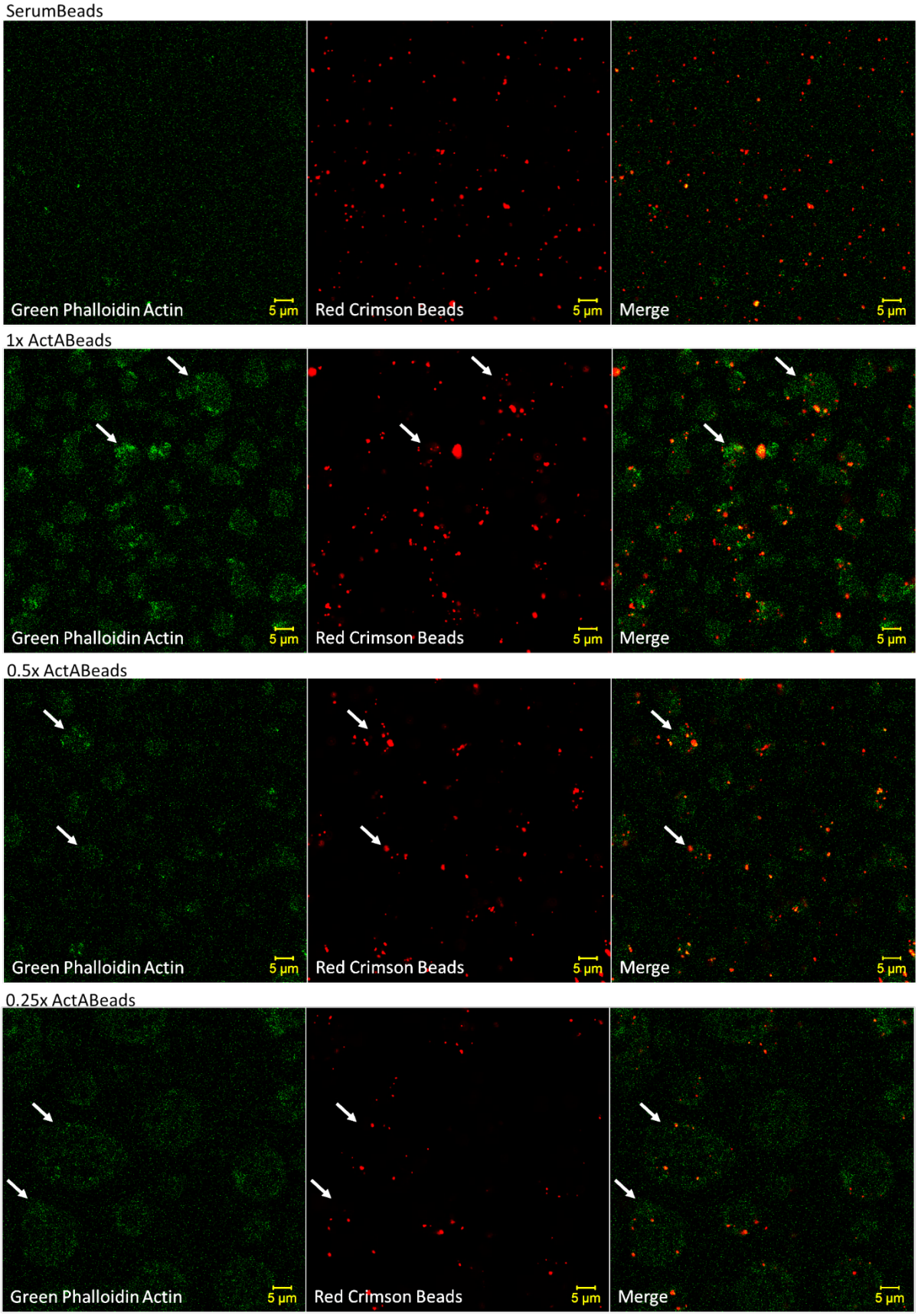

Figure 4.9: Actin polymerisation induced by exposure to ActABeads. Panels indicate marked actin polymerisation 'clouds' when exposed to 1x (45.00µg), 0.5x (22.50µg) and 0.25x (11.25µg) ActABeads (**white arrows**), compared to SerumBeads control at the same time point. All frames indicate polymerisation at 70 min after introduction of beads.

4.2.4. *In Vitro* Validation of Actin Polymerisation

The macrophages shown in **Figure 4.10** were exposed to live *L. monocytogenes* and allowed to infect cells for 3 hours. Live cell time lapse images were collected with phase contrast to determine analysis time points for later LLOActABeads infection. From 2 hours post infection the cells showed actin polymerisation (white arrows), induced by *L. monocytogenes* infection. When comparing this to a different cell population at ~5 min post infection, no such actin polymerisation is observed, rather extension of pseudopodia is seen. Importantly, the phenomenon of membranous actin polymerisation is also seen when cells are exposed to synthesised effectors (**Figure 4.11**), supporting induction of similar cellular processes when exposed to our synthetic microbe coated beads. Previous reports have shown these membrane actin spikes (Ishida et al., 2019), however, those present are significantly more in comparison. Additionally, marked cell shrinkage can be observed at 3 hours post infection, likely a process related to expulsion and intracellular pathogen load. (One limitation of this experiment was the inability to visualise *L. monocytogenes* associated actin comets. This is due to the inability of labelling live cells with the phalloidin actin stain. A pilot study was launched to determine possible phagocytosis of the label (**Appendix 5**), however, the stain remained within phagosomes, isolated from cytosolic actin filaments.)

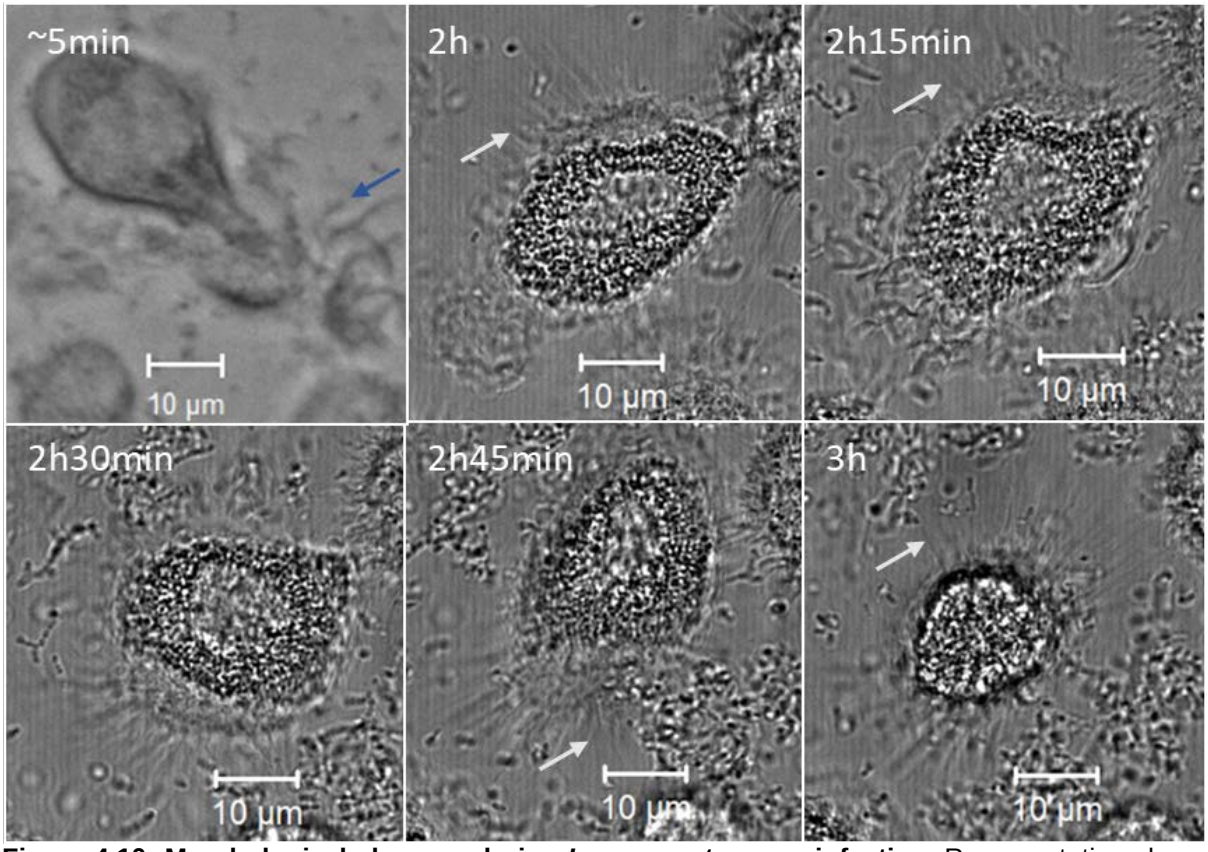

Figure 4.10: Morphological changes during *L. monocytogenes* infection. Representative phase contrast images show actin polarisation of a primary human M1 macrophage, as evidenced by membranous "spikes" protruding from the macrophage membrane (**white arrows**).

Actin polymerisation induced by LLOActABeads was also confirmed *in vitro* using confocal microscopy (**Figure 4.11**). After two hours of exposure to LLOActABeads, human primary M1 macrophages exhibited greater actin polymerisation and membrane extensions or 'spikes' (white arrows) compared to cells at 1-hour, as well as previous reports of homeostatic membrane 'spikes' (Ishida et al., 2019). This is apparent when considering that only membrane extrusions, likely associated with cell movement, is observed in the SerumBeads control group. No rigid actin spikes can be seen protruding from membranes at either 1-hour or 2-hour time points during SerumBeads infection. These findings were satisfactory to progress this protocol into high throughput assessment for quantitative evaluation.

Control: SerumBeads

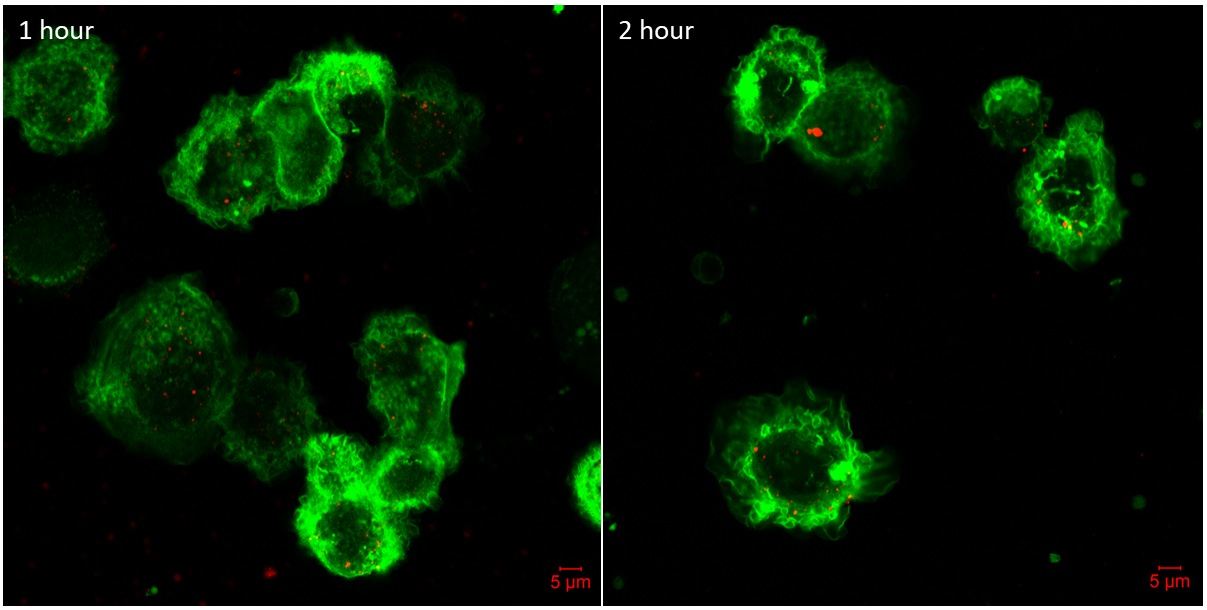

Treated: LLOActABeads

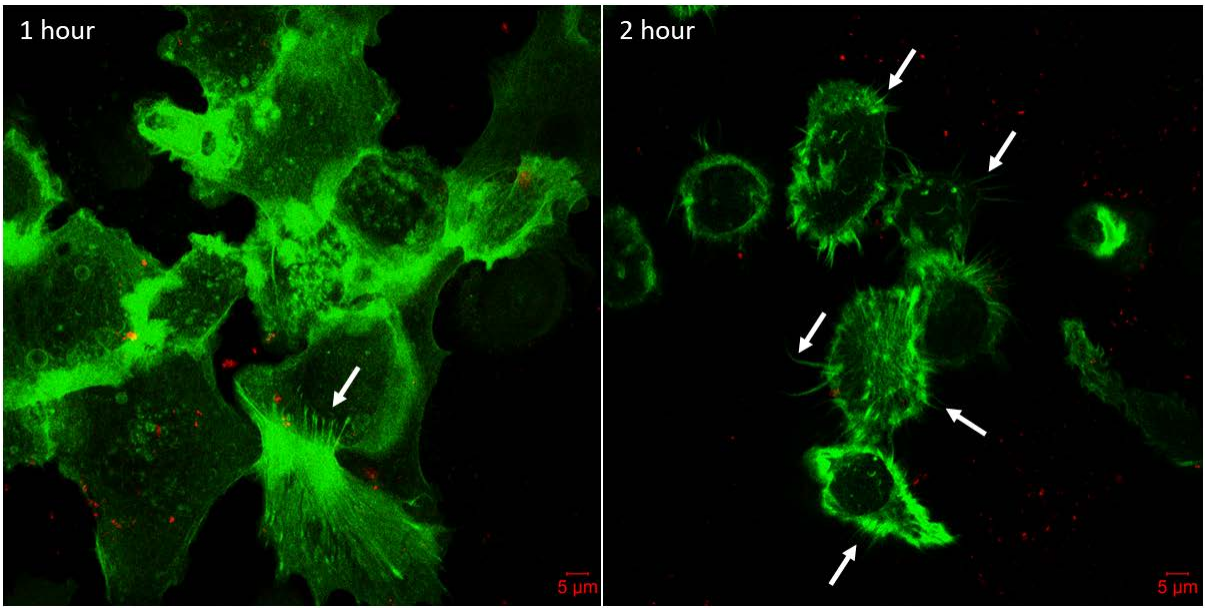

Figure 4.11: Confocal microscope assessment of actin polymerisation. Images of separate cell populations exposed to SerumBeads and LLOActABeads, indicating extent of actin polymerisation (**white arrows**) at two time points.

4.3. Cargo Expulsion: Quantitative Data

Representative images of morphological changes in cells undergoing different engulfment and expulsion phases are presented in **Figure 4.12**. Bead count and localisation is observed as well as pseudopodia (blue arrows) and actin polymerisation ("membrane spikes") (white arrows). Pseudopodia protrude from macrophages under both SerumBeads and LLOActABeads conditions at the 15 min time point, indicating

that engulfment is initiated in similar time frames while the coated effectors has not yet been activated (rows A and E of **Figure 4.12**). Accumulation of beads inside macrophages over time was observed in cells exposed to SerumBeads, but not those exposed to LLOActABeads (rows A-D and rows E-H of **Figure 4.12**, respectively). Almost all cells produced membrane spikes when exposed to LLOActABeads (rows F-H of **Figure 4.12**). This was particularly pronounced at 75 min and suggests that expulsion of beads through these spikes had occurred (**Figure 4.12**). Of interest, when considering the location of beads still inside host macrophages (**Figure 4.13**), SerumBeads seemed to be homogenously distributed throughout cells whereas LLOActABeads tend to localise toward the periphery. This could potentially be linked to the occurrence of actin polymerisation and should be quantitatively evaluated as an additional marker indicative of bead expulsion efficacy.

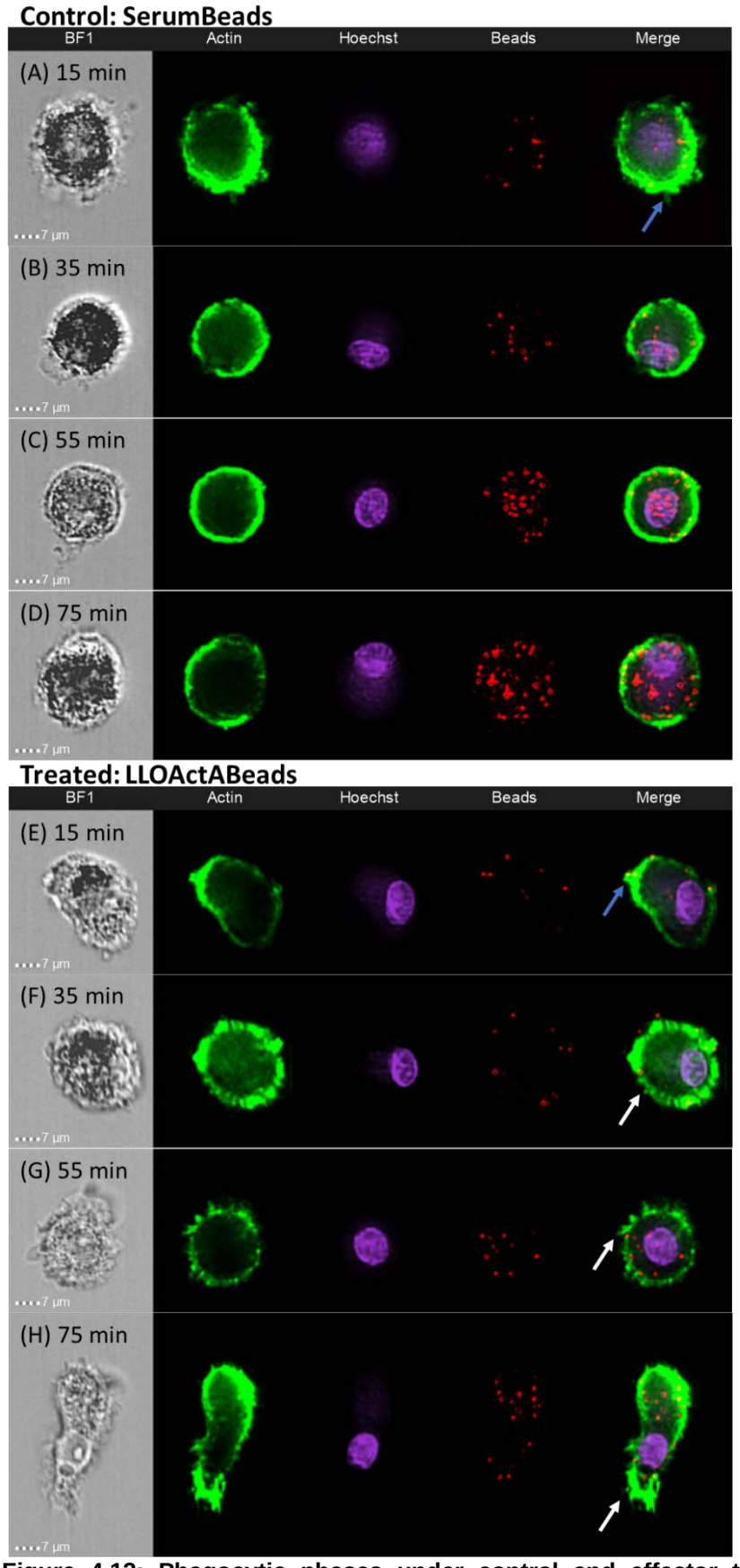

Figure 4.12: Phagocytic phases under control and effector treated conditions over time. Macrophage populations were exposed to SerumBeads or LLOActABeads for different time periods. **Blue arrows**: pseudopodia. **White arrows**: actin membrane spikes. Accumulation of beads is seen under SerumBeads exposure. **BF1**: first bright-field channel.

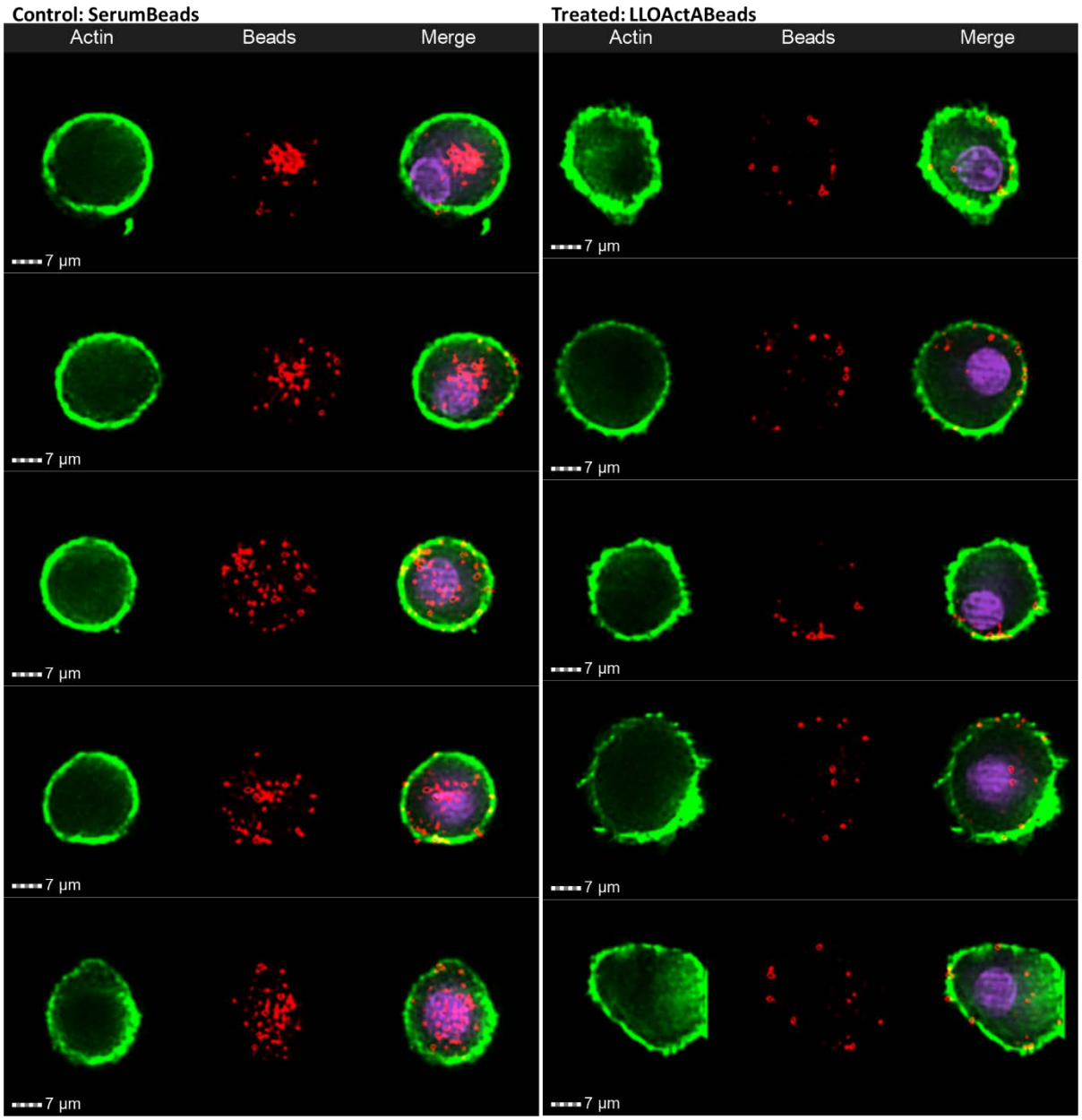

Figure 4.13: Intracellular bead location at 75min post infection. Representative images of macrophages at the same time point suggest a tendency for bead distribution predominating at the periphery of cells during LLOActABeads exposure.

Most significant in terms of the current aim, was the intracellular accumulation of SerumBeads in macrophages over time, while a significantly smaller accumulation of LLOActABeads was recorded (ANOVA main effect of treatment, $p < 0.01$; **Figure 4.14**).

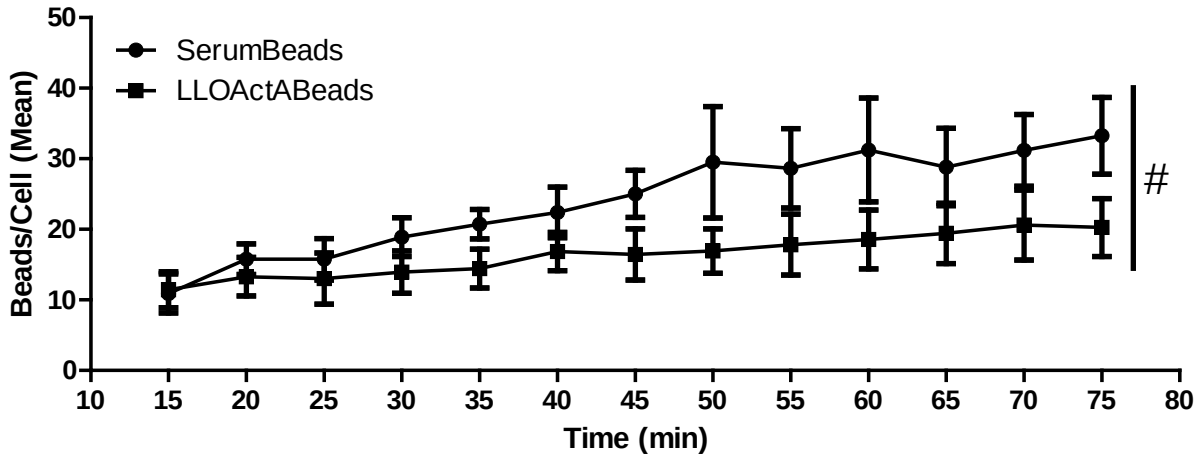

Figure 4.14: Number of beads per cell during exposure to SerumBeads and LLOActABeads. Average number of beads per cell given for effector treated (LLOActABeads) and control (SerumBeads) over time. Data points are means and error bars indicate SEM. **Statistics**: #, ANOVA main effect of treatment, $p < 0.01$.

In addition, the percentage of cells containing intracellular beads (i.e. cells actively participating in phagocytosis) remained similar for the two treatment conditions (**Figure 4.15**). No significant inhibitory effect of effector coating on cellular bead uptake was observed (**Figure 4.15**). Furthermore, our pilot data showed satisfactory engulfment of 4 µm beads when coated with LLO (**Appendix 6**). Additionally, both conditions had a near identical bead/cell average at the 15min time point (**Figure 4.14**), further hinting that exposure to effectors does not have an inhibitory effect on cellular bead uptake. Together, this suggests that the reduced number of beads seen under LLOActABeads exposure can only be attributed to a progressive loss or expulsion of beads from cells (**Figure 4.14**).

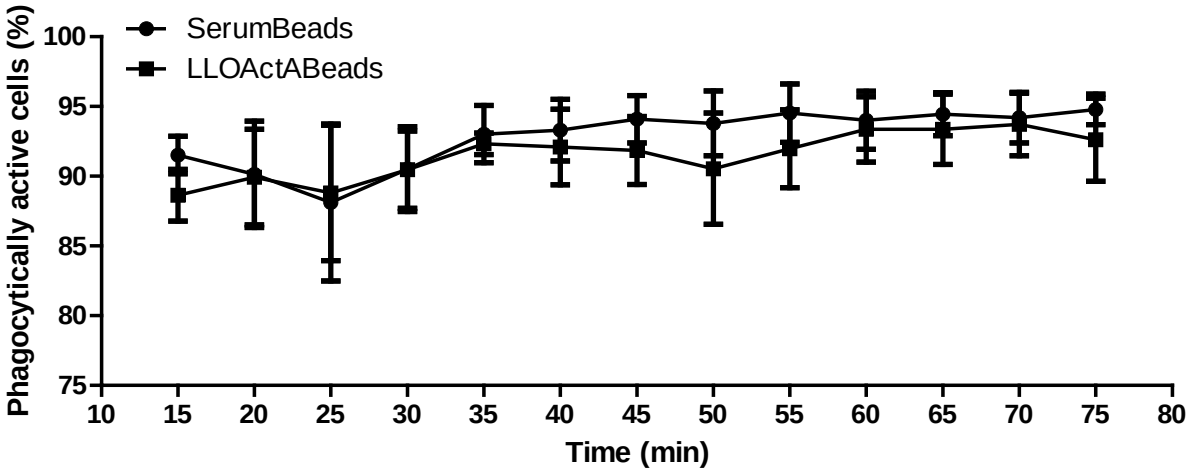

Figure 4.15: Percentage of cells actively participating in phagocytosis during SerumBeads and LLOActABeads exposure. Percentage of bead containing cells per population over time, indicate a similar number of cells during both conditions. Data points are means and error bars indicate SEM. **Statistics**: ANOVA main effect of treatment, p = 0.75.

Chapter 5: Discussion

The majority of research focused on host-microbe interaction to date has been aimed at prevention of microbial infection or dissemination through identifying the active effectors or characterizing the redundant signalling pathways involved (Proal et al., 2017; Ireton et al., 2018). In contrast, with this project we set out to identify functionality and utilisation of microbial effectors for therapeutic outcome. This builds on our previous work where ingestion and intracellular preservation of cargo has been achieved, while maintaining the transmembrane migratory capacity of carrier cells (Visser et al., 2018). In a paradigm-shifting approach, we decided to re-use this knowledge of microbes in a novel manner: our approach was to engineer a system that would promote dissemination of beneficial components/compounds rather than microbes themselves. In particular, we proposed to facilitate release of therapeutic cargo from carrier cells through the activity of specific microbial effectors and their manipulation of the host cell signalling pathways involved in expulsion mechanisms. Our previous work utilised microbial metabolites in a similar manner to induce phagosome maturation arrest and subsequent preservation of ingested cargo (Visser et al., 2018). Maturation arrest is however only transiently induced (with these metabolites and other compounds) allowing a period in which macrophages can move toward the target area before maturation arrest is lost and expulsion initiated. In this regard non-lytic release is advantageous as deposition of additional M1 type carrier macrophages into target areas would facilitate resolution of infection/inflammation (Abbas et al., 2014). In order to achieve our initial aim of identifying adequate microbial effectors, the current literature needed to be evaluated in terms of the efficacy of inducing expulsion from carrier cells. Adequate knowledge of known expulsion-inducing effectors with their signalling pathways and the possibility to obtain these effectors for experimental testing also needed to be addressed (**Chapter 2**). Following identification, focus was placed on how effectors could be synthesised, validated for purity and activity and tested *in vitro*. The subsequent sections will discuss how our methodological approach, and the results obtained, aided in the development of a cell-based drug delivery system.

5.1. Microbial Effector Identification

An important hallmark for effector identification was non-lytic release of cargo from carrier cells. As mentioned elsewhere, this would deposit additional functional M1 macrophages to the target site. Due to macrophage plasticity (Mosser et al., 2008) these cells could then shift toward a M2 phenotype and contribute to resolution of inflammation/damage. Therefore, focus was initially placed on the vomocytosis capability of *Cryptococcus neoformans* due to the possibility of maintaining carrier cell viability following this form of expulsion (Johnston et al., 2010). However, our initial experimentation elucidated that vomocytosis is a rare event (7 out of 100 000 cells) and responsible effectors are largely unidentified (**Appendix 7**). This could be attributed to the fact that *C. neoformans* does not seem to have directly evolved with the purpose of evading the host immune system (Steenbergen et al., 2003) – at least in part because it seems dependent on host immunity for its ability to infect host cells, as poor infective capacity has been reported for *C. neoformans* in the absence of opsonisation (Johnston et al., 2013). Conversely, others have shown engulfment of *L. monocytogenes* to be independent of opsonisation (Pierce et al., 1996), a finding confirmed by our own results (**Figure 4.9**). Therefore, we shifted our attention to effectors already identified in other intracellular pathogens which are known to successfully evade host immunity. The keystone bacterium *Porphyromonas gingivalis* exhibits similar mechanisms of expulsion, with the advantage (at least in the current context) of almost exclusively disseminating in a non-lytic fashion (Takeuchi et al., 2011). The high incidence of expulsion from host cells made this microbe a more desirable candidate compared to *C. neoformans.* Reports indicate 44% infection after 24h incubation of uninfected cells with *P. gingivalis* containing cells (Yilmaz et al., 2006), indicating the effectivity with which this bacterium can spread throughout the periodontium. These mechanisms are likely actin dependant and evade humoral immunity through direct cell-to-cell spread. However, the mechanisms of action responsible for this effective dissemination are even less well understood than those of *C. neoformans*. Nonetheless, from our review of the literature (as presented in **Chapter 2**), we identified a key similarity in these and other reports on microbial egress: the majority of literature consulted seems to describe a requirement for phagocytic engulfment with phagosomal manipulation by the microbe to maintain its own viability and even assist in its proliferation. This immune evasion technique is then

commonly followed by an actin polymerisation-dependent mechanism of egress from the host cell. Therefore, we shifted our focus to the better understood mechanisms of *L. monocytogenes*.

5.1.1 Mechanisms of *Listeria* Effectors LLO and ActA

The main effectors responsible for *L. monocytogenes* egress are LLO and ActA. Briefly, LLO create pores in the phagosomal membrane when under acidic pH conditions, to induce its escape into the cytosol (Alberti-Segui et al., 2007). Once in the cytosol, activity of ActA is reported to induce actin polymerisation in the more physiological pH of the cytosol (Skoble et al., 2000). These effectors are not produced by other microbes; however, similar mechanisms of action are employed, and homologues do exist. Pore forming toxins other than LLO are produced by other bacteria and not only induce pore formation but also manipulate carrier cell ion concentration, manipulating infected cells in more subtle ways (Dal Peraro et al., 2016). Furthermore, a similar actin polymerizing factor to ActA is produced in *Shigella flexneri* (IcsA) (Welch et al., 2013). ActA and IcsA are not homologues and induce polymerisation in distinct manners, but still achieve a similar outcome. For example, LLO negative mutants of *L. monocytogenes* are able to infect neighbouring cells via cell-to-cell spread but are unable to escape from these host cells. These microbes are harboured inside double membrane vesicles and are unable to disseminate due to absence of LLO pore formation (Gedde et al., 2000). Similarly, the absence of ActA in *L. monocytogenes* infection has been reported to render intracellular bacteria immotile and markedly non-infectious (Pillich et al., 2017). Thus, these effectors are of pivotal importance for *L. monocytogenes* dissemination and survival and use of these effectors in a synthetic microbe system would be advantageous. Purchased microbial effectors are expensive, and availability is limited. In addition, a substantial amount of effector would be needed for experimentation in a novel project like this. Given the risk involved in an ambitious endeavour such as proposed here, the high cost of effectors could not be justified. Practically, 50 µg of LLO costs ~$263 (Abcam) whereas we produced >50 mg/L for ~$145 ($0.145 per 50µg) In addition, we could only source ActA from MyBioSource at ~$775 for 50 µg and delivery to South Africa is limited. Furthermore, commercially available effectors are limited to those that are well-studied and commercially viable. This limits the combinations of effectors that can be used,

especially if working with novel effectors. In order to overcome these limitations heterologous expression was utilized.

5.2. Effector Synthesis

Previously, LLO has been purified from *L. monocytogenes* directly - however, these methods resulted in low yield and were relatively time consuming (Traub et al., 1995). Other authors turned to purification of LLO from *E. coli* to increase yields while lowering production time (Churchill et al., 2005). Methods for purification of ActA have also been established (Kocks et al., 1993; Welch et al., 1998; Noireaux et al., 2000; Skoble et al., 2000). These purified proteins had appropriate activity by either erythrocyte lysis (LLO) or actin polymerisation (ActA). Most notably, recombinant LLO has been used for the effective delivery of several compounds to the cytosol of cells (Mandal et al., 2002; Provoda et al., 2003; Stier et al., 2005). However, yields needed to be further improved for our application.

Fusion of proteins to GFP for heterologous expression have been previously reported. This fusion helps in soluble expression of functional proteins and has recently been reported by our group for the expression of lanthipeptides (van Staden et al., 2019) (used in **Chapter 3**). Similar methods have also been employed for the expression of LLO (Kwiatkowska et al., 2017) and ActA (Noireaux et al., 2000). However, these studies did not focus on increasing protein yields or using GFP fluorescence during purification. Using this method, we isolated sufficient protein for experimentation in our synthetic microbe system, while maintaining appropriate haemolytic and actin polymerizing activity for synthesised LLO and ActA, respectively. Of note is the heterologous GFP-linked expression method used for LLO resulting in significantly greater yields (> 50 mg/L) when compared to previously reported yields of 3.5 – 8 mg/L (Churchill et al., 2005). In terms of haemolytic capacity of LLO in particular, a noteworthy additional finding was that GFP-fused LLO showed appropriate pH dependant haemolytic capacity of similar potency when compared to unbound LLO, suggesting that GFP-fusion does not affect activity of LLO. This is particularly interesting as GFP fusion could be used in future studies to easily determine the intracellular location of exogenous LLO, while maintaining the pH-dependent pore forming capacity of this toxin.

The pH-dependant nature of LLO pore formation is advantageous in a synthetic microbe system as this opens possible manipulation methods. For example, the pore forming capacity can be controlled for by inducing phagosome maturation arrest, leading to prolonged phagosome alkalinity. Thus, allowing a window period during which the carrier cells are able to reach the target location for delivery. Upon reaching the site, transient maturation arrest would be lost, and acidification induced LLO pore formation occurs to release the therapeutic cargo. In this regard, we have conducted a pilot study to determine the temporal limit of phagosome maturation arrest at between 2-3 hours post exposure to a phagosome maturation arrest inducing cocktail (**Appendix 8**).

The use of a dual tagged system has previously been used for the expression of ActA (Noireaux et al., 2000). In this study the authors used an N-terminal GST-tag and a C-terminal His-tag, without removal of the N-terminal tag after purification. Using the method described in our study we were able to visualize expression (through GFP fluorescence) during the different purification steps as well as the degradation that takes place. Furthermore, by removing the N-terminal GFP-tag our construct more closely resembles that of native ActA found on the membrane of *L. monocytogenes.*

5.3. Validation of *In Vitro* Effector Activity

Following confirmation of appropriate activity in solution, these effectors were coated onto beads to determine their capacity to induce expulsion from carrier cells. These beads represented the cargo of interest. Carboxylate modified beads were used as previous reports indicate that ActA does not bind to hydrophobic latex (Footer et al., 2008). In addition, 0.2 µm beads were chosen due to previous reports of directional actin polymerisation-induced movement following coating of 0.5 µm carboxylate modified beads with ActA (Cemeron et al., 1999). Furthermore, current drug delivery systems utilise cargo of ~ 0.2 µm in size (Kleynhans et al., 2019), similar to the size of our cargo.

These findings indicated a good likelihood for these LLOActABeads to induce expulsion from carrier cells. Initial evaluations were conducted via confocal microscopy and time lapse imaging to pinpoint expulsion. However, due to the lower optical range of 0.2 µm on the confocal microscope and the abundance of beads

present in samples, an unbiased evaluation could not be guaranteed. Larger beads conjugated with the required fluorophore could also not be sourced, thus 0.2 µm beads had to be used. The inability to differentiate a released bead from beads that have not yet been taken up was also problematic. Furthermore, this process was extremely time consuming and costly with a relatively low experimental success rate. Thus, we opted for high throughput assessment where the entire sample could be quantitatively analysed to determine cellular bead content. We acknowledge the importance of time lapse microscopy as definitive visual proof. However, our option of imaging flow cytometry is superior to time lapse confocal microscopy in terms of generation of quantitative data. Our approach allowed for greater statistical power and takes the entire sample into consideration, thereby generating an unbiased quantitative data set.

High throughput analysis showed accumulation of intracellular beads under control conditions with a significantly lower accumulation during effector exposure. This phenomenon indicates that effector exposure induced either expulsion of intracellular beads or reduced the initial uptake of beads. The percentage of cells containing any number of beads were counted during each time point and treatment condition. This number indicates the percentage of cells that were able to phagocytose the cargo. A reduction in this percentage indicates that less cells were able to phagocytose the beads, and this would be reflected in the number of beads per cell. Here we found that the percentage of cells containing any number of beads remained the same for time and treatment (**Figure 4.15)**. The number of beads per cell in the earliest 15 min time point of **Figure 4.14** is also surprisingly similar for LLOActABeads and SerumBeads, indicating a similar propensity for engulfment under both conditions. Thus, LLOActABeads exposure induced expulsion of these beads over time and reduction thereof cannot be attributed to weaker bead engulfment. This is a novel discovery as no previous reports have shown intended and induced expulsion of cargo from carrier cells, using microbial effectors, in the absence of infection.

Macrophages exposed to LLOActABeads presented marked actin polymerisation as well as clear membranous actin spikes. This is in accordance with reports of actin propelled membrane protrusions that are taken up by adjacent cells during *L. monocytogenes* dissemination (Pizarro-Cerda et al., 2012). Listeriolysin-O damages the plasma membrane of these protrusions resulting in surface presentation of the inner membrane leaflet lipid, phosphatidylserine (PS). These PS+ protrusions are

recognised by the T cell immunoglobulin and mucin-domain containing protein 4 (TIM-4) on macrophages, which subsequently mediates the uptake of PS+ protrusions (Czuczman et al., 2014). Expelled bacteria may also be packed into PS+ vesicles, formed as a result of Ca^{2+} dependent membrane repair and scission of the initial PS+ protrusion (Czuczman et al., 2014). Both PS+ vesicles and protrusions are similarly taken up by neighbouring cells via TIM-4. This method of cell-to-cell spread was however not observed in the current study. One reason for this could be that cells were located to sparsely relative to each other in this *in vitro* model, so that reuptake could not readily happen. An alternative reason could be that the actin polarisation may have interfered with PS vesicle formation, so that expelled cargo was not associated with PS, and thus not readily taken up via TIM-4. There is the possibility that residual LLO itself could serve as opsonin for reuptake into neighbouring cells, but if this was to occur, one would not expect to see the clear decrease in the number of intracellular beads in the LLOActABeads group. Thus, although this remains to be definitively confirmed in an *in vivo* model, this does not take away from our data which indicates successful bead expulsion.

For the sake of comprehensiveness, potential alternative interpretations for current data should be considered. The fact that each cell could not be labelled and followed individually to visually exact bead uptake and expulsion mechanisms, raises the possibility that beads could have been expelled *via* other mechanisms than that suggested here. For example, it could be argued that beads were able to passively move through the cell membrane, as has been shown for nanoparticles in the past (Tammam et al., 2017). However, in the current scenario, it is unlikely that passive movement of beads would have resulted in the average number of beads per cell being significantly different between the two treatment conditions, as was the case here. Seeing as this average was statistically different, it can only be argued that the presence of LLOActABeads indeed influenced the cells to induce significantly “loss” of beads.

Furthermore, our data indicated that LLO itself served as an opsonin to upregulate bead uptake (**Appendix 6**). Thus, if no bead expulsion had occurred, one would expect a larger percentage of phagocytically active cells and a larger number of beads per cell in the LLOActABeads group when compared to the control – the opposite of what if reflected in current data

It is also necessary to consider that beads may have been expelled *via* mechanisms other than the currently known mechanisms of LLO and ActA. Firstly, it is theoretically possible that these effectors induced homeostatic recycling of cargo from macrophages, in a manner similar to nutrient digestion and excretion. To determine this, one would need to stain for secretory granules and their markers. Nonetheless, this is still unlikely as our initial findings indicated a significant influence of ActA on actin, evidenced by actin membrane spikes as well as actin 'clouds'. Furthermore, appropriate pH-dependent activity of LLO was also observed. Secondly, considering that secretory granules alkalinise during exocytosis (Li, 2017), it could also be possible that the effectors induced cellular exocytosis in a manner independent of LLO activity. To this end, the phagosome could have alkalinised in preparation to expel its cargo into the extracellular matrix, thus, leading to inactivity of LLO in this alkaline environment but still ultimately ending in expulsion. This could be addressed in a number of ways that will be discussed in the future recommendations section. This being said, reports have indicated some effects of LLO on host cell genetic material (Hernández-Flores et al., 2015). It could therefore be possible that modulation of gene expression induced expulsion from the cell. This option remains to be revisited as more information becomes available on the intracellular interactions of LLO, to fully explore this possibility. However, none of the aforementioned alternative interpretations provides sufficient arguments against our finding that LLOActABeads treatment induced some mechanism by which ingested beads exited from the cells without damaging them.

On a technical note, actin spikes observed during LLOActABeads exposure may be misinterpreted as pseudopodia. However, there is a marked difference in rigidity between the two extruding structures: pseudopodia present as more curved structures (See **Figure 4.10 and Figure 5.1** for examples) - as expected when considering that pseudopodia need to encircle the material of interest in order to engulf it – whereas actin spikes present as linear, rigid structures. These actin spikes observed in the current study are likely the fluorescent remnants of a bead that has been expelled through the membrane via ActA induced actin polymerisation originating from within the cytosol. Thus, the expression of high numbers of these spikes in the LLOActABeads group confirms that beads were continually being expelled. In addition, it is important to note morphological differences between primary isolated

monocyte/macrophages and established cell lines such as J774 cells. These cells could present marked differences during phagocytosis or expulsion of cargo. One example from our group could be mentioned in this regard, where treatment of primary macrophages with phagosome maturation arresting agents did not significantly affect cell viability, however, treatment of J774 cells with these agents resulted in significant viable cell loss (data not shown).

Furthermore, although LLO is able to perforate membranes, carrier macrophages did not exhibit apparent cellular perturbations evidenced by intact cell nuclei. In addition, other authors have reported internalisation of LLO coated beads as well as entry of noninvasive *Listeria innocua* into cells, indicating that these effectors are likely more opsonising in nature (Vadia et al., 2011). Therefore, we propose that the number of beads per cell – and by extension the percentage of phagocytically active cells – would be elevated under conditions of LLOActABeads exposure rather than inhibited.

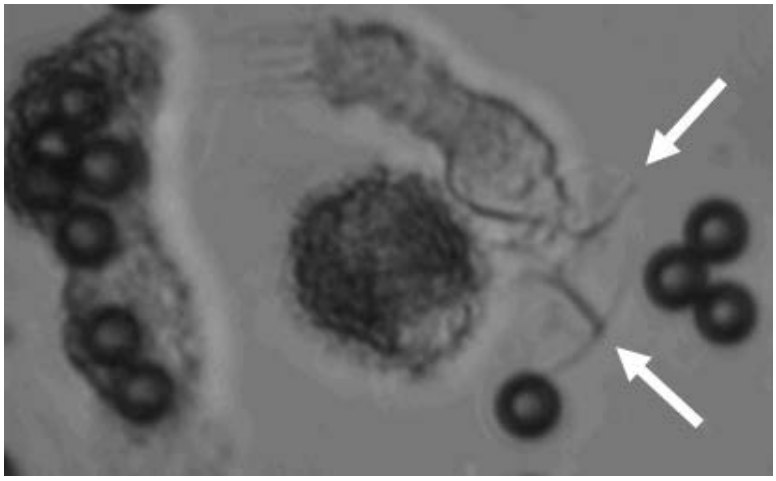

Figure 5.1: Differentiation between pseudopodia and actin spikes. Human macrophage extending pseudopodia toward 4 µm polystyrene beads coated with serum. Another macrophage containing 7 polystyrene beads is also shown.

Together, this provides evidence that the correct combination of synthesised effectors can be used to effectively mimic microbial effects on cellular processes, such as matter expulsion from phagosomes. Thus, this is novel evidence of how microbial processes may be harnessed for therapeutic benefit.

Chapter 6: Conclusion and Future Recommendations

The findings presented here illustrate a novel prototype drug delivery system – the synthetic microbe – by which to achieve drug expulsion from human macrophage shuttles. A particularly novel approach is the use of harnessing microbial effectors to facilitate expulsion, in the absence of infection or micro-organisms, which largely negates concerns about risk to the patient recipient. Current data illustrate that the microbial effectors, LLO and ActA, can be employed to achieve their native affect without adverse outcomes to host carrier cells. This could initiate a paradigm shifting research area into the treatment of a plethora of diseases, which are currently hampered by limitations such as poor blood supply or high toxicity of pharmaceuticals.

The exact mechanism with which LLO and ActA induce expulsion also need to be addressed by utilising time lapse microscopy. This was not a focus point during the current study as the possibility of expulsion needed to be indicated before one could endeavour into the exact mechanisms by which this is achieved and determine if the above stated mechanisms are at all true. The phagosome of macrophages would firstly need to be labelled with Rab5, Rab7 and LAMP1 to determine normal phagosome maturation. This would support the acidic activation of LLO and determine of the cargo exits the phagosome before expulsion or not. Additionally, to more precisely determine this, one could add the acidification marker pHrodo (Thermo Fisher) to cells. This marker emits at wavelength 533nm once inside an acidic environment and has no excitation/emission at above pH 6 (Visser et al., 2018). Thus, it is able to determine if the phagosomes acidify prior to expulsion – supporting activity of LLO – or if the phagosomes alkalinise before expulsion – supporting the induction of exocytosis in a more homeostatic manner. Furthermore, one could conduct transcriptomics to determine a genetic adaptation of host cells due to LLO exposure, as previous reports have indicated transcriptional modification (Hamon et al., 2007, 2012).

Additional follow-on experiments of the current study include testing of different effector concentrations coated onto beads. Future studies could include lower and higher concentrations of LLO and ActA to determine a possible dose response in bead expulsion over time. This would prevent, possible, over exposure of the patient to LLO and/or ActA and limit costs associated with protein synthesis.

The processing time required for isolation, culture and manipulation of cells in the current project, is a limitation in regard to acute treatment regimes. In an attempt to circumvent extended culture periods, we assessed the migratory capacity of phagosome maturation arrested monocytes. Unfortunately, this pilot study showed no migration of manipulated monocytes. However, these monocytes were able to phagocytose cargo. Thus, it is possible that cargo expulsion could also be induced within these monocytes, if the need for delaying expulsion is not necessary, making this prototype more applicable to acute as well as chronic diseases.

Together with our previously described prototype – a macrophage drug shuttle – we believe that we have now arrived at a complete system for drug delivery which is ready for *in vivo* testing. Aspects which can only be accurately assessed and optimised in an *in vivo* model, include: a) the rate and extent of bead expulsion from host macrophages, b) identification of additional components to incorporate into the synthetic microbe with which to modulate these aspects for more control over the expulsion process, c) confirming the accuracy with which drug delivery occurs focally at the intended delivery site only and d) the effect of carrier macrophages on inflammation and other cellular and tissue recovery processes after drug delivery.

Additional aspects regarding development of a polymer coating evaluated through *in vitro* investigation include a) optimisation of cargo coating and effector ratios, b) investigation into additional or more effective effectors to incorporate into the multi-layered polymer coating and c) controlling the accuracy of drug delivery by adapting this polymer coating.

Transient phagosome maturation arrest would need to be utilised to lengthen the period of cargo harbouring before effectors are activated and expulsion induced. Preliminary findings have been promising to indicate a prolonged period of cargo retention before expulsion is initiated. This would allow time for carrier macrophages to reach the intended area. The better this resolution of phagosome maturation arrest can be controlled, the more likely a burst release of cargo can be achieved. This would alleviate previous limitations in conventional drug delivery by administering an adequate dose to the target area. In addition, this would prevent excessive host drug exposure. Thus, a smaller amount of drug, at a higher concentration can be administered to the target area only.

The use of a multi-layered nanoparticle coating may also be necessary to facilitate more controlled delivery. An outermost pH sensitive layer may lengthen the period of cargo harbouring, with incorporation of escape inducing agents (i.e. LLO and ActA) into a middle layer (**Chapter 2**). This will allow time for transient phagosome maturation arrest to expire, subsequently lowering phagosomal pH and degrading the outermost layer before reaching and releasing this effector treated layer. Furthermore, an additional inner most coating could be included to protect the cargo itself from phagosomal pH drop and degradation. In addition, this layer could ensure cargo is kept intact. This innermost protective layer could also be designed so that it may be externally broken down by e.g. ultrasound administration. This would prevent host exposure to drugs deposited at unwanted locations. The need for controlled delivery can only be evaluated once an in vivo trial has been executed. Similarly, we envisage that the type of polymer and/or external triggers will be dictated by the specific application for which the synthetic microbe is required.

In terms of specificity of delivery to required sites, deposition of cargo at unwanted locations is unlikely, as macrophages infiltrate into damaged/infected areas during the inflammatory process – which is expected to prevail at sites of infection. However, this potential risk cannot be ignored, and *in vivo* evaluation is required to confirm specificity of focal delivery. For this reason, patients receiving this treatment would likely need to be evaluated beforehand to ensure that no additional sites of inflammation exist. This is not an uncommon procedure as patients are readily kept for screening before therapeutic intervention. Practically, drug and cell location within the host could still be evaluated in real time, during or post treatment. To this end, GFP bound LLO was shown to have similar activity to unbound LLO. Thus, pre-clinical *in vivo* (likely zebrafish) testing and optimisation of drug deposition locations should be conducted. Furthermore, cell labels such as CellTracker Violet (Thermo Fisher) can be used to determine locations of carrier cells during zebrafish *in vivo* testing.

Finally, migration of carrier cells to target locations could potentially alleviate inflammation due to macrophage phenotype plasticity. Once the delivered drug had exerted its antimicrobial effect, the extracellular milieu will change. We hypothesise that this may result the carrier M1 macrophages to undergo a phenotype shift toward M2 anti-inflammatory macrophages. These macrophages would be able to contribute to resolution of inflammation/infection.

Taken together, we believe that the findings reported here present a prototype which – after rigorous in vivo evaluation and optimisation – has a high likelihood for translation into clinical practice.

Chapter 7: References

1. Abbas, A. K.; Lichtman, A. H.; Pillai, S., 2014: *Basic Immunology: Functions and Disorders of the Immune System* 4th edn. Elsevier Ltd, Philadelphia.
2. Abla, N.; Naik, A.; Guy, R. H.; Kalia, Y. N., 2005: Effect of Charge and Molecular Weight on Transdermal Peptide Delivery by Iontophoresis. *Pharmaceutical Research*., **22**, 2069–2078.
3. Africa, L. D.; Smith, C., 2015a: Using a simulated blood-brain barrier to investigate potential modulators of HIV-1-associated neuro-inflammatory processes in vitro. *Journal of Research in Biology*., **5**, 5–20.
4. Africa, L. D.; Smith, C., 2015b: Sutherlandia frutescens may exacerbate HIV-associated neuroinflammation. *Journal of Negative Results in BioMedicine*., **14**, 1–9.
5. Ahsan, F.; Rivas, I. P.; Khan, M. A.; Torres Suarez, A. I., 2002: Targeting to macrophages: role of physicochemical properties of particulate carriers--liposomes and microspheres--on the phagocytosis by macrophages. *Journal of controlled release : official journal of the Controlled Release Society*., **79**, 29–40.
6. Akbar, M. A.; Tracy, C.; Kahr, W. H.; Krämer, H., 2011: The full-of-bacteria gene is required for phagosome maturation during immune defense in Drosophila. *The Journal of Cell Biology*., **192**, 383–390.
7. Alberti-Segui, C.; Goeden, K. R.; Higgins, D. E., 2007: Differential function of Listeria monocytogenes listeriolysin O and phospholipases C in vacuolar dissolution following cell-to-cell spread. *Cellular Microbiology*., **9**, 179–195.
8. Alexis, F.; Pridgen, E.; Molnar, L. K.; Farokhzad, O. C., 2008: Factors Affecting the Clearance and Biodistribution of Polymeric Nanoparticles. *Molecular Pharmaceutics*., **5**, 505–515.
9. Alkilani, A. Z.; McCrudden, M. T. C.; Donnelly, R. F., 2015: Transdermal Drug Delivery: Innovative Pharmaceutical Developments Based on Disruption of the Barrier Properties of the stratum corneum. *Pharmaceutics*., **7**, 438–470.
10. Alli, O. A.; Gao, L. Y.; Pedersen, L. L.; Zink, S.; Radulic, M.; Doric, M.; Abu Kwaik, Y., 2000: Temporal pore formation-mediated egress from macrophages and alveolar epithelial cells by Legionella pneumophila. *Infection and immunity*., **68**, 6431–6440.
11. Anderson, R.; Wadee, A. A., 2012: Innate immune mechanisms confer essential first-line host defence against the unrelenting threat posed by environmental microbial and viral pathogens. *Continuing Medical Education*., **30**, 273–277.
12. Arellano-Reynoso, B.; Lapaque, N.; Salcedo, S.; Briones, G.; Ciocchini, A. E.; Ugalde, R.; Moreno, E.; Moriyón, I.; Gorvel, J. P., 2005: Cyclic β-1,2-glucan is a brucella virulence factor required for intracellular survival. *Nature Immunology*., **6**, 618–625.
13. Arnold, L.; Henry, A.; Poron, F.; Baba-Amer, Y.; van Rooijen, N.; Plonquet, A.; Gherardi, R. K.; Chazaud, B., 2007a: Inflammatory monocytes recruited after skeletal muscle injury switch into antiinflammatory macrophages to support myogenesis. *The Journal of Experimental Medicine*., **204**, 1057–1069.
14. Arnold, L.; Henry, A.; Poron, F.; Baba-Amer, Y.; van Rooijen, N.; Plonquet, A.; Gherardi, R.; Chazaud, B., 2007b: Inflammatory monocytes recruited after skeletal muscle injury switch into antiinflammatory macrophages to support myogenesis. *Journal of Experimental Medicine*., **204**, 1057–1069.
15. Augenstreich, J.; Arbues, A.; Simeone, R.; Haanappel, E.; Wegener, A.; Sayes, F.; Le Chevalier, F.; Chalut, C.; Malaga, W.; Guilhot, C.; Brosch, R.; Astarie-Dequeker, C., 2017: ESX-1 and phthiocerol dimycocerosates of *Mycobacterium tuberculosis* act in concert to cause phagosomal rupture and host cell apoptosis. *Cellular Microbiology*., **19**, e12726.
16. Bachman, M. A.; Swanson, M. S., 2001: RpoS co-operates with other factors to induce Legionella pneumophila virulence in the stationary phase. *Molecular Microbiology*., **40**, 1201–1214.
17. Backer, J. M., 2008: The regulation and function of Class III PI3Ks: novel roles for Vps34. *Biochemical Journal*., **410**, 1–17.
18. Baeck, C.; Wehr, A.; Karlmark, K. R.; Heymann, F.; Vucur, M.; Gassler, N.; Huss, S.; Klussmann, S.; Eulberg, D.; Luedde, T.; Trautwein, C.; Tacke, F., 2012: Pharmacological inhibition of the chemokine CCL2 (MCP-1) diminishes liver macrophage infiltration and steatohepatitis in chronic hepatic injury. *Gut*., **61**, 416–426.
19. Bakowski, M. A.; Braun, V.; Lam, G. Y.; Yeung, T.; Do Heo, W.; Meyer, T.; Finlay, B. B.; Grinstein, S.; Brumell, J. H., 2010: The Phosphoinositide Phosphatase SopB Manipulates Membrane Surface Charge and Trafficking of the Salmonella-Containing Vacuole. *Cell Host &*

Microbe., **7**, 453–462.
20. Banerjee, A.; Qi, J.; Gogoi, R.; Wong, J.; Mitragotri, S., 2016: Role of nanoparticle size, shape and surface chemistry in oral drug delivery. *Journal of Controlled Release*., **238**, 176–185.
21. Bardoel, B. W.; Van Strijp, J. A. G., 2011: Molecular battle between host and bacterium: Recognition in innate immunity. *Journal of Molecular Recognition*., **24**, 1077–1086.
22. Bärlocher, K.; Welin, A.; Hilbi, H., 2017: Formation of the Legionella Replicative Compartment at the Crossroads of Retrograde Trafficking. *Frontiers in Cellular and Infection Microbiology*., **7**, 482.
23. Barros-Becker, F.; Lam, P. Y.; Fisher, R.; Huttenlocher, A., 2017: Live imaging reveals distinct modes of neutrophil and macrophage migration within interstitial tissues. *Journal of Cell Science*., **130**, 3801–3808.
24. Batrakova, E. V.; Gendelman, H. E.; Kabanov, A. V., 2011: Cell-Mediated Drugs Delivery. *Expert Opin Drug Deliv*., **8**, 415–433.
25. Becken, U.; Jeschke, A.; Veltman, K.; Haas, A., 2010: Cell-free fusion of bacteria-containing phagosomes with endocytic compartments. *Proceedings of the National Academy of Sciences*., **107**, 20726–20731.
26. Beemiller, P.; Hoppe, A. D.; Swanson, J. A., 2006: A phosphatidylinositol-3-kinase-dependent signal transition regulates ARF1 and ARF6 during Fcgamma receptor-mediated phagocytosis. *Public Library of Science Biology*., **4**, 0987–0999.
27. Beningo, K.; Wang, Y. li, 2002: Fc-receptor-mediated phagocytosis is regulated by mechanical properties of the target. *Journal of cell science*., **115**, 849–856.
28. Bertrand, N.; Wu, J.; Xu, X.; Kamaly, N.; Farokhzad, O. C., 2014: Cancer nanotechnology: The impact of passive and active targeting in the era of modern cancer biology. *Advanced Drug Delivery Reviews*., **66**, 2–25.
29. Betts-Hampikian, H. J.; Fields, K. A., 2010: The Chlamydial Type III Secretion Mechanism: Revealing Cracks in a Tough Nut. *Frontiers in microbiology*., **1**, 114.
30. Birmingham, C. L.; Canadien, V.; Kaniuk, N. A.; Steinberg, B. E.; Higgins, D. E.; Brumell, J. H., 2008: Listeriolysin O allows Listeria monocytogenes replication in macrophage vacuoles. *Nature*., **451**, 350–354.
31. Blaudszun, A. R.; Lian, Q.; Schnabel, M.; Loretz, B.; Steinfeld, U.; Lee, H. H.; Wenz, G.; Lehr, C. M.; Schneider, M.; Philippi, A., 2014: Polyester-idarubicin nanoparticles and a polymer-photosensitizer complex as potential drug formulations for cell-mediated drug delivery. *International Journal of Pharmaceutics*., **474**, 70–79.
32. Bojarczuk, A.; Miller, K. A.; Hotham, R.; Lewis, A.; Ogryzko, N. V.; Kamuyango, A. A.; Frost, H.; Gibson, R. H.; Stillman, E.; May, R. C.; Renshaw, S. A.; Johnston, S. A., 2016: Cryptococcus neoformans Intracellular Proliferation and Capsule Size Determines Early Macrophage Control of Infection. *Scientific Reports*., **6**, 21489.
33. Boschiroli, M. L.; Ouahrani-Bettache, S.; Foulongne, V.; Michaux-Charachon, S.; Bourg, G.; Allardet-Servent, A.; Cazevieille, C.; Liautard, J. P.; Ramuz, M.; O'Callaghan, D., 2002: The Brucella suis virB operon is induced intracellularly in macrophages. *Proceedings of the National Academy of Sciences*., **99**, 1544–1549.
34. Botelho, R. J.; Teruel, M.; Dierckman, R.; Anderson, R.; Wells, A.; York, J. D.; Meyer, T.; Grinstein, S., 2000: Localized biphasic changes in phosphatidylinositol- 4,5-bisphosphate at sites of phagocytosis. *The Journal of Cell Biology*., **151**, 1353–1368.
35. Braun, V.; Wong, A.; Landekic, M.; Hong, W. J.; Grinstein, S.; Brumell, J. H., 2010: Sorting nexin 3 (SNX3) is a component of a tubular endosomal network induced by Salmonella and involved in maturation of the Salmonella-containing vacuole. *Cellular Microbiology*., **12**, 1352–1367.
36. Bujny, M. V; Ewels, P. A.; Humphrey, S.; Attar, N.; Jepson, M. A.; Cullen, P. J., 2008: Sorting nexin-1 defines an early phase of Salmonella-containing vacuole-remodeling during Salmonella infection. *Journal of cell science*., **121**, 2027–2036.
37. Candiano, G.; Bruschi, M.; Musante, L.; Santucci, L.; Ghiggeri, G. M.; Carnemolla, B.; Orecchia, P.; Zardi, L.; Righetti, P. G., 2004: Blue silver: A very sensitive colloidal Coomassie G-250 staining for proteome analysis. *ELECTROPHORESIS*., **25**, 1327–1333.
38. Capmany, A.; Damiani, M. T., 2010: Chlamydia trachomatis Intercepts Golgi-Derived Sphingolipids through a Rab14-Mediated Transport Required for Bacterial Development and Replication. (Valdivia, R. H., Ed.)*PLoS ONE*., **5**, e14084.
39. Celli, J.; de Chastellier, C.; Franchini, D. M.; Pizarro-Cerda, J.; Moreno, E.; Gorvel, J. P., 2003: Brucella evades macrophage killing via VirB-dependent sustained interactions with the endoplasmic reticulum. *The Journal of experimental medicine*., **198**, 545–556.
40. Celli, J., 2006: Surviving inside a macrophage: The many ways of Brucella. *Research in*

Microbiology., **157**, 93–98.
41. Celli, J., 2015: The changing nature of the Brucella-containing vacuole. *Cellular microbiology*., **17**, 951–958.
42. Cemeron, L. A.; Footer, M. J.; Van Oudenaarden, A.; Theriot, J. A., 1999: Motility of ActA protein-coated microspheres driven by actin polymerization. *Biophysics*., **96**, 4908–4913.
43. Chakraborty, S.; Mizusaki, H.; Kenney, L. J., 2015: A FRET-Based DNA Biosensor Tracks OmpR-Dependent Acidification of Salmonella during Macrophage Infection. *PLoS Biology*., **13**.
44. Champion, J. A.; Mitragotri, S., 2006: Role of target geometry in phagocytosis. *Proceedings of the National Academy of Sciences of the United States of America*., **103**, 4930–4934.
45. Chang, Y. N.; Guo, H.; Li, J.; Song, Y.; Zhang, M.; Jin, J.; Xing, G.; Zhao, Y., 2013: Adjusting the Balance between Effective Loading and Vector Migration of Macrophage Vehicles to Deliver Nanoparticles. (Pintus, G., Ed.)*PLoS ONE*., **8**, e76024.
46. Chazaud, B.; Brigitte, M.; Yacoub-Youssef, H.; Arnold, L.; Gherardi, R.; Sonnet, C.; Lafuste, P.; Chretien, F., 2009: Dual and beneficial roles of macrophages during skeletal muscle regeneration. *Exercise and Sport Sciences Reviews*., **37**, 18–22.
47. Chen, F.; He, Y., 2009: Caspase-2 Mediated Apoptotic and Necrotic Murine Macrophage Cell Death Induced by Rough Brucella abortus. (May, R. C., Ed.)*PLoS ONE*., **4**, e6830.
48. Chen, F.; Ding, X.; Ding, Y.; Xiang, Z.; Li, X.; Ghosh, D.; Schurig, G. G.; Sriranganathan, N.; Boyle, S. M.; He, Y., 2011: Proinflammatory caspase-2-mediated macrophage cell death induced by a rough attenuated Brucella suis strain. *Infection and immunity*., **79**, 2460–2469.
49. Chen, J.; de Felipe, K. S.; Clarke, M.; Lu, H.; Anderson, O. R.; Segal, G.; Shuman, H. A., 2004: Legionella effectors that promote nonlytic release from protozoa. *Science (New York, N.Y.)*., **303**, 1358–1361.
50. Chen, J.; Reyes, M.; Clarke, M.; Shuman, H. A., 2007: Host cell-dependent secretion and translocation of the LepA and LepB effectors of Legionella pneumophila. *Cellular Microbiology*., **9**, 1660–1671.
51. Chen, M.; Xing, Y.; Lu, A.; Fang, W.; Sun, B.; Chen, C.; Liao, W.; Meng, G., 2015: Internalized *Cryptococcus neoformans* Activates the Canonical Caspase-1 and the Noncanonical Caspase-8 Inflammasomes. *The Journal of Immunology*., **195**, 4962–4972.
52. Chen, Y.; Shen, Y.; Guo, X.; Zhang, C.; Yang, W.; Ma, M.; Liu, S.; Zhang, M.; Wen, L. P., 2006: Transdermal protein delivery by a coadministered peptide identified via phage display. *Nature Biotechnology*., **24**, 455–460.
53. Cheng, S.; Wang, L.; Liu, Q.; Qi, L.; Yu, K.; Wang, Z.; Wu, M.; Liu, Y.; Fu, J.; Hu, M.; Li, M.; Zhou, D.; Liu, X., 2017: Identification of a Novel *Salmonella* Type III Effector by Quantitative Secretome Profiling. *Molecular & Cellular Proteomics*., **16**, 2219–2228.
54. Chin, E.; Kirker, K.; Zuck, M.; James, G.; Hybiske, K., 2012: Actin recruitment to the Chlamydia inclusion is spatiotemporally regulated by a mechanism that requires host and bacterial factors. *PloS one*., **7**, e46949.
55. Churchill, R. L. T.; Lee, H.; Hall, J. C., 2005: Rapid purification of recombinant listeriolysin O (LLO) from Escherichia coli. *Journal of Industrial Microbiology and Biotechnology*., **32**, 355–363.
56. Cohen, S.; Yoshioka, T.; Lucarelli, M.; Hwang, L.; Langer, R., 1991: Controlled delivery systems for proteins based on poly(lactic/glycolic acid) microspheres. *Pharmacological Research*., **8**, 713–720.
57. Comerci, D. J.; Martínez-Lorenzo, M. J.; Sieira, R.; Gorvel, J. P.; Ugalde, R. A., 2001: Essential role of the VirB machinery in the maturation of the Brucella abortus-containing vacuole. *Cellular microbiology*., **3**, 159–168.
58. Cullen, P. J.; Korswagen, H. C., 2011: Sorting nexins provide diversity for retromer-dependent trafficking events. *Nature cell biology*., **14**, 29–37.
59. Curtis, L. M.; Gluck, S., 2005: Distribution of Rab GTPases in mouse kidney and comparison with vacuolar H+-ATPase. *Nephron Physiology*., **100**, 31–42.
60. Czuczman, M. A.; Fattouh, R.; Van Rijn, J. M.; Canadien, V.; Osborne, S.; Muise, A. M.; Kuchroo, V. K.; Higgins, D. E.; Brumell, J. H., 2014: Listeria monocytogenes exploits efferocytosis to promote cell-to-cell spread. *Nature*., **509**, 230–234.
61. D'Costa, V. M.; Braun, V.; Landekic, M.; Shi, R.; Proteau, A.; McDonald, L.; Cygler, M.; Grinstein, S.; Brumell, J. H., 2015: Salmonella Disrupts Host Endocytic Trafficking by SopD2-Mediated Inhibition of Rab7. *Cell Reports*., **12**, 1508–1518.
62. Dal Peraro, M.; van der Goot, F. G., 2016: Pore-forming toxins: ancient, but never really out of fashion. *Nature reviews. Microbiology*., **14**, 77–92.
63. Davis, M. J.; Eastman, A. J.; Qiu, Y.; Gregorka, B.; Kozel, T. R.; Osterholzer, J. J.; Curtis, J. L.; Swanson, J. A.; Olszewski, M. A., 2015: Cryptococcus neoformans-induced macrophage

lysosome damage crucially contributes to fungal virulence. *Journal of immunology (Baltimore, Md. : 1950)*., **194**, 2219–2231.
64. de Almeida, A. C.; Barbosa, S. M.; de Lourdes Rios Barjas-Castro, M.; Olalla-Saad, S. T.; Condino-Neto, A., 2012: IFN-beta, IFN-gamma, and TNF-alpha decrease erythrophagocytosis by human monocytes independent of SIRP-alpha or SHP-1 expression. *Immunopharmacology and Immunotoxicology*., **34**, 1054–1059.
65. de Jonge, M. I.; Pehau-Arnaudet, G.; Fretz, M. M.; Romain, F.; Bottai, D.; Brodin, P.; Honoré, N.; Marchal, G.; Jiskoot, W.; England, P.; Cole, S. T.; Brosch, R., 2007: ESAT-6 from Mycobacterium tuberculosis dissociates from its putative chaperone CFP-10 under acidic conditions and exhibits membrane-lysing activity. *Journal of bacteriology*., **189**, 6028–6034.
66. Desjardins, M., 1995: Biogenesis of phagolysosomes: the “kiss and run” hypothesis. *Trends Cell Biology*., **5**, 183–186.
67. Ding, A. G.; Shenderova, A.; Schwendeman, S. P., 2006: Prediction of Microclimate pH in Poly(lactic- c o -glycolic Acid) Films. *Journal of the American Chemical Society*., **128**, 5384–5390.
68. Doshi, N.; Swiston, A. J.; Gilbert, J. B.; Alcaraz, M. L.; Cohen, R. E.; Rubner, M. F.; Mitragotri, S., 2011: Cell-based drug delivery devices using phagocytosis-resistant backpacks. *Advanced materials (Deerfield Beach, Fla.)*., **23**, H105-9.
69. Dou, H.; Destache, C. J.; Morehead, J. R.; Mosley, R. L.; Boska, M. D.; Kingsley, J.; Gorantla, S.; Poluektova, L.; Nelson, J. A.; Chaubal, M.; Werling, J.; Kipp, J.; Rabinow, B. E.; Gendelman, H. E., 2006: Development of a macrophage-based nanoparticle platform for antiretroviral drug delivery. *Blood*., **108**, 2827–2835.
70. Dreaden, E. C.; Mwakwari, S. C.; Austin, L. A.; Kieffer, M. J.; Oyelere, A. K.; El-Sayed, M. A., 2012: Small Molecule-Gold Nanorod Conjugates Selectively Target and Induce Macrophage Cytotoxicity towards Breast Cancer Cells. *Small*., **8**, 2819–2822.
71. Edwards, D. A., 1997: Large Porous Particles for Pulmonary Drug Delivery. *Science*., **276**, 1868–1872.
72. Evans, M. A.; Huang, P. J.; Iwamoto, Y.; Ibsen, K. N.; Chan, E. M.; Hitomi, Y.; Ford, P. C.; Mitragotri, S., 2018: Macrophage-mediated delivery of light activated nitric oxide prodrugs with spatial, temporal and concentration control. *Chemical science*., **9**, 3729–3741.
73. Fairn, G. D.; Grinstein, S., 2012: How nascent phagosomes mature to become phagolysosomes. *Trends in Immunology*., **33**, 397–405.
74. Fan, C. H.; Lee, Y. H.; Ho, Y. J.; Wang, C. H.; Kang, S. T.; Yeh, C. K., 2018: Macrophages as Drug Delivery Carriers for Acoustic Phase-Change Droplets. *Ultrasound in Medicine & Biology*., **44**, 1468–1481.
75. Feng, S.; Cui, S.; Jin, J.; Gu, Y., 2014: Macrophage as cellular vehicles for delivery of nanoparticles. *Journal of Innovative Optical Health Sciences*., **07**, 1450023.
76. Ferrari, G.; Langen, H.; Naito, M.; Pieters, J., 1999: A coat protein on phagosomes involved in the intracellular survival of mycobacteria. *Cell*., **97**, 435–447.
77. Footer, M. J.; Lyo, J. K.; Theriot, J. A., 2008: Close Packing of Listeria monocytogenes ActA , a Natively Unfolded Protein , Enhances F-actin Assembly without Dimerization. *Journal of Biological Chemistry*., **283**, 23852–23862.
78. Fratti, R. A.; Backer, J. M.; Gruenberg, J.; Corvera, S.; Deretic, V., 2001: Role of phosphatidylinositol 3-kinase and Rab5 effectors in phagosomal biogenesis and mycobacterial phagosome maturation arrest. *Journal of Cell Biology*., **154**, 631–644.
79. Freeman, S. A.; Grinstein, S., 2014: Phagocytosis: Receptors, signal integration, and the cytoskeleton. *Immunological Reviews*., **262**, 193–215.
80. Friedrich, N.; Hagedorn, M.; Soldati-Favre, D.; Soldati, T., 2012: Prison Break: Pathogens’ Strategies To Egress from Host Cells. *Microbiology and Molecular Biology Reviews*., **76**, 707–720.
81. Fu, M. S.; Coelho, C.; De Leon-Rodriguez, C. M.; Rossi, D. C. P.; Camacho, E.; Jung, E. H.; Kulkarni, M.; Casadevall, A., 2018: Cryptococcus neoformans urease affects the outcome of intracellular pathogenesis by modulating phagolysosomal pH. (May, R. C., Ed.)*PLOS Pathogens*., **14**, e1007144.
82. Gao, L. Y.; Abu Kwaik, Y., 1999: Activation of caspase 3 during Legionella pneumophila-induced apoptosis. *Infection and immunity*., **67**, 4886–4894.
83. Gaur, N. A.; Hasek, J.; Brickner, D. G.; Qiu, H.; Zhang, F.; Wong, C. M.; Malcova, I.; Vasicova, P.; Brickner, J. H.; Hinnebusch, A. G., 2013: Vps factors are required for efficient transcription elongation in budding yeast. *Genetics*., **193**, 829–851.
84. Gedde, M. M.; Higgins, D. E.; Tilney, L. G., 2000: Role of Listeriolysin O in Cell-to-Cell Spread of

Listeria monocytogenes. *Infection and immunity*., **68**, 999–1003.
85. Gerhardt, H.; Walz, M. J.; Faigle, M.; Northoff, H.; Wolburg, H.; Neumeister, B., 2000: Localization of Legionella bacteria within ribosome-studded phagosomes is not restricted to Legionella pneumophila. *FEMS microbiology letters*., **192**, 145–152.
86. Ghalanbor, Z.; Körber, M.; Bodmeier, R., 2010: Improved Lysozyme Stability and Release Properties of Poly(lactide-co-glycolide) Implants Prepared by Hot-Melt Extrusion. *Pharmaceutical Research*., **27**, 371–379.
87. Ghosh, S.; O'Connor, T. J., 2017: Beyond Paralogs: The Multiple Layers of Redundancy in Bacterial Pathogenesis. *Frontiers in Cellular and Infection Microbiology*., **7**, 467.
88. Gilbert, A. S.; Seoane, P. I.; Sephton-Clark, P.; Bojarczuk, A.; Hotham, R.; Giurisato, E.; Sarhan, A. R.; Hillen, A.; Velde, G. Vande; Gray, N. S.; Alessi, D. R.; Cunningham, D. L.; Tournier, C.; Johnston, S. A.; May, R. C., 2017: Vomocytosis of live pathogens from macrophages is regulated by the atypical MAP kinase ERK5. *Science advances*., **3**, e1700898.
89. Gillooly, D. J.; Morrow, I. C.; Lindsay, M.; Gould, R.; Bryant, N. J.; Gaullier, J. M.; Parton, R. G.; Stenmark, H., 2000: Localization of phosphatidylinositol 3-phosphate in yeast and mammalian cells. *European Molecular Biology Organization Journal*., **19**, 4577–4588.
90. Gnanadhas, D. P.; Dash, P. K.; Sillman, B.; Bade, A. N.; Lin, Z.; Palandri, D. L.; Gautam, N.; Alnouti, Y.; Gelbard, H. A.; McMillan, J.; Mosley, R. L.; Edagwa, B.; Gendelman, H. E.; Gorantla, S., 2017: Autophagy facilitates macrophage depots of sustained-release nanoformulated antiretroviral drugs. *The Journal of clinical investigation*., **127**, 857–873.
91. Gogulamudi, V. R.; Dubey, M. L.; Kaul, D.; Atluri, V. S. R.; Sehgal, R., 2015: Downregulation of host tryptophan-aspartate containing coat (TACO) gene restricts the entry and survival of Leishmania donovani in human macrophage model. *Frontiers in Microbiology*., **6**, 1–10.
92. Guyton, C.; Hall, E., 2011: *Medical Physiology* 12th edn. Elsevier Ltd, Philadelphia.
93. Hamon, M. A.; Batsche, E.; Regnault, B.; Tham, T. N.; Seveau, S.; Muchardt, C.; Cossart, P., 2007: Histone modifications induced by a family of bacterial toxins. *Proceedings of the National Academy of Sciences*., **104**, 13467–13472.
94. Hamon, M. A.; Ribet, D.; Stavru, F.; Cossart, P., 2012: Listeriolysin O: the Swiss army knife of Listeria. *Trends in Microbiology*., **20**, 360–368.
95. Harrison, R. E.; Bucci, C.; Vieira, O. V.; Schroer, T. A.; Grinstein, S., 2003: Phagosomes fuse with late endosomes and/or lysosomes by extension of membrane protrusions along microtubules: role of Rab7 and RILP. *Molecular and Cellular Biology*., **23**, 6494–6506.
96. Henry, R.; Shaughnessy, L.; Loessner, M. J.; Alberti-Segui, C.; Higgins, D. E.; Swanson, J. A., 2006: Cytolysin-dependent delay of vacuole maturation in macrophages infected with Listeria monocytogenes. *Cellular Microbiology*., **8**, 107–119.
97. Hernández-Flores, K. G.; Vivanco-Cid, H., 2015: Biological Effects of Listeriolysin O: Implications for Vaccination. *BioMed Research International*., **2015**, 1–9.
98. Hersh, D.; Monack, D. M.; Smith, M. R.; Ghori, N.; Falkow, S.; Zychlinsky, A., 1999: The Salmonella invasin SipB induces macrophage apoptosis by binding to caspase-1. *Microbiology*., **96**, 2396–2401.
99. Hickey, C. M.; Wickner, W., 2010: HOPS initiates vacuole docking by tethering membranes before trans-SNARE complex assembly. *Molecular Biology of the Cell*., **21**, 2297–2305.
100. Hong, P. C.; Tsolis, R. M.; Ficht, T. A., 2000: Identification of genes required for chronic persistence of Brucella abortus in mice. *Infection and immunity*., **68**, 4102–4107.
101. Horiuchi, H.; Lippe, R.; McBride, H. M.; Rubino, M.; Woodman, P.; Stenmark, H.; Rybin, V.; Wilm, M.; Ashman, K.; Mann, M.; Zeria, M., 1997: A novel Rab5 GDP/GTP exchange factor complexed to Rabaptin-5 links nucleotide exchange to effector recruitment and function. *Cell*., **90**, 1149–1159.
102. Hoshyar, N.; Gray, S.; Han, H.; Bao, G., 2016: The effect of nanoparticle size on in vivo pharmacokinetics and cellular interaction. *Nanomedicine*., **11**, 673–692.
103. Huang, W. C.; Chiang, W. H.; Cheng, Y. H.; Lin, W. C.; Yu, C. F.; Yen, C. Y.; Yeh, C. K.; Chern, C. S.; Chiang, C. S.; Chiu, H. C., 2015: Tumortropic monocyte-mediated delivery of echogenic polymer bubbles and therapeutic vesicles for chemotherapy of tumor hypoxia. *Biomaterials*., **71**, 71–83.
104. Hughes, D.; Andersson, D. I., 2015: Evolutionary consequences of drug resistance: shared principles across diverse targets and organisms. *Nature Reviews Genetics*., **16**, 459–471.
105. Huynh, K. K.; Kay, J. G.; Stow, J. L.; Grinstein, S., 2007: Fusion, fission, and secretion during phagocytosis. *Physiology Bethesda*., **22**, 366–372.
106. Hybiske, K.; Stephens, R. S., 2007: Mechanisms of host cell exit by the intracellular bacterium Chlamydia. *Proceedings of the National Academy of Sciences*., **104**, 11430–11435.

107. Imhof, B. A.; Aurrand-Lions, M., 2004: Adhesion mechanisms regulating the migration of monocytes. *Nature Reviews Immunology*., **4**, 432–444.
108. Ireton, K.; Van Ngo, H.; Bhalla, M., 2018: Interaction of microbial pathogens with host exocytic pathways. *Cellular Microbiology*., **20**, 1–10.
109. Ishida, T.; Fujihara, N.; Nishimura, T.; Funabashi, H.; Hirota, R.; Ikeda, T.; Kuroda, A., 2019: Live-cell imaging of macrophage phagocytosis of asbestos fibers under fluorescence microscopy. *Genes and Environment*., **41**, 14.
110. Jahraus, A.; Storrie, B.; Griffiths, G.; Desjardins, M., 1994: Molecular characterization of phagosomes. *Journal of Cell Science*., **107**, 145–157.
111. Jahraus, A.; Tjelle, T. E.; Berg, T.; Habermann, A.; Storrie, B.; Ullrich, O.; Griffiths, G., 1998: In vitro fusion of phagosomes with different endocytic organelles. *Journal of Biological Chemistry*., **273**, 30379–30390.
112. Jesenberger, V.; Procyk, K. J.; Yuan, J.; Reipert, S.; Baccarini, M., 2000: Salmonella -Induced Caspase-2 Activation in Macrophages. *The Journal of Experimental Medicine*., **192**, 1035–1046.
113. Johansson, M.; Rocha, N.; Zwart, W.; Jordens, I.; Janssen, L.; Kuijl, C.; Olkkonen, V. M.; Neefjes, J., 2007: Activation of endosomal dynein motors by stepwise assembly of Rab7-RILP-p150Glued, ORP1L, and the receptor betaIII spectrin. *The Journal of Cell Biology*., **176**, 459–471.
114. Johnston, S. A.; May, R. C., 2010: The Human Fungal Pathogen Cryptococcus neoformans Escapes Macrophages by a Phagosome Emptying Mechanism That Is Inhibited by Arp2/3 Complex-Mediated Actin Polymerisation. (Levitz, S. M., Ed.)*PLoS Pathogens*., **6**, e1001041.
115. Johnston, S. A.; May, R. C., 2013: Cryptococcus interactions with macrophages: Evasion and manipulation of the phagosome by a fungal pathogen. *Cellular Microbiology*., **15**, 403–411.
116. Khan, M. A.; Muzammil, S.; Musarrat, J., 2002: Differential binding of tetracyclines with serum albumin and induced structural alterations in drug-bound protein. *International Journal of Biological Macromolecules*., **30**, 243–249.
117. Kim, H. K.; Park, T. G., 1999: Microencapsulation of human growth hormone within biodegradable polyester microspheres: Protein aggregation stability and incomplete release mechanism. *Biotechnology and Bioengineering*., **65**, 659–667.
118. Kinchen, J. M.; Doukoumetzidis, K.; Almendinger, J.; Stergiou, L.; Tosello-Trampont, A.; Sifri, C. D.; Hengartner, M. O.; Ravichandran, K. S., 2008: A pathway for phagosome maturation during engulfment of apoptotic cells. *Nature Cell Biology*., **10**, 556–566.
119. Kirby, J. E.; Vogel, J. P.; Andrews, H. L.; Isberg, R. R., 1998: Evidence for pore-forming ability by Legionella pneumophila. *Molecular Microbiology*., **27**, 323–336.
120. Kleynhans, J.; Elgar, D.; Ebenhan, T.; Zeevaart, J. R.; Kotzé, A.; Grobler, A., 2019: A toxicity profile of the Pheroid® technology in rodents. *Toxicology Reports*., **6**, 940–950.
121. Klyachko, N. L.; Haney, M. J.; Zhao, Y.; Manickam, D. S.; Mahajan, V.; Suresh, P.; Hingtgen, S. D.; Mosley, R. L.; Gendelman, H. E.; Kabanov, A. V; Batrakova, E. V, 2014: Macrophages offer a paradigm switch for CNS delivery of therapeutic proteins. *Nanomedicine (London, England)*., **9**, 1403–1422.
122. Knuff, K.; Finlay, B. B., 2017: What the SIF Is Happening-The Role of Intracellular Salmonella-Induced Filaments. *Frontiers in cellular and infection microbiology*., **7**, 335.
123. Kocks, C.; Hellio, R.; Gounon, P.; Ohayon, H.; Cossart, P., 1993: Polarized distribution of Listeria monocytogenes surface protein ActA at the site of directional actin assembly. *Journal of cell science*., **105 (Pt 3**, 699–710.
124. Kruger, M. J.; Myburgh, K. H.; Smith, C., 2014: Contusion injury with chronic in vivo polyphenol supplementation: leukocyte responses. *Medicine and science in sports and exercise*., **46**, 225–231.
125. Kwiatkowska, A.; Granicka, L. H.; Grzeczkowicz, A.; Stachowiak, R.; Kamiński, M.; Grubek, Z.; Bielecki, J.; Strawski, M.; Szklarczyk, M., 2017: Stabilized nanosystem of nanocarriers with an immobilized biological factor for anti-tumor therapy. *PloS one*., **12**, e0170925.
126. Langenau, D. M.; Ferrando, A. A.; Traver, D.; Kutok, J. L.; Hezel, J. P. D.; Kanki, J. P.; Zon, L. I.; Look, A. T.; Trede, N. S., 2004: In vivo tracking of T cell development, ablation, and engraftment in transgenic zebrafish. *Proceedings of the National Academy of Sciences of the United States of America*., **101**, 7369–7374.
127. Langer, R.; Folkman, J., 1976: Polymers for the sustained release of proteins and other macromolecules. *Nature*., **263**, 797–800.
128. LaRock, D. L.; Chaudhary, A.; Miller, S. I., 2015: Salmonellae interactions with host processes. *Nature Reviews Microbiology*., **13**, 191–205.
129. Lee, K. D.; Oh, Y. K.; Portnoy, D. A.; Swanson, J. A., 1996: Delivery of macromolecules into

cytosol using liposomes containing hemolysin from Listeria monocytogenes. *The Journal of biological chemistry*., **271**, 7249–7252.
130. Lee, Y.; Ryu, J. W.; Chang, H.; Sohn, J. Y.; Lee, K. W.; Woo, C. W.; Kang, H. J.; Jeong, S. Y.; Choi, E. K.; Lee, J. S., 2010: In vivo MR evaluation of the effect of the CCR2 antagonist on macrophage migration. *Magnetic Resonance in Medicine*., **64**, 72–79.
131. Lerm, B.; Kenyon, C.; Schwartz, I. S.; Kroukamp, H.; de Witt, R.; Govender, N. P.; de Hoog, G. S.; Botha, A., 2017: First report of urease activity in the novel systemic fungal pathogen Emergomyces africanus: a comparison with the neurotrope Cryptococcus neoformans. *FEMS yeast research*., **17**.
132. Li, W. hong, 2017: Probes for monitoring regulated exocytosis. *Cell Calcium*., **64**, 65–71.
133. Li, Z.; Zheng, Q.; Xue, X.; Shi, X.; Zhou, Y.; Da, F.; Qu, D.; Hou, Z.; Luo, X., 2016: Pyroptosis of Salmonella Typhimurium-infected macrophages was suppressed and elimination of intracellular bacteria from macrophages was promoted by blocking QseC. *Scientific Reports*., **6**, 37447.
134. Liu, W.; Xiao, X.; Demirci, G.; Madsen, J.; Li1, X. C., 2013: The innate NK cells and macrophages recognize and reject allogeneic non-self in vivo via different mechanisms. *The Journal of Immunology*., **188**, 2703–2711.
135. Lv, Y.; Hao, L.; Hu, W.; Ran, Y.; Bai, Y.; Zhang, L., 2016: Novel multifunctional pH-sensitive nanoparticles loaded into microbubbles as drug delivery vehicles for enhanced tumor targeting. *Scientific Reports*., **6**, 1–9.
136. Mallo, G. V; Espina, M.; Smith, A. C.; Terebiznik, M. R.; Alemán, A.; Finlay, B. B.; Rameh, L. E.; Grinstein, S.; Brumell, J. H., 2008: SopB promotes phosphatidylinositol 3-phosphate formation on Salmonella vacuoles by recruiting Rab5 and Vps34. *The Journal of cell biology*., **182**, 741–752.
137. Mandal, M.; Lee, K. D., 2002: Listeriolysin O-liposome-mediated cytosolic delivery of macromolecule antigen in vivo: Enhancement of antigen-specific cytotoxic T lymphocyte frequency, activity, and tumor protection. *Biochimica et Biophysica Acta - Biomembranes*., **1563**, 7–17.
138. McGourty, K.; Thurston, T. L.; Matthews, S. A.; Pinaud, L.; Mota, L. J.; Holden, D. W., 2012: Salmonella inhibits retrograde trafficking of mannose-6-phosphate receptors and lysosome function. *Science (New York, N.Y.)*., **338**, 963–967.
139. Mia, S.; Warnecke, A.; Zhang, X. M.; Malmström, V.; Harris, R. A., 2014: An optimized protocol for human M2 macrophages using M-CSF and IL-4/IL-10/TGF-β yields a dominant immunosuppressive phenotype. *Scandinavian Journal of Immunology*., **79**, 305–314.
140. Miller, M. A.; Zheng, Y. rong; Gadde, S.; Pfirschke, C.; Zope, H.; Engblom, C.; Kohler, R. H.; Iwamoto, Y.; Yang, K. S.; Askevold, B.; Kolishetti, N.; Pittet, M.; Lippard, S. J.; Farokhzad, O. C.; Weissleder, R., 2015: Tumour-associated macrophages act as a slow-release reservoir of nano-therapeutic Pt(IV) pro-drug. *Nature Communications*., **6**, 1–13.
141. Mills, C. D., 2012: M1 and M2 Macrophages: Oracles of Health and Disease. *Critical reviews in immunology*., **32**, 463–488.
142. Mills, C. D.; Ley, K.; Buchmann, K.; Canton, J., 2015: Sequential Immune Responses: The Weapons of Immunity. *Journal of Innate Immunity*., **7**, 443–449.
143. Misawa, T.; Takahama, M.; Kozaki, T.; Lee, H.; Zou, J.; Saitoh, T.; Akira, S., 2013: Microtubule-driven spatial arrangement of mitochondria promotes activation of the NLRP3 inflammasome. *Nature immunology*., **14**, 454–460.
144. Mitchell, G.; Ge, L.; Huang, Q.; Chen, C.; Kianian, S.; Roberts, M. F.; Schekman, R.; Portnoy, D. A., 2015: Avoidance of autophagy mediated by PlcA or ActA is required for Listeria monocytogenes growth in macrophages. *Infection and immunity*., **83**, 2175–2184.
145. Mitragotri, S.; Burke, P. A.; Langer, R., 2014: Overcoming the challenges in administering biopharmaceuticals: formulation and delivery strategies. *Nature Reviews Drug Discovery*., **13**, 655–672.
146. Molmeret, M., 2002: icmT Is Essential for Pore Formation-Mediated Egress of Legionella pneumophila from Mammalian and Protozoan Cells. *Infection and Immunity*., **70**, 69–78.
147. Molmeret, M.; Zink, S. D.; Han, L.; Abu-Zant, A.; Asari, R.; Bitar, D. M.; Abu Kwaik, Y., 2004: Activation of caspase-3 by the Dot/Icm virulence system is essential for arrested biogenesis of the Legionella-containing phagosome. *Cellular microbiology*., **6**, 33–48.
148. Moradin, N.; Descoteaux, A., 2012: Leishmania promastigotes: building a safe niche within macrophages. *Frontiers in cellular and infection microbiology*., **2**, 1–6.
149. Morishita, M.; Peppas, N. A., 2006: Is the oral route possible for peptide and protein drug delivery? *Drug Discovery Today*., **11**, 905–910.
150. Mosser, D. M.; Edwards, J. P., 2008: Exploring the full spectrum of macrophage activation.

Nature reviews. Immunology., **8**, 958–969.
151. Na, H. N.; Yoo, Y. H.; Yoon, C. N.; Lee, J. S., 2015: Unbiased Proteomic Profiling Strategy for Discovery of Bacterial Effector Proteins Reveals that Salmonella Protein PheA Is a Host Cell Cycle Regulator. *Chemistry & Biology*., **22**, 453–459.
152. Nance, E. A.; Woodworth, G. F.; Sailor, K. A.; Shih, T. Y.; Xu, Q.; Swaminathan, G.; Xiang, D.; Eberhart, C.; Hanes, J., 2012: A Dense Poly(Ethylene Glycol) Coating Improves Penetration of Large Polymeric Nanoparticles Within Brain Tissue. *Science Translational Medicine*., **4**, 149ra119-149ra119.
153. Ng, E. L.; Wang, Y.; Tang, B. L., 2007: Rab22B's role in trans-Golgi network membrane dynamics. *Biochemical and Biophysical Research Communications*., **361**, 751–757.
154. Nicola, A. M.; Robertson, E. J.; Albuquerque, P.; Derengowski, L. da S.; Casadevall, A., 2011: Nonlytic exocytosis of Cryptococcus neoformans from macrophages occurs in vivo and is influenced by phagosomal pH. *mBio*., **2**, e00167-11.
155. Nicola, A. M.; Albuquerque, P.; Martinez, L. R.; Dal-Rosso, R. A.; Saylor, C.; De Jesus, M.; Nosanchuk, J. D.; Casadevall, A., 2012: Macrophage autophagy in immunity to Cryptococcus neoformans and Candida albicans. *Infection and immunity*., **80**, 3065–3076.
156. Nimse, S. B.; Pal, D., 2015: Free radicals, natural antioxidants, and their reaction mechanisms. *RSC Advances*., **5**, 27986–28006.
157. Noireaux, V.; Golsteyn, R. M.; Friederich, E.; Prost, J.; Antony, C.; Louvard, D.; Sykes, C., 2000: Growing an actin gel on spherical surfaces. *Biophysical journal*., **78**, 1643–1654.
158. Oh, N.; Park, J. H., 2014: Endocytosis and exocytosis of nanoparticles in mammalian cells. *International journal of nanomedicine*., **9 Suppl 1**, 51–63.
159. Owen, M. R.; Byrne, H. M.; Lewis, C. E., 2004: Mathematical modelling of the use of macrophages as vehicles for drug delivery to hypoxic tumour sites. *Journal of theoretical biology*., **226**, 377–391.
160. Pang, L.; Qin, J.; Han, L.; Zhao, W.; Liang, J.; Xie, Z.; Yang, P.; Wang, J., 2016: Exploiting macrophages as targeted carrier to guide nanoparticles into glioma. *Oncotarget*., **7**, 37081–37091.
161. Pasut, G.; Veronese, F. M., 2012: State of the art in PEGylation: The great versatility achieved after forty years of research. *Journal of Controlled Release*., **161**, 461–472.
162. Patki, V.; Lawe, D. C.; Corvera, S.; Virbasius, J. V.; Chawla, A., 1998: A functional PtdIns(3)P-binding motif. *Nature*., **394**, 433–434.
163. Patra, J. K.; Das, G.; Fraceto, L. F.; Campos, E. V. R.; Rodriguez-Torres, M. del P.; Acosta-Torres, L. S.; Diaz-Torres, L. A.; Grillo, R.; Swamy, M. K.; Sharma, S.; Habtemariam, S.; Shin, H. S., 2018: Nano based drug delivery systems: recent developments and future prospects. *Journal of Nanobiotechnology*., **16**, 71.
164. Pei, J.; Turse, J. E.; Wu, Q.; Ficht, T. A., 2006: Brucella abortus Rough Mutants Induce Macrophage Oncosis That Requires Bacterial Protein Synthesis and Direct Interaction with the Macrophage. *Infection and Immunity*., **74**, 2667–2675.
165. Pei, J.; Wu, Q.; Kahl-McDonagh, M.; Ficht, T. A., 2008: Cytotoxicity in macrophages infected with rough Brucella mutants is type IV secretion system dependent. *Infection and immunity*., **76**, 30–37.
166. Pei, J.; Kahl-McDonagh, M.; Ficht, T. A., 2014: Brucella dissociation is essential for macrophage egress and bacterial dissemination. *Frontiers in cellular and infection microbiology*., **4**, 23.
167. Perfettini, J. L.; Hospital, V.; Stahl, L.; Jungas, T.; Verbeke, P.; Ojcius, D. M., 2003: Cell death and inflammation during infection with the obligate intracellular pathogen, Chlamydia. *Biochimie*., **85**, 763–769.
168. Petersen, K. S.; Smith, C., 2016: Ageing-Associated Oxidative Stress and Inflammation Are Alleviated by Products from Grapes. *Oxidative medicine and cellular longevity*., **2016**, 6236309.
169. Pierce, M. M.; Gibson, R. E.; Rodgers, F. G., 1996: Opsonin-independent adherence and phagocytosis of Listeria monocytogenes by murine peritoneal macrophages. *Journal of medical microbiology*., **45**, 258–262.
170. Pillich, H.; Puri, M.; Chakraborty, T., 2017: ActA of Listeria monocytogenes and Its Manifold Activities as an Important Listerial Virulence Factor. *Current topics in microbiology and immunology*., **399**, 113–132.
171. Pizarro-Cerda, J.; Kuhbacher, A.; Cossart, P., 2012: Entry of Listeria monocytogenes in Mammalian Epithelial Cells: An Updated View. *Cold Spring Harbor Perspectives in Medicine*., **2**, a010009–a010009.
172. Pizarro-Cerdá, J.; Moreno, E.; Sanguedolce, V.; Mege, J. L.; Gorvel, J. P., 1998: Virulent Brucella abortus prevents lysosome fusion and is distributed within autophagosome-like

compartments. *Infection and immunity*., **66**, 2387–2392.
173. Press, B.; Feng, Y.; Hoflack, B.; Wandinger-Ness, A., 1998: Mutant Rab7 causes the accumulation of cathepsin D and cation-independent mannose 6-phosphate receptor in an early endocytic compartment. *The Journal of Cell Biology*., **140**, 1075–1089.
174. Proal, A. D.; Lindseth, I. A.; Marshall, T. G., 2017: Microbe-microbe and host-microbe interactions drive microbiome dysbiosis and inflammatory processes. *Discovery medicine*., **23**, 51–60.
175. Provoda, C. J.; Stier, E. M.; Lee, K. D., 2003: Tumor cell killing enabled by listeriolysin O-liposome-mediated delivery of the protein toxin gelonin. *Journal of Biological Chemistry*., **278**, 35102–35108.
176. Qin, Q. M.; Luo, J.; Lin, X.; Pei, J.; Li, L.; Ficht, T. A.; de Figueiredo, P., 2011: Functional Analysis of Host Factors that Mediate the Intracellular Lifestyle of Cryptococcus neoformans. (Andrianopoulos, A., Ed.)*PLoS Pathogens*., **7**, e1002078.
177. Queval, C. J.; Song, O. R.; Carralot, J. P.; Saliou, J. M.; Bongiovanni, A.; Deloison, G.; Deboosère, N.; Jouny, S.; Iantomasi, R.; Delorme, V.; Debrie, A. S.; Park, S. J.; Gouveia, J. C.; Tomavo, S.; Brosch, R.; Yoshimura, A.; Yeramian, E.; Brodin, P., 2017: Mycobacterium tuberculosis Controls Phagosomal Acidification by Targeting CISH-Mediated Signaling. *Cell Reports*., **20**, 3188–3198.
178. Quigley, J.; Hughitt, V. K.; Velikovsky, C. A.; Mariuzza, R. A.; El-Sayed, N. M.; Briken, V., 2017: The Cell Wall Lipid PDIM Contributes to Phagosomal Escape and Host Cell Exit of Mycobacterium tuberculosis. *mBio*., **8**, e00148-17.
179. Rai, M. N.; Sharma, V.; Balusu, S.; Kaur, R., 2015: An essential role for phosphatidylinositol 3-kinase in the inhibition of phagosomal maturation, intracellular survival and virulence in Candida glabrata. *Cellular Microbiology*., **17**, 269–287.
180. Redpath, S.; Ghaza, I. P.; Gascoigne, N. R., 2001: Hijacking and exploitation of IL-10 by intracellular pathogens. *Trends in Microbiology*., **9**, 86–92.
181. Renshaw, P. S.; Panagiotidou, P.; Whelan, A.; Gordon, S. V; Hewinson, R. G.; Williamson, R. A.; Carr, M. D., 2002: Conclusive evidence that the major T-cell antigens of the Mycobacterium tuberculosis complex ESAT-6 and CFP-10 form a tight, 1:1 complex and characterization of the structural properties of ESAT-6, CFP-10, and the ESAT-6*CFP-10 complex. Implications for p. *The Journal of biological chemistry*., **277**, 21598–21603.
182. Roy, C. R.; Berger, K. H.; Isberg, R. R., 1998: Legionella pneumophila DotA protein is required for early phagosome trafficking decisions that occur within minutes of bacterial uptake. *Molecular Microbiology*., **28**, 663–674.
183. Ruytinx, P.; Proost, P.; Van Damme, J.; Struyf, S., 2018: Chemokine-Induced Macrophage Polarization in Inflammatory Conditions. *Frontiers in immunology*., **9**, 1930.
184. Rzomp, K. A.; Scholtes, L. D.; Briggs, B. J.; Whittaker, G. R.; Scidmore, M. A., 2003: Rab GTPases are recruited to chlamydial inclusions in both a species-dependent and species-independent manner. *Infection and immunity*., **71**, 5855–5870.
185. Samie, M. A.; Xu, H., 2014: Lysosomal exocytosis and lipid storage disorders. *Journal of lipid research*., **55**, 995–1009.
186. Sano, G.; Takada, Y.; Goto, S.; Maruyama, K.; Shindo, Y.; Oka, K.; Matsui, H.; Matsuo, K., 2007: Flagella Facilitate Escape of Salmonella from Oncotic Macrophages. *Journal of Bacteriology*., **189**, 8224–8232.
187. Santos, J. C.; Duchateau, M.; Fredlund, J.; Weiner, A.; Mallet, A.; Schmitt, C.; Matondo, M.; Hourdel, V.; Chamot-Rooke, J.; Enninga, J., 2015: The COPII complex and lysosomal VAMP7 determine intracellular *Salmonella* localization and growth. *Cellular Microbiology*., **17**, 1699–1720.
188. Schafer, D. A.; Jennings, P. B.; Cooper, J. A., 1998: Rapid and efficient purification of actin from nonmuscle sources. *Cell Motility and the Cytoskeleton*., **39**, 166–171.
189. Schägger, H., 2006: Tricine-SDS-PAGE. *Nature Protocols*., **1**, 16–22.
190. Schlame, M.; Rua, D.; Greenberg, M. L., 2000: The biosynthesis and functional role of cardiolipin. *Progress in Lipid Research*., **39**, 257–288.
191. Schroeder, G. N., 2018: The Toolbox for Uncovering the Functions of Legionella Dot/Icm Type IVb Secretion System Effectors: Current State and Future Directions. *Frontiers in Cellular and Infection Microbiology*., **7**, 528.
192. Schubert, M.; Steude, A.; Liehm, P.; Kronenberg, N. M.; Karl, M.; Campbell, E. C.; Powis, S. J.; Gather, M. C., 2015: Lasing within Live Cells Containing Intracellular Optical Microresonators for Barcode-Type Cell Tagging and Tracking. *Nano letters*., **15**, 5647–5652.
193. Scidmore, M. A.; Fischer, E. R.; Hackstadt, T., 2003: Restricted Fusion of Chlamydia

trachomatis Vesicles with Endocytic Compartments during the Initial Stages of Infection. *INFECTION AND IMMUNITY*., **71**, 973–984.
194. Scott, C. C.; Cuellar-Mata, P.; Matsuo, T.; Davidson, H. W.; Grinstein, S., 2002: Role of 3-phosphoinositides in the maturation of Salmonella-containing vacuoles within host cells. *The Journal of Biological Chemistry*., **277**, 12770–12776.
195. Sendide, K.; Deghmane, A. E.; Pechkovsky, D.; Av-Gay, Y.; Talal, A.; Hmama, Z., 2005: Mycobacterium bovis BCG attenuates surface expression of mature Class II molecules through IL-10–dependent inhibition of cathepsin S. *The Journal of Immunology*., **175**, 5324–5332.
196. Seto, S.; Matsumoto, S.; Tsujimura, K.; Koide, Y., 2010: Differential recruitment of CD63 and Rab7-interacting-lysosomal-protein to phagosomes containing Mycobacterium tuberculosis in macrophages. *Microbiology and Immunology*., **54**, 170–174.
197. Seto, S.; Tsujimura, K.; Koide, Y., 2011: Rab GTPases Regulating Phagosome Maturation Are Differentially Recruited to Mycobacterial Phagosomes. *Traffic*., **12**, 407–420.
198. Shaughnessy, L. M.; Hoppe, A. D.; Christensen, K. A.; Swanson, J. A., 2006: Membrane perforations inhibit lysosome fusion by altering pH and calcium in Listeria monocytogenes vacuoles. *Cellular Microbiology*., **8**, 781–792.
199. Shi, M.; Zhang, Y.; Liu, L.; Zhang, T.; Han, F.; Cleveland, J.; Wang, F.; McKeehan, W. L.; Li, Y.; Zhang, D., 2016: MAP1S protein regulates the phagocytosis of bacteria and toll-like receptor (TLR) signaling. *Journal of Biological Chemistry*., **291**, 1243–1250.
200. Shi, Y.; Moon, M.; Dawood, S.; McManus, B.; Liu, P. P., 2011: Mechanisms and management of doxorubicin cardiotoxicity. *Herz*., **36**, 296–305.
201. Simeone, R.; Sayes, F.; Song, O.; Gröschel, M. I.; Brodin, P.; Brosch, R.; Majlessi, L., 2015: Cytosolic access of Mycobacterium tuberculosis: critical impact of phagosomal acidification control and demonstration of occurrence in vivo. *PLoS pathogens*., **11**, e1004650.
202. Simonsen, A.; Lippe, R.; Christoforidis, S.; Gaullier, J. M.; Brech, A.; Callaghan, J.; Toh, B. H.; Murphy, C.; Zerial, M.; Stenmark, H., 1998: EEA1 links PI3K function to Rab5 regulation of endosome fusion. *Nature*., **394**.
203. Simpkins, F.; Flores, A.; Chu, C.; Berek, J. S.; Lucci, J.; Murray, S.; Bauman, J.; Struemper, H.; Germaschewski, F.; Jonak, Z.; Gardner, O.; Toso, J.; Coukos, G., 2013: Chemoimmunotherapy Using Pegylated Liposomal Doxorubicin and Interleukin-18 in Recurrent Ovarian Cancer: A Phase I Dose-Escalation Study. *Cancer Immunology Research*., **1**, 168–178.
204. Sishi, B. J. N.; Loos, B.; van Rooyen, J.; Engelbrecht, A. M., 2013a: Autophagy upregulation promotes survival and attenuates doxorubicin-induced cardiotoxicity. *Biochemical Pharmacology*., **85**, 124–134.
205. Sishi, B. J. N.; Loos, B.; van Rooyen, J.; Engelbrecht, A. M., 2013b: Doxorubicin induces protein ubiquitination and inhibits proteasome activity during cardiotoxicity. *Toxicology*., **309**, 23–29.
206. Skoble, J.; Portnoy, D. A.; Welch, M. D., 2000: Three regions within ActA promote Arp2/3 complex-mediated actin nucleation and listeria monocytogenes motility. *Journal of Cell Biology*., **150**, 527–537.
207. Smith, C.; Kruger, M. J.; Smith, R. M.; Myburgh, K. H., 2008: The Inflammatory Response to Skeletal Muscle Injury. *Sports Medicine*., **38**, 947–969.
208. Smith, E. P.; Miller, C. N.; Child, R.; Cundiff, J. A.; Celli, J., 2016: Postreplication Roles of the Brucella VirB Type IV Secretion System Uncovered via Conditional Expression of the VirB11 ATPase. *mBio*., **7**, e01730-16.
209. Smith, G. A.; Marquis, H.; Jones, S.; Johnston, N. C.; Portnoy, D. A.; Goldfine, H., 1995: The two distinct phospholipases C of Listeria monocytogenes have overlapping roles in escape from a vacuole and cell-to-cell spread. *Infection and immunity*., **63**, 4231–4237.
210. Smith, L. M.; Dixon, E. F.; May, R. C., 2015: The fungal pathogen *C ryptococcus neoformans* manipulates macrophage phagosome maturation. *Cellular Microbiology*., **17**, 702–713.
211. Starr, T.; Ng, T. W.; Wehrly, T. D.; Knodler, L. A.; Celli, J., 2008: Brucella Intracellular Replication Requires Trafficking Through the Late Endosomal/Lysosomal Compartment. *Traffic*., **9**, 678–694.
212. Starr, T.; Child, R.; Wehrly, T. D.; Hansen, B.; Hwang, S.; López-Otin, C.; Virgin, H. W.; Celli, J., 2012: Selective Subversion of Autophagy Complexes Facilitates Completion of the Brucella Intracellular Cycle. *Cell Host & Microbe*., **11**, 33–45.
213. Steele-Mortimer, O.; Méresse, S.; Gorvel, J. P.; Toh, B. H.; Finlay, B. B., 1999: Biogenesis of Salmonella typhimurium-containing vacuoles in epithelial cells involves interactions with the early endocytic pathway. *Cellular microbiology*., **1**, 33–49.
214. Steenbergen, J. N.; Casadevall, A., 2003: The origin and maintenance of virulence for the human pathogenic fungus Cryptococcus neoformans. *Microbes and infection*., **5**, 667–675.

215. Stephens, R.; Kalman, S.; Mitchell, W.; Marathe, R.; Lammel, C.; Fan, J.; Hyman, R. W.; Olinger, L.; Grimwood, J.; Davis, R. W., 1999: Comparative genomes of Chlamydia pneumoniae and C. trachomatis. *Nature Genetics*., **21**, 385–389.
216. Stier, E. M.; Mandal, M.; Lee, K. D., 2005: Differential cytosolic delivery and presentation of antigen by listeriolysin O-liposomes to macrophages and dendritic cells. *Molecular Pharmaceutics*., **2**, 74–82.
217. Strahl, T.; Thorner, J., 2007: Synthesis and function of membrane phosphoinositides in budding yeast, Saccharomyces cerevisiae. *Biochimica et Biophysica Acta*., **1771**, 353–404.
218. Sturgill-Koszycki, S.; Schlesinger, P. H.; Chakraborty, P.; Haddix, P. L.; Collins, H. L.; Fok, A. K.; Allen, R. D.; Gluck, S. L.; Heuser, J.; Russell, D. G., 1994: Lack of acidification in Mycobacterium phagosomes produced by exclusion of the vesicular proton-ATPase. *Science (New York, N.Y.)*., **263**, 678–681.
219. Sugahara, K. N.; Teesalu, T.; Karmali, P. P.; Kotamraju, V. R.; Agemy, L.; Greenwald, D. R.; Ruoslahti, E., 2010: Coadministration of a Tumor-Penetrating Peptide Enhances the Efficacy of Cancer Drugs. *Science*., **328**, 1031–1035.
220. Swanson, J. A.; Hoppe, A. D., 2004: The coordination of signaling during Fc receptor-mediated phagocytosis. *Journal of Leukocyte Biology*., **76**, 1093–1103.
221. Takeuchi, H.; Furuta, N.; Morisaki, I.; Amano, A., 2011: Exit of intracellular Porphyromonas gingivalis from gingival epithelial cells is mediated by endocytic recycling pathway. *Cellular Microbiology*., **13**, 677–691.
222. Tammam, S. N.; Azzazy, H. M. E.; Lamprecht, A., 2017: The effect of nanoparticle size and NLS density on nuclear targeting in cancer and normal cells; impaired nuclear import and aberrant nanoparticle intracellular trafficking in glioma. *Journal of Controlled Release*., **253**, 30–36.
223. Tanei, T.; Leonard, F.; Liu, X.; Alexander, J. F.; Saito, Y.; Ferrari, M.; Godin, B.; Yokoi, K., 2016: Redirecting Transport of Nanoparticle Albumin-Bound Paclitaxel to Macrophages Enhances Therapeutic Efficacy against Liver Metastases. *Cancer research*., **76**, 429–439.
224. Tilney, L. G.; Harb, O. S.; Connelly, P. S.; Robinson, C. G.; Roy, C. R., 2001: How the parasitic bacterium Legionella pneumophila modifies its phagosome and transforms it into rough ER: implications for conversion of plasma membrane to the ER membrane. *Journal of cell science*., **114**, 4637–4650.
225. Traub, W. H.; Bauer, D., 1995: Simplified purification of Listeria monocytogenes listeriolysin O and preliminary application in the enzyme-linked immunosorbent assay (ELISA). *Zentralblatt fur Bakteriologie : international journal of medical microbiology*., **283**, 29–42.
226. Tucker, S. C.; Casadevall, A., 2002: Replication of Cryptococcus neoformans in macrophages is accompanied by phagosomal permeabilization and accumulation of vesicles containing polysaccharide in the cytoplasm. *Proceedings of the National Academy of Science of the United States of America*., **99**, 3165–3170.
227. Underhill, D. M.; Goodridge, H. S., 2012: Information processing during phagocytosis. *Nature reviews. Immunology*., **12**, 492–502.
228. Vadia, S.; Arnett, E.; Haghighat, A. C.; Wilson-Kubalek, E. M.; Tweten, R. K.; Seveau, S., 2011: The pore-forming toxin listeriolysin O mediates a novel entry pathway of L. monocytogenes into human hepatocytes. *PLoS pathogens*., **7**, e1002356.
229. Van Goethem, E.; Poincloux, R.; Gauffre, F.; Maridonneau-Parini, I.; Le Cabec, V., 2010: Matrix Architecture Dictates Three-Dimensional Migration Modes of Human Macrophages: Differential Involvement of Proteases and Podosome-Like Structures. *The Journal of Immunology*., **184**, 1049–1061.
230. van Staden, A. D. P.; Brand, A. M.; Dicks, L. M. T., 2012: Nisin F-loaded brushite bone cement prevented the growth of Staphylococcus aureus in vivo. *Journal of applied microbiology*., **112**, 831–840.
231. van Staden, A. D. P.; Faure, L. M.; Vermeulen, R. R.; Dicks, L. M. T.; Smith, C., 2019: Functional Expression of GFP-Fused Class I Lanthipeptides in Escherichia coli. *ACS Synthetic Biology*., **8**, 2220–2227.
232. Veiga, E.; Cossart, P., 2005: Listeria hijacks the clathrin-dependent endocytic machinery to invade mammalian cells. *Nature Cell Biology*., **7**, 894–900.
233. Vergne, I.; Chua, J.; Deretic, V., 2003: Mycobacterium tuberculosis Phagosome Maturation Arrest: Selective Targeting of PI3P-Dependent Membrane Trafficking. *Traffic*., **4**, 600–606.
234. Vergne, I.; Chua, J.; Lee, H. H.; Lucas, M.; Belisle, J.; Deretic, V., 2005: Mechanism of phagolysosome biogenesis block by viable Mycobacterium tuberculosis. *Proceedings of the National Academy of Sciences of the United States of America*., **102**, 4033–4038.
235. Vieira, O. V.; Botelho, R. J.; Rameh, L.; Brachmann, S. M.; Matsuo, T.; Davidson, H. W.;

Schreiber, A.; Backer, J. M.; Cantley, L. C.; Grinstein, S., 2001: Distinct roles of class I and class III phosphatidylinositol 3-kinases in phagosome formation and maturation. *Journal of Cell Biology*., **155**, 19–25.
236. Vieira, O. V; Botelho, R. J.; Grinstein, S., 2002: Phagosome maturation: aging gracefully. *The Biochemical Journal*., **366**, 689–704.
237. Vinet, A. F.; Fukuda, M.; Turco, S. J.; Descoteaux, A., 2009: The Leishmania donovani Lipophosphoglycan Excludes the Vesicular Proton-ATPase from Phagosomes by Impairing the Recruitment of Synaptotagmin. *Public Library of Science Pathogens*., **5**, e1000628.
238. Visser, J. G.; Smith, C., 2018: Development of a transendothelial shuttle by macrophage modification. *Journal of Tissue Engineering and Regenerative Medicine*., **12**, e1889–e1898.
239. Visser, J. G.; Van Staden, A. D. P.; Smith, C., 2019: Harnessing macrophages for controlled-release drug delivery: Lessons from microbes. *Frontiers in Pharmacology*., **9**, 1–18.
240. Volceanov, L.; Herbst, K.; Biniossek, M.; Schilling, O.; Haller, D.; Nölke, T.; Subbarayal, P.; Rudel, T.; Zieger, B.; Häcker, G., 2014: Septins arrange F-actin-containing fibers on the Chlamydia trachomatis inclusion and are required for normal release of the inclusion by extrusion. *mBio*., **5**, e01802-14.
241. von Bargen, K.; Gorvel, J. P.; Salcedo, S. P., 2012: Internal affairs: Investigating the Brucella intracellular lifestyle. *FEMS Microbiology Reviews*.
242. Walburger, A.; Koul, A.; Ferrari, G.; Nguyen, L.; Prescianotto-Baschong, C.; Huygen, K.; Klebl, B.; Thompson, C.; Bacher, G.; Pieters, J., 2004: Protein kinase G from pathogenic mycobacteria promotes survival within macrophages. *Science (New York, N.Y.)*., **304**, 1800–1804.
243. Wang, Q.; Liu, S.; Hu, D.; Wang, Z.; Wang, L.; Wu, T.; Wu, Z.; Mohan, C.; Peng, A., 2016: Identification of apoptosis and macrophage migration events in paraquat-induced oxidative stress using a zebrafish model. *Life sciences*., **157**, 116–124.
244. Warstler, A.; Bean, J., 2016: Antimicrobial-induced cognitive side effects. *Mental Health Clinician*., **6**, 207–214.
245. Watson, K. G.; Holden, D. W., 2010: Dynamics of growth and dissemination of Salmonella in vivo. *Cellular Microbiology*., **12**, 1389–1397.
246. Weigele, B. A.; Orchard, R. C.; Jimenez, A.; Cox, G. W.; Alto, N. M., 2017: A systematic exploration of the interactions between bacterial effector proteins and host cell membranes. *Nature Communications*., **8**, 532.
247. Welch, M. D.; Rosenblatt, J.; Skoble, J.; Portnoy, D. A.; Mitchison, T. J., 1998: Interaction of Human Arp2/3 Complex and the Listeria monocytogenes ActA Protein in Actin Filament Nucleation. *Science*., **281**, 105–109.
248. Welch, M. D.; Way, M., 2013: Arp2/3-mediated actin-based motility: a tail of pathogen abuse. *Cell host & microbe*., **14**, 242–255.
249. Wong, D.; Bach, H.; Sun, J.; Hmama, Z.; Av-Gay, Y., 2011: Mycobacterium tuberculosis protein tyrosine phosphatase (PtpA) excludes host vacuolar-H+-ATPase to inhibit phagosome acidification. *Proceedings of the National Academy of Sciences of the United States of America*., **108**, 19371–19376.
250. Wozniak, K. L.; Levitz, S. M., 2008: Cryptococcus neoformans enters the endolysosomal pathway of dendritic cells and is killed by lysosomal components. *Infection and immunity*., **76**, 4764–4771.
251. Xu, L.; Luo, Z. Q., 2013: Cell biology of infection by Legionella pneumophila. *Microbes and Infection*., **15**, 157–167.
252. Yasinzai, M.; Khan, M.; Nadhman, A.; Shahnaz, G., 2013: Drug resistance in leishmaniasis: current drug-delivery systems and future perspectives. *Future Medicinal Chemistry*., **5**, 1877–1888.
253. Yilmaz, O.; Verbeke, P.; Lamont, R. J.; Ojcius, D. M., 2006: Intercellular Spreading of Porphyromonas gingivalis Infection in Primary Gingival Epithelial Cells. *Infection and Immunity*., **74**, 703–710.
254. Yousefpour, P.; Chilkoti, A., 2014: Co-opting biology to deliver drugs. *Biotechnology and bioengineering*., **111**, 1699–1716.
255. Youshia, J.; Lamprecht, A., 2016: Size-dependent nanoparticulate drug delivery in inflammatory bowel diseases. *Expert Opinion on Drug Delivery*., **13**, 281–294.
256. Zaragoza, O.; Chrisman, C. J.; Castelli, M. V.; Frases, S.; Cuenca-Estrella, M.; Rodríguez-Tudela, J. L.; Casadevall, A., 2008: Capsule enlargement in Cryptococcus neoformans confers resistance to oxidative stress suggesting a mechanism for intracellular survival. *Cellular microbiology*., **10**, 2043–2057.
257. Zareifopoulos, N.; Panayiotakopoulos, G., 2017: Neuropsychiatric Effects of Antimicrobial

Agents. *Clinical Drug Investigation*., **37**, 423–437.
258. Zhang, Q.; Raoof, M.; Chen, Y.; Sumi, Y.; Sursal, T.; Junger, W.; Brohi, K.; Itagaki, K.; Hauser, C. J., 2010: Circulating mitochondrial DAMPs cause inflammatory responses to injury. *Nature*., **464**, 104–107.
259. Zhang, Q.; Wang, D.; Jiang, G.; Liu, W.; Deng, Q.; Li, X.; Qian, W.; Ouellet, H.; Sun, J., 2016: EsxA membrane-permeabilizing activity plays a key role in mycobacterial cytosolic translocation and virulence: effects of single-residue mutations at glutamine 5. *Scientific Reports*., **6**, 32618.
260. Zhao, L.; Seth, A.; Wibowo, N.; Zhao, C. X.; Mitter, N.; Yu, C.; Middelberg, A. P. J., 2014: Nanoparticle vaccines. *Vaccine*., **32**, 327–337.
261. Zhao, Y.; Haney, M. J.; Mahajan, V.; Reiner, B. C.; Dunaevsky, A.; Mosley, R. L.; Kabanov, A. V; Gendelman, H. E.; Batrakova, E. V, 2011: Active Targeted Macrophage-mediated Delivery of Catalase to Affected Brain Regions in Models of Parkinson's Disease. *Journal of nanomedicine & nanotechnology*., **S4**.

Appendices

Appendix 1: Basic macrophage biology and the Molecular Basis of Phagocytosis

The M1 macrophage phenotype is the only phenotype to have been shown to migrate through endothelial barriers (Arnold et al., 2007 b; Chazaud et al., 2009). This phenotype is also honed toward particle engulfment and digestion, and is the main phenotype to which inflammatory monocytes differentiate (Imhof et al., 2004; Freeman et al., 2014). Monocytes have a relatively short lifespan in circulation (10-20 hours) (Guyton et al., 2011). Extravasation of monocytes is needed to induce differentiation into resident tissue macrophages. This process ensures a significant increase in lifespan through the protective and nutrient- and chemokine-rich extra-circulatory environment that augment cell survival. The M2 phenotype is more closely associated with resolution of inflammation (Abbas et al., 2014) and macrophages do present with some phenotype plasticity (Mosser et al., 2008). Thus, it is an additional future aspect of this project to determine if delivered M1 macrophages are able to shift toward the M2 phenotype after deposition of cargo. This would have to be tested *in vivo*.

Recognition

Macrophages recognise matter as foreign via binding to different pattern recognition receptors (PRRs) found on immune cells of both the innate and adaptive branch (Anderson et al., 2012). PRRs differentiate between molecules released from dying self-cells and foreign material through binding to damage-associated molecular patterns (DAMPs) and pathogen-associated molecular patterns (PAMPs), respectively (Abbas et al., 2014). Self-cells undergoing necrosis release formylated peptides such as N-formylmethionine from damaged mitochondria (Zhang et al., 2010). These self-originating DAMPs can bind to formyl peptide receptors on monocytic cells, initiating chemotaxis and eventualy phagocytosis (Bardoel et al., 2011). Recognition of PAMPs is oriented toward many PRR subtypes, such as NOD-like receptors (NLRs) (recognise DAMPs as well), RIG-like receptors (RLRs) and Toll-like receptors (TLRs). NLRs are mainly associated with sterile inflammation like gout via NLRP3 associated inflammasome formation (Misawa et al., 2013). The membrane bound TLRs bind bacterial hallmark molecules. The TLR5 subtype typically binds to flagella, while TLR2 and TLR4 binds bacterial cell wall components like peptidoglycan and lipopolysaccharide (LPS), respectively (Abbas et al., 2014).

IgG receptors are more closely associated with phagocytosis. IgG antibodies attach to microbes to opsonise them. This opsonisation facilitates phagocytosis of material. Macrophages recognise the constant γ heavy chain in Fc regions of IgG antibodies with Fcγ receptors (CD64) on their cell surface. Recognition induces FcγR clustering and subsequent actin polymerization and engulfment through pseudopod extension (Swanson et al., 2004). Pseudopodia formation and actin polymerization is dependent on PI3k recruitment for production of phosphatidylinositides. FcγR mediated phagocytosis is the main form of phagocytosis simulated in experimental phagocytosis models, because engulfment does not require stimulation by other cells types like T cells or NK cells (Liu et al., 2013).

Pseudopodia and Encapsulation

Phagocytosis is initiated by extension of pseudopodia. Internalisation and nascent phagosome formation are completed within 5 min (Visser & Smith, unpublished data). Macrophages are extremely ambitious in their phagocytic ability and are able to engulf particles that are closely comparable with their own size (Huynh et al., 2007). This leads to the question of where the extra membrane is produced. This can be addressed by looking at the type III PI3k.

The type III PI3ks consists of one catalytic subunit in humans, hVPS34. Type III PI3ks phosphorylate phosphatidylinositol (PI) to PI3P on endosomes and autophagosomal structures (Backer, 2008). Formation of PI3P is accompanied by the closure of the phagocytic cup and subsequent disappearance of PI(4,5)P2 (Botelho et al., 2000) that lead to and are essential for maturation of newly formed phagosomes (Vieira et al., 2001). Thus, PI3P function is centred more around phagosomal/endosomal maturation than as a source of extra membrane during engulfment.

Nascent Phagosomal Stage

This stage can be distinguished from engulfment by phagocytic cup closure behind the engulfed material of interest. Pseudopod closure is dependent on type I PI3k, PIP_3 and PI(4,5)P2. Inhibition of PI3k with, LY294002, prevented antibody opsonized particle engulfment as a result of unsuccessful pseudopod closure (Beemiller et al., 2006).

The successfully engulfed material is encapsulated into a nascent phagosome expressing Rab5 (Fairn et al., 2012). Rabex-5 is requited an activates Rab5 (Horiuchi et al., 1997). Rab5 then recruits endosomal early antigen 1 (EEA1) (Scott et al., 2002) and the type III PI3k, hVPS34, (Kinchen et al., 2008) to the phagosome. PI3P is generated by hVPS34 on the cytosolic side of the nascent phagosome and serves as a docking station for other maturation effectors. EEA1 can then dock onto PI3P and ensures EEA1-mediated tethering and fusion of phagosomes with late endosomes for further maturation (Vieira et al., 2002). EEA1 thus plays a central role in phagosome maturation.

Late Phagosomal Stage

GTPase-activating protein (GAP) mediates Rab5 inactivation and dissociation, marking the late phagosomal stage (Fairn et al., 2012). This is accompanied by Rab7 recruitment, late endosome fusion, expression of markers like mannose-6-phosphate receptor (MPR), lysobisphosphatidic acid (Fratti et al., 2001) and LAMP (Desjardins, 1995). During this stage, PI3P is incorporated and degraded inside the phagosome (Gillooly et al., 2000). Elimination of PI3P is likely necessary for removal of nascent phagosomal markers, dependent on PI3P expression, such as EEA1. The late phagosomal stage is initiated, *in vitro*, at about 10-30 min after formation of the nascent phagosome (Fratti et al., 2001). This coincides with PI3P disappearance at 10 min after its formation (Vieira et al., 2001).

The expression of Rab7 on both late endosomes and late phagosomes allows Rab7 to regulate membrane trafficking between nascent phagosomes, late phagosomes and lysosomes (Press et al., 1998). Fusion between nascent phagosomes and late endosomes could allow for close proximity of Rab7 and PI3P that facilitates SNX retromer functioning (Cullen et al., 2011). Thus, SNX retromers likely recycle cargo between nascent phagosomes and late phagosomes. Rab7 accelerates maturation to the phagolysosome biogenesis stage via the action of Rab7-interacting-lysosomal-protein (RILP) (Harrison et al., 2003). RILP and oxysterol-binding protein related-

protein 1 (ORP1L) together link phagosomes to dynein (Johansson et al., 2007), for centripetal movement of late phagosomes along microtubules toward lysosomes for fusion (Harrison et al., 2003). Dynein mediated lysosome fusion is likely dependent on Rab7 and the HOPS complex (Akbar et al., 2011). HOPS acts as a tethering protein, keeping phagosomes and lysosomes in close proximity to each other, similar to the function of EEA1 (Hickey et al., 2010).

Phagolysosome Biogenesis Stage

Lysosomal fusion with phagosomes is the final stage in maturation, referred to as phagolysosome biogenesis (Seto et al., 2011). This stage is achieved around 1 h after formation of nascent phagosomes, under *in vitro* conditions (Jahraus et al., 1998). SNARE proteins mediate fusion (syntaxin 7, syntaxin 8, VAMP7 and VAMP8) (Becken et al., 2010) and provide phagolysosomes with proteases (e.g. cathepsin D), reactive nitrogen species (RNS) and reactive oxygen species (ROS) with which to neutralize ingested particles. Fusion also elevates LAMP expression and facilitates an acidic phagosomal lumen (Jahraus et al., 1994).

Phagolysosomal degradation of protein is hugely dependant on proteases such as cathepsin D. Delivery of this protease is controlled by the trans-Golgi network-localised Rabs (22b, 32, 34,38 and 43) (Ng et al., 2007). Blockage of cathepsin D delivery resulted in phagosome maturation arrest. The ER-localized Rab20, was reported to co-localize with V-ATPases on phagosomes, suggesting its involvement during phagosome acidification (Curtis et al., 2005).

It seems that phagocytosis has evolved from endocytic nutrient processing to a specialized self-defence mechanism conserved uniquely to professional phagocytes. This phenomenon can, however, still be manipulated and applied to therapy, as the focus of the current study.

Appendix 2: ActA Expression Optimisation

Expression of ActA proved difficult as degradation was evident when separated via SDS-PAGE. Initial experiments using GFP-ActA resulted in significant degradation even at different incubation times after expression (**Figure 1**). Cleavage of GFP-ActA with WELQut protease resulted in dropouts corresponding to ActA and GFP, but with significant degradation (**Figure 2**). In order to better visualize the degradation, a second fluorescent marker (mCherry) was incorporated at the C-terminal of GFP-ActA. Before and after cleavage of GFP-ActA-mCherry with WELQuet protease and separation using SDS-PAGE, clear degradation patterns could be observed (**Figure 3**). From the fluorescent image of the SDS-PAGE gel multiple red fluorescent bands could be observed, which corresponds to different ActA-mCherry products (intact ActA-mCherry and degradation products). The degradation patterns do not give much insight into where the degradation takes place, due to the aberrant migration of ActA in SDS-PAGE gels. It is possible that some *E. coli* proteases that are co-purified with various ActA constructs cause the degradation. Therefore, it was ultimately decided to utilize a dual purification method as to reduce the capture of degradation products and possible proteases that are co-purified (as the two affinity purification methods are fundamentally different).

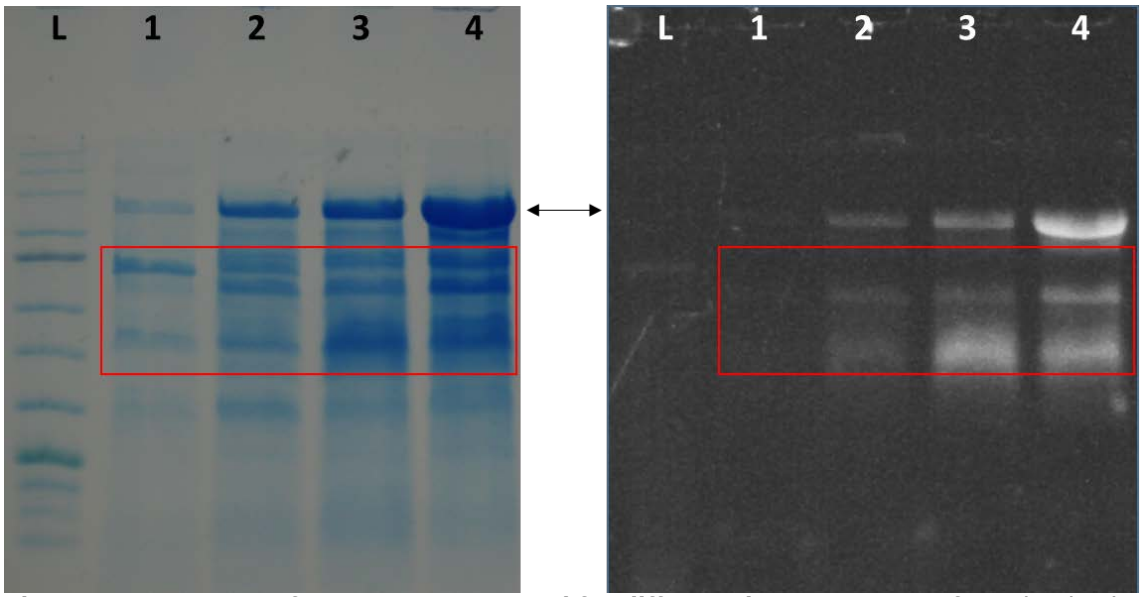

Figure 1: SDS-PAGE of GFP-ActA expressed for different times at 26°C. **Left**: Stained gel, **Right**: Fluorescent image of GFP-ActA and degradation products. **L**: Ladder (NEB ladder #P7712), **1-4**: 2, 4, 6, 18 hours expression, respectively. Black arrow indicates GFP-ActA. Degradation products are outlined in red.

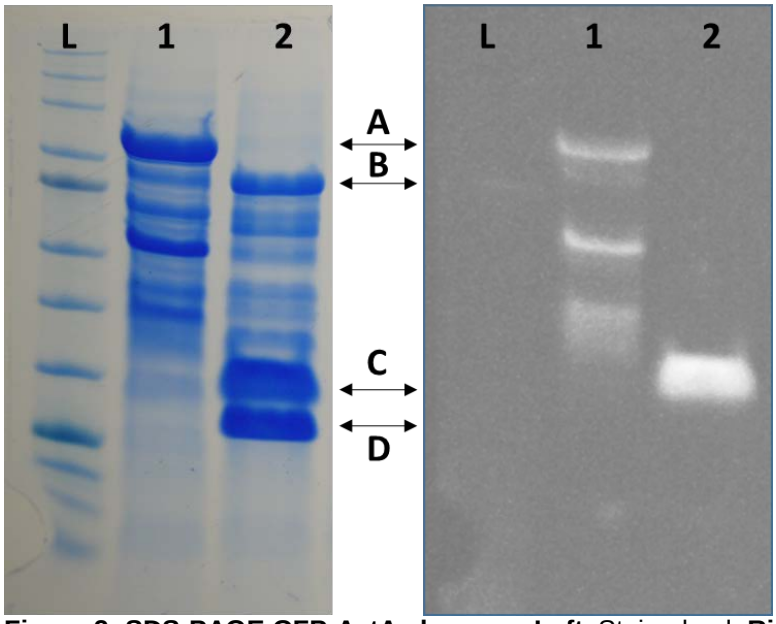

Figure 2: SDS-PAGE GFP-ActA cleavage. **Left**: Stained gel, **Right**: Fluorescent image of GFP-ActA and GFP. **L**: Ladder (NEB ladder #P7712), **1**: Uncut GFP-ActA, **2**: GFP-ActA cut with WELQut protease. **A**: GFP-ActA, **B**: ActA, **C**: GFP, **D**: WELQut protease.

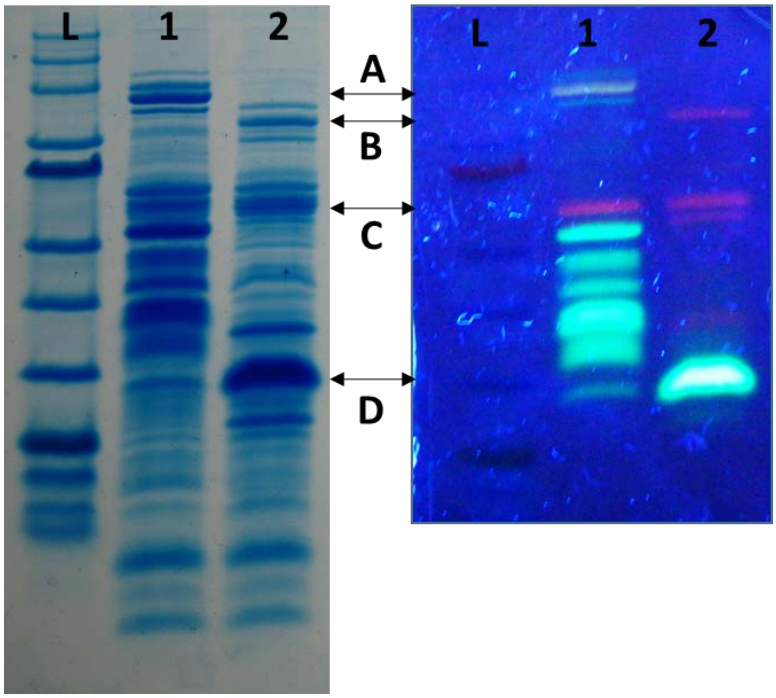

Figure 3: SDS-PAGE GFP-ActA-mCherry cleavage. **Left**: Stained gel, **Right**: Fluorescent image. **L**: Ladder (NEB ladder #P7712), **1**: Uncut GFP-ActA-mCherry, **2**: ActA-mCherry cut with WELQut protease. **A**: GFP-ActA-mCherry, **B**: ActA-mCherry, **C**: truncated ActA-mCherry, **D**: GFP.

Appendix 3: Preparation of Macrophages for Imaging Flow Cytometry

A pilot study was launched to determine the most effective method of lifting macrophages from culture surfaces, while maintaining labelled fluorescent markers. Live cell imaging has the advantage to record cells in an unhindered state, but, in the case of imaging flow cytometry cells need to be lifted from culture surfaces without damaging membranes or confounding experimental outcomes. Primary macrophages are also notoriously hard to lift from surfaces in a viable state. Thus, different methods of fixing cells prior to lifting and fixing after lifting was tested (**Figure 4**). In **Figure 4** the methods are ranked according to effectiveness with optimal combinations for viable cell yield ranked highest on the y-axis and optimal combinations for membrane marker retention ranked highest on the x-axis. Generally, lifting cells prior to fixing with PBS containing 1mM ethylenediaminetetraacetic acid (EDTA) resulted in higher cell viability (determined via Hoechst staining), compared to commercially available Accutase lifting. However, PBS-EDTA treatment led to incomplete retention of the fluorescent membrane marker (CellMask Orange). This is particularly interesting when considering that complete (100% of cells recorded) membrane marker retention was recorded with 23˚C Accutase treatment. Thus, it is important to compare different cell detachment methods, especially during flow cytometric analysis, as the use of PBS-EDTA could have confounded results obtained from further experimentation. To this end, 23˚C Accutase Fix was deemed as the superior detachment method in this study.

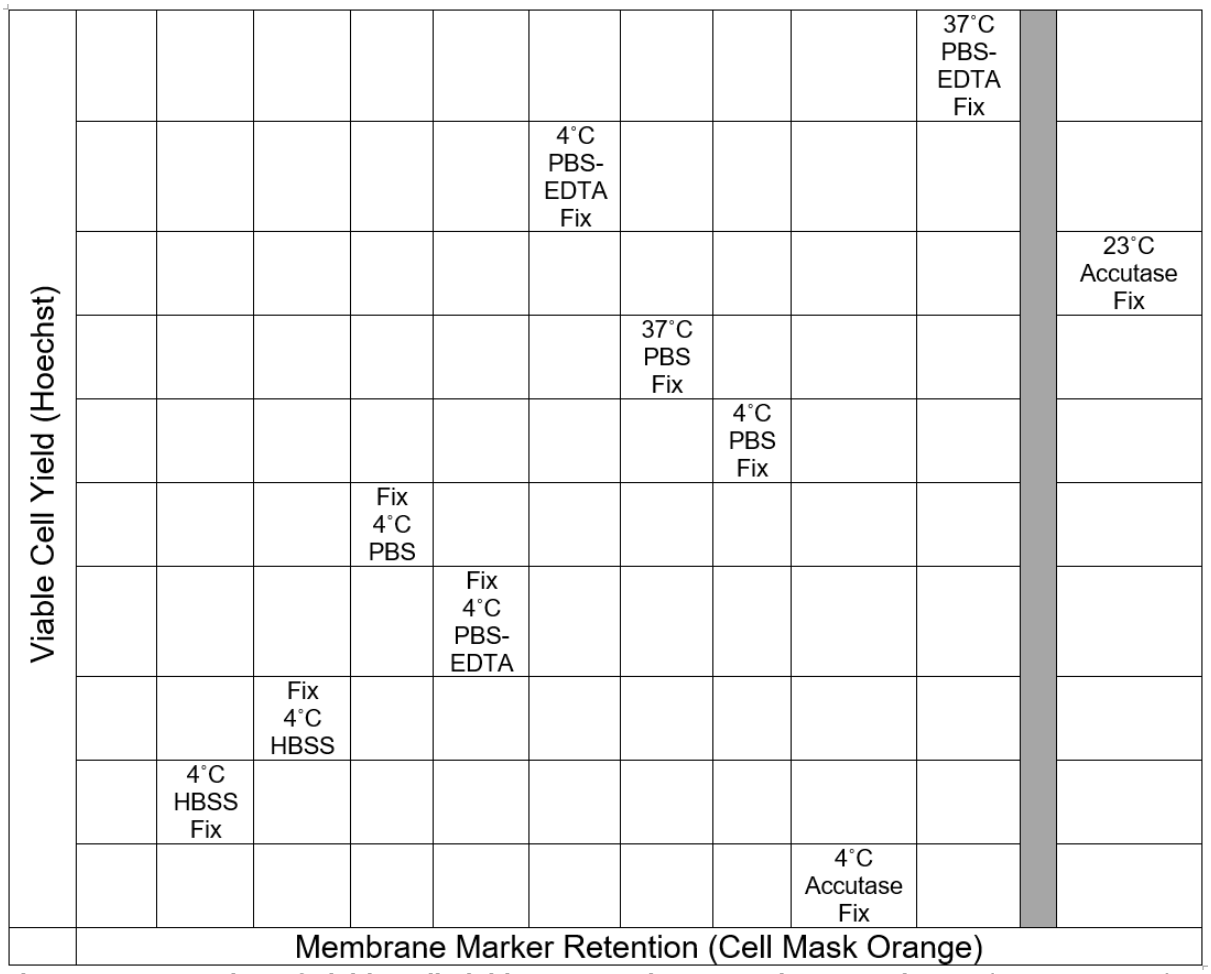

Figure 4: Expression of viable cell yield over membrane marker retention. Values expressed as absolute cell yield over percentage of membrane positive cells. Plotted according to (x;y) co-ordinates. 37˚C PBS-EDTA Fix (23.46%;11426), 4˚C PBS-EDTA Fix (0.0950%;5438), 23˚C Accutase Fix (100%;4868), 37˚C PBS Fix (0.1952%;3360), 4˚C PBS Fix (0.2364%;3151), Fix 4˚C PBS (0.0061%;2069), Fix 4˚C PBS-EDTA (0.0127%;1933), Fix 4˚C HBSS (0.0018%;1780), 4˚C HBSS Fix (0.0003%;1614), 4˚C Accutase Fix (2.034%;100). A threshold for marker retention is indicated in grey.

Appendix 4: GFP-LLO Migration in Gels

Separation of GFP-LLO using SDS-PAGE resulted in a band corresponding to a size slightly lower than that predicted for GFP-LLO (~ 85kDa). In order to visualize GFP fluorescence in SDS-PAGE gels samples are not boiled, which may result in faster migration through the gel. In order to confirm this, GFP-LLO was incubated with SDS-PAGE sampling buffer at 37°C for 30 min or boiled for 5 min. Gels were electrophoresed as described in **Chapter 3**. From SDS-PAGE gels it is evident that treatment of the sample before loading does indeed influence its migration through the gel (**Figure 5**). Boiling the samples resulted in a single band corresponding to the correct size of GFP-LLO (**Figure 5 B**). Cleaved and purified LLO does not suffer the same discrepancy with regards to migration through the gel.

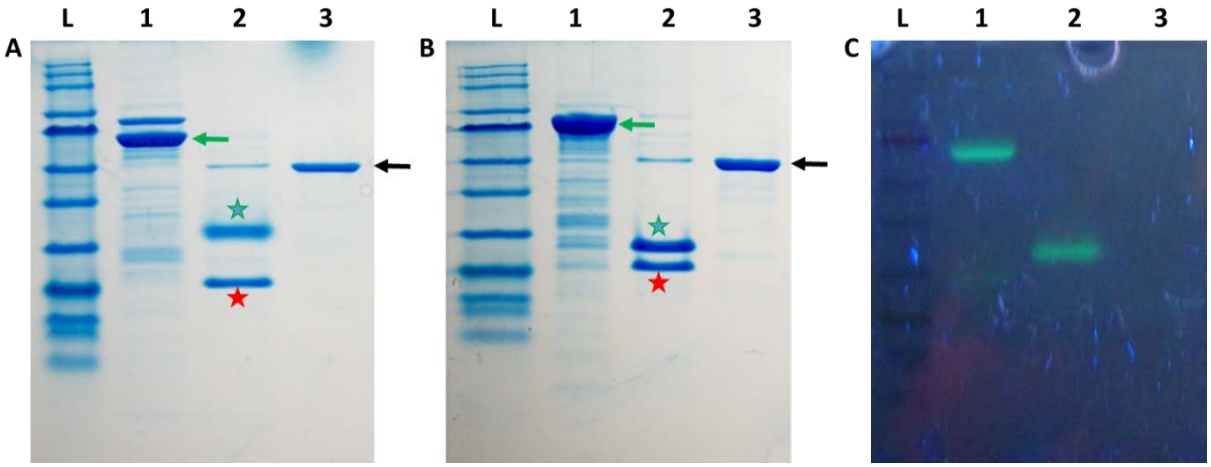

Figure 5: SDS-PAGE GFP-LLO and LLO treated at 37°C (A) or 100°C (B) before SDS-PAGE separation. **Left**: Stained gel, **Right**: Fluorescent image of GFP-LLO (37˚C). **L**: Ladder (NEB ladder #P7712), **1**: GFP-LLO eluted from IMAC column, **2**: GFP and WELQut eluted from column after GFP-LLO digestion, **3**: Flow through from IMAC column containing LLO. GFP-LLO and LLO indicated with green and black arrows, respectively. GFP and WELQut protease indicated with green and red stars, respectively. **C**) Fluorescent image of Gel depicted in figure (**A**).

Appendix 5: Phalloidin Actin Staining in Live Cells

The possibility of labelling live cells with the phalloidin actin stain was determined (**Figure 6**). The stain was taken up by live primary isolated macrophages, however, it remained within intracellular phagosomes throughout the experimental period. Thus, only fixed cells were labelled with the actin stain.

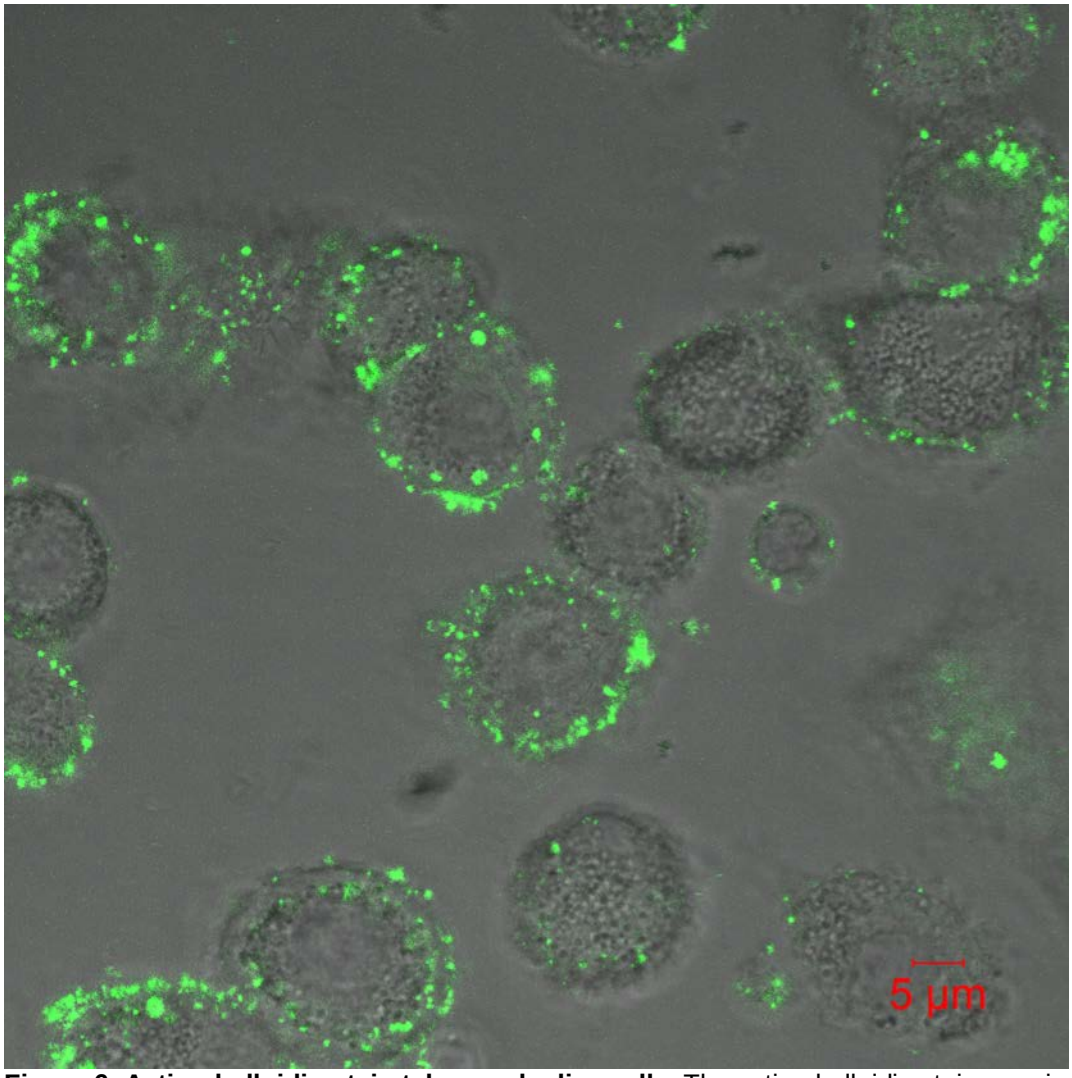

Figure 6: Actin phalloidin stain taken up by live cells. The actin phalloidin stain remained inside phagosomes when taken up by primary macrophages.

Appendix 6: Opsonising Effect of LLO

The capacity of macrophages to engulf beads coated with microbial effectors was determined by coating 4 µm carboxylate modified polystyrene beads with LLO. Satisfactory engulfment was observed 30 min post introduction of LLO coated beads (**Figure 7**). Engulfment increased until all observed cells contained beads. Previously fluorescent antibody coated beads needed to be exposed to serum in order to opsonise the beads and induce engulfment. These findings indicate that LLO is opsonic in nature. Thus, exposure of macrophages to LLOActABeads would more readily result in a normal (or upregulated) engulfment rate, than inhibition thereof.

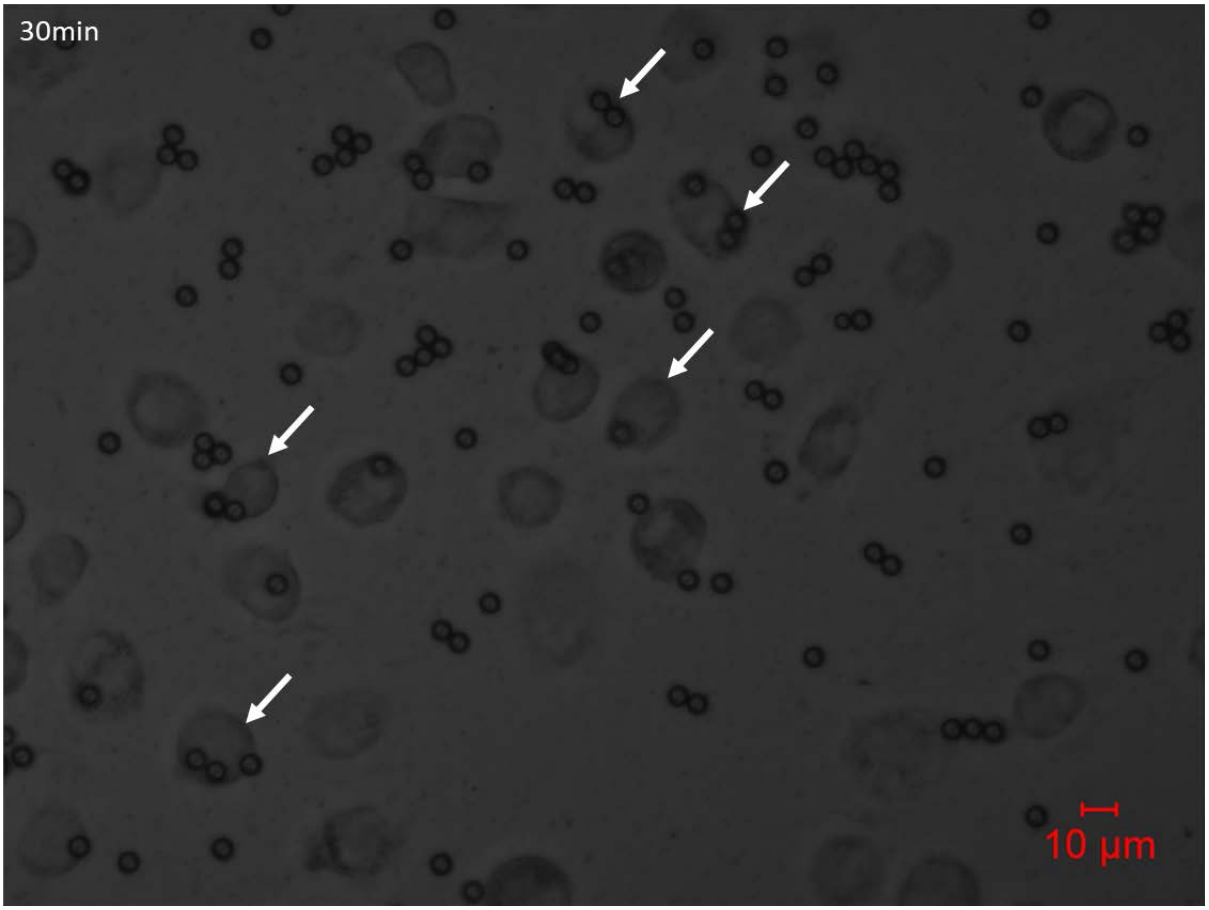

Figure 7: Engulfment of LLO coated beads. Primary macrophages readily engulfed LLO coated beads. Intracellular beads indicated by **white arrows**.

Appendix 7: Incidence of *Cryptococcus neoformans* Vomocytosis

A pilot study was conducted to determine the incidence of vomocytosis. J774 macrophages were infected with *C. neoformans* and vomocytosis only occurred in ~7 out of 100 000 infected cells. Representative images of vomocytosis are given in **Figure 8**. Due to the very low occurrence of vomocytosis in this micro-organism, attention was shifted toward the more effective egress inducing pathogen, *Listeria monocytogenes*.

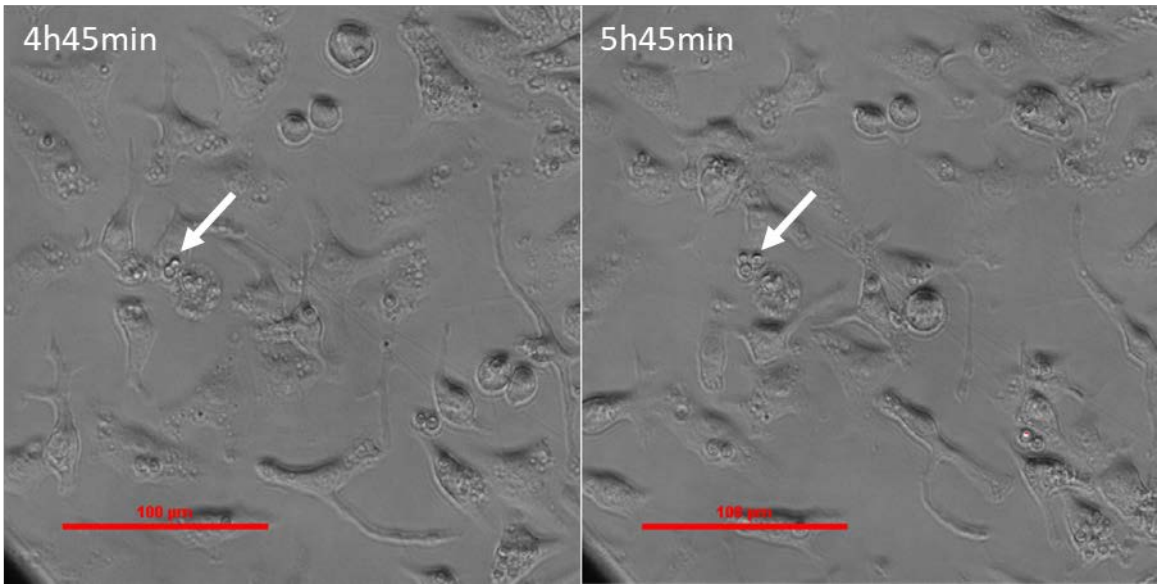

Figure 8: Incidence of *Cryptococcus neoformans* vomocytosis. Infected J774 macrophages indicate vomocytosis of 3 *Cryptococcus neoformans* cells (**white arrows**).

Appendix 8: Delaying Cargo Expulsion

Cargo delivery with the synthetic microbe model needs to be time dependant as carrier cells need to be able to reach target destinations before expulsion of drugs or cargo. Thus, carrier macrophages were treated with phagosome maturation arresting agents to prevent acidification of phagosomes that in turn prevents activation of LLO, subsequently delaying the effect of ActA to induce cargo expulsion. The percentage of non-effector exposed cells carrying degraded cargo is plotted over time (**Figure 9**). A marginal difference in the number of cells with degraded cargo can be seen during the 2-hour time point. This degradation process is increased around 3 hours where after it reaches control conditions. This curve indicates that phagosome maturation arrest is maintained for around 2 hours post treatment with arrest inducing agents.

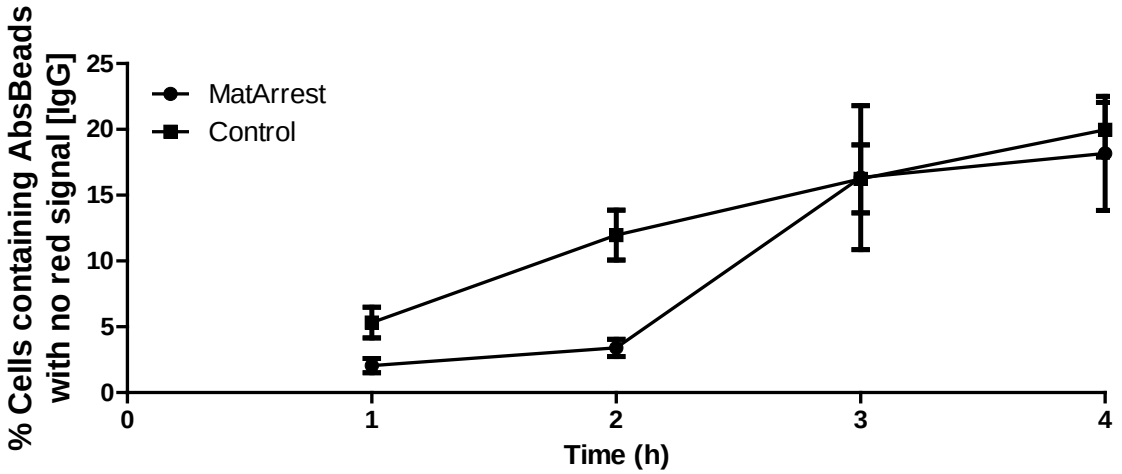

Figure 9: Degradation of Cargo. Values expressed averages with errors bars indicating SEM.

The temporal limit of phagosome maturation arrest during LLOActABeads exposure was determined (**Figure 10**). Preliminary results indicate a marked reduction in the arrested period to about less than 30 min. Indicated by a steep increase in the number of beads per cell (**Figure 10**) until around 30 min, after which the number of beads per cell plateau out. This could be attributed to bead expulsion being induces from the 30 min time point or to a limit in bead uptake being reached at 30 min. However, additional data would need to be collected to adequately determine this.

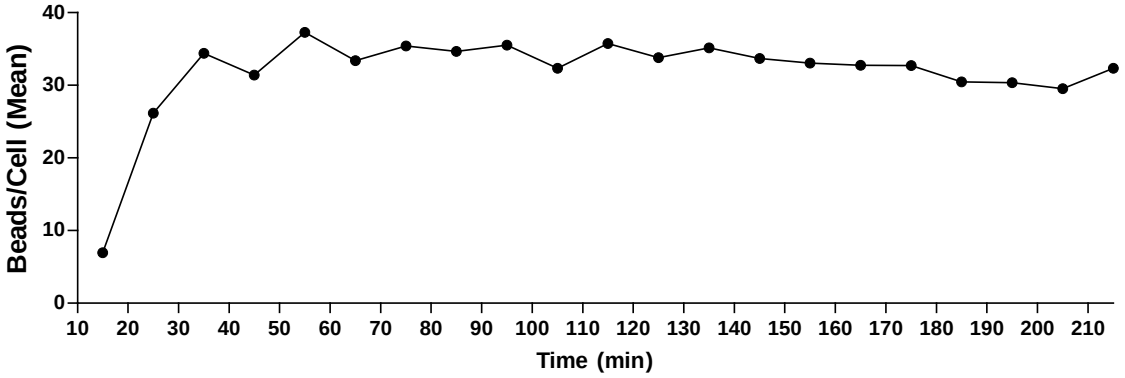

Figure 10: Expulsion efficiency during phagosome maturation arrest. Graph indicate the number of average beads per cell during macrophage phagosome maturation arrest. Values expressed averages with errors bars indicating SEM.

Table 1.1: Examples of drug delivery systems: Reticuloendothelial System (RES), Gastrointestinal Tract (GIT). **1**: (Langer et al., 1976; Cohen et al., 1991; Kim et al., 1999; Ding et al., 2006) **2**: (Sugahara et al., 2010; Nance et al., 2012; Bertrand et al., 2014; Zhao et al., 2014; Hoshyar et al., 2016) **3**: (Ghalanbor et al., 2010) **4**: (Pasut et al., 2012) **5**: (Edwards, 1997) **6**: (Abla et al., 2005; Chen et al., 2006; Alkilani et al., 2015) **7**: (Morishita et al., 2006).